SYNTHESIS AND MECHANISTIC STUDIES OF CHROMIUM(III) PORPHYRAZINES

by

NALEDI HARRIET SEHERI

Submitted in fulfilment of the requirements for the Degree of Master of Science in the Department of Chemistry, Faculty of Agriculture, Science and Technology, North West University, Mafikeng campus.

SUPERVISOR

Dr D. A. ISABIRYE

DATE SUBMITTED:

JUNE 2006

DECLARATION

"I hereby declare that this thesis for the degree of Master of Science, at the North West University hereby submitted, has not previously been submitted by me for a degree at this or any other university, that it is my own work in design and execution and that all material contained herein has been duly acknowledged"

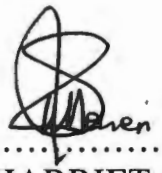

.....

NALEDI HARRIET SEHERI

CERTIFICATE OF ACCEPTANCE

FOR EXAMINATION

This thesis entitled " Synthesis and mechanistic studies of chromium(III) porphyrazines" written by Naledi Harriet Seheri, Student no. 10227326 of the Department of Chemistry in the Faculty of Agriculture, Science and Technology, is hereby recommended for acceptance for examination.

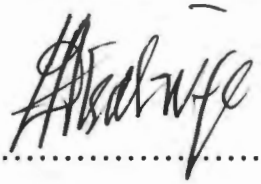

.....

Supervisor : Dr D. A. Isabirye

Department : Chemistry

Faculty : Agriculture, Science and Technology

University : North West University (Mafikeng Campus)

ACKNOWLEDGEMENTS

I would like to thank my Supervisor Dr D.A. Isabirye for his valuable support, guidance, encouragements and advice throughout the entire project.

Thanks to my colleagues Mr F Mtunzi and Mr M J Motaung for their motivational support.

Thanks to the NRF and North West University (Mafikeng Campus) for the financial assistance provided for the entire research project.

I gratefully thank my family, Oupa, Sinah, Onalenna and grandma for their love and encouragements throughout the entire years of my studies.

Thanks to the almighty God for giving me the strength and power throughout.

ABSTRACT

The octakis(propyl)porphyrazinemagnesium(II) complex has been prepared by the addition of bromine to 4-octyne in the presence of acetic acid to produce a *trans*-dibromoalkene. These vinylic dibromides have been converted to fumaronitriles via a Rosenmund - von Braun reaction.[1] The fumaronitriles have been photoisomerised to the corresponding maleonitriles. Mixed Linstead macrocyclisation of the maleonitrile in the presence of magnesium butoxide has yielded the octakis(propyl)porphyrazinemagnesium(II) complex.

2,3,9,10,16,17,23,24octa-substituted phthalocyanine has been prepared by reacting a solution of 4-nitrophthalonitrile with phenol in the presence of tetrahydrofuran, at lower temperatures to form the 1,2-diisocyano-4-phenoxybenzene. The phenoxybenzene has been further reacted with 1,8 diazabicyclo[5,4,0]-undec-7-ene, in the presence of methanol to give the 2,3,9,10,16,17,23,24octa-substituted phthalocyanine.

The octakis(propyl)porphyrazinemagnesium(II) complex has been demetallated with trifluoroacetic acid, to give a freebase compound which has been metallated centrally with cobalt(II) and chromium(III) ions.

In addition the octakis(propyl)porphyrazinemagnesium(II) complex and the 2,3,9,10,16,17,23,24octa-substituted phthalocyanine have been metallated centrally with chromium(III) ion.

The reduction of octakis(propyl)porphyrazinechromium(III) complex using octakis(propyl)porphyrazine cobalt(II) complex has been investigated.

The kinetics of both the chromium(III) insertion into the octakis(propyl)porphyrazinemagnesium(II) complex and the 2,3,9,10,16,17,23,24octa-substituted phthalocyanine and reduction of octakis(propyl)porphyrazinechromium(III) complex with octakis(propyl) porphyrazinecobalt(II) complex have been followed spectrophotometrically at temperatures ranging from 15°C to 35°C. The reactions have been found to follow pseudo-first order kinetics.

Mechanisms of the insertion and reduction of chromium(III) ion have been proposed.

ABBREVIATIONS

THF	Tetrahydrofuran
$CHCl_3$	Chloroform
Mg(II)-Pz	Octakis(propyl)porphyrazinemagnesium(II) complex
Co(II)-Pz	Octakis(propyl) porphyrazinecobalt(II) complex
Cr(III)-Pz	Octakis(propyl)porphyrazinechromium(III) complex
Freebase	Octakis(propyl)porphyrazine ligand
Octa-Phthalo	2,3,9,10,16,17,23,24-octasubstituted phthalocyanine
TCNQ	Tetracyanoquinodimethane
ODMAPz	2,3,7,8,12,13,17,18-octakis(dimethylamino)porphyrazine
Et_2dtc	Diethyl dithiocarbamato
OPTAP	2,3,7,8,12,13,17,18-octa(propyl)tetraazaporphyrazinato
$[pzS_2]_4^{8-}$	Porphyrazineoctathiolate
$[pz(S_2)(Pc)_3]^2$	Porphyrazinedithiolate
$Cr(ox)_2(py.3COOEt)_2^-$	*trans*-dioxalatobis(ethylnicotinate)chromium(III)
sh	Sharp
w	Weak
vw	Very weak
m	Medium

TABLE OF CONTENTS

PAGE No.

CHAPTER ONE
INTRODUCTION

1.1 INTRODUCTION

The considerable interest shown in porphyrazines by the scientific community has been attributed to their potential applications in technology and their relationships to biologically important porphyrins such as chlorophyll and haemoglobin.[1,2]

Porphyrazines are macrocyclic ligands composed of four pyrrole rings bridged by aza nitrogens as shown in Figure 1.[3,4] These aza bridges have little effect on the metal to *pi* donation. They are square-planar with high symmetry and electronic delocalization.[5] The C_{α}-C_{β} bonds are long compared to typical aromatic C-C distances.[6] Electronic absorption spectra of porphyrazines like phthalocyanines show an intense B Soret band at wavelength less than 400 nm and a Q band that has its principal absorption at a wavelength larger than 600 nm.[7,8]

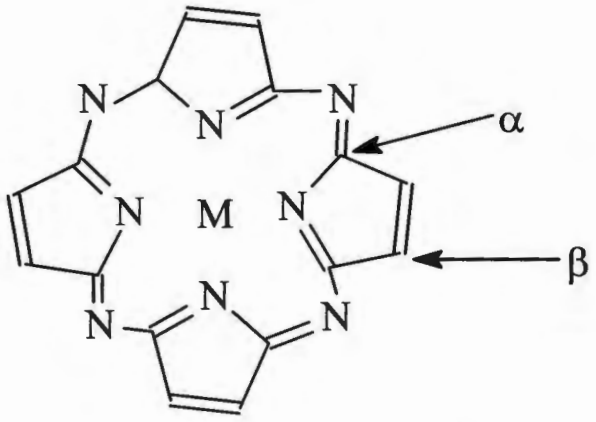

Figure 1, Metallated porphyrazine

1.2 STUDIES ON PORPHYRAZINES

1.2.1 Unsymmetrical porphyrazines

Lange and co-workers[9] studied the unsymmetrical porphyrazines of the form $M[pz(A_n;B_{4-n})]$, where A and B are the functional groups fused directly to the β-position of the pyrroles and M is the central coordinated metal ion. The peripheral A moieties generally involve heteroatoms such as S, N and O which usually bind the exocyclic metal ion. The B groups can be designed to optimise the yields, introduce novel or redox properties and to confer for desired solubility. The ability to vary the types and numbers (n) of A and B allows for even greater control over the physical properties of the macrocycle.[8,9,10,11,12]

These compounds were separated by column chromatography over silica gel, using THF and hexane and they were studied through X-ray crystallography, cyclic voltammetry and ultraviolet-visible spectroscopy.

The ultraviolet-visible spectra of these compounds showed an intense Soret transition between 300 nm and 350 nm and a broadened Q-band transition between 650 nm- 700 nm.[8,9,10]

1.2.2 Symmetrical and unsymmetrical magnesium(II)porphyrazines

Barrets and his co-workers.[9,13,14,15,16] studied and characterised the unsymmetrical porphyrazinehexaamines, that include $Mg[pz(H_2)(NMe_2)_6]$, $Mg[pz(H_2)(Ar)_6]$ (Ar = tert-butylphenyl), $Mg[pz(NMe_2)_8]$ and dinitroporphyrazines and the symmetrical $Mg[pz(Ar)_8]$ which were separated by column chromatography.

1.2.3 Octakis(dimethylamino)porphyrazinato]-magnesium(II)

Montalban and his co-workers[17,18,19] studied and characterised the [octakis(dimethylamino)porphyrazinato]magnesium(II) complex.

The magnesium(II)porphyrazine was demetallated to give a freebase porphyrazine ligand which was more readily oxidised and formed charge transfer complexes with tetracyanoquinodimethane (TCNQ) and C_{10}.[13,20] The ultraviolet-visible spectra of magnesium(II)porphyrazine showed the Q-band at 752 nm, and intense peak at 599 nm, and a band in the Soret region at 335 nm. The proton NMR spectrum showed a single resonance that

corresponded to *N*-methyl groups. The freebase showed a loss of symmetry where the Q band shifted to 709 nm and 531 nm. The microanalysis and high resolution mass ion measurement were consistent with the loss of the magnesium(II) cation.[17,19]

1.2.4 Zinc(II)*seco*-porhyrazines

Montalban and his co-workers[17,18,19,21] also studied and characterised the zinc(II)*seco*-porphyrazines. The acid mediated demetallation of magnesium(II)porphyrazine resulted in peripheral oxidation of one pyrrole ring to form the *seco*-porphyrazine. This *seco*-porphyrazine was metallated with zinc acetate to form a zinc(II)*seco*-porphyrazine. The electronic absorption spectra of zinc(II)porphyrazine has a distinct Q band at 600 nm which consists of two absorption features assigned to the non-degenerate and perpendicular Q_x and Q_y transitions broadened by vibronic structure effect of the two amine groups. When the pyrrole bond is cleaved to form the *seco*-zinc porphyrazine, the Q band splits into two sharp peaks. This is because the two carboxamine groups do not strongly interact with the central ring thus removing the broadening effect.[6] ^{1}H and ^{13}C NMR spectra for the *seco*-porphyrazine showed five distinct N-methyl groups, six ring carbons and amide carbonyl, which are consistent with the structure.[17,19,21]

1.2.5 Nickel(II)porphyrazines

Barrets and his co-workers.[9,13,14,15,16] also studied and characterised the nickel(II)dinitroporphyrazines. Treatment of the freebase H_2ODMAPz in dichloromethane with a solution of nitrogen dioxide in hexane resulted in the formation of dinitroporphyrazine. This dinitroporphyrazine was metallated by nickel(II) to form nickel(II)porphyrazine. This nickel(II)porphyrazine showed an intense Soret band at 343 nm and a Q band at 613 nm. The spectra of the freebase showed a split Q band having Q_x and Q_y absorbances at 586 nm and 656 nm. The bands at 467 nm and 435 nm in the nickel(II)porphyrazine were due to the n-π^* transition from nonbonding electrons on the meso nitrogen atoms of the macrocycle. The propyl substituted porphyrazine displayed a split Q band at 559 nm and 617 nm.[9,13]

1.2.6 Manganese(III)porphyrazines and peripheral metallation

Goldberg and his co-workers[22] studied the X-ray structural characterisation of two manganese(III)porphyrazine complexes, [Mn(Et_2dtc)ODMAPz)] (Et_2dtc=diethyl-dithiocarbamato) and Mn(cl)ODMAPz] ,(ODMAPz)= Octakis(dimethylamino)-porphyrazinato). The peripheral dimethylamino groups make the ODMAPz macrocycle extremely electron rich.[13] As a result, the freebase form H_2ODMAPz(porphyrazine ligand) is readily

oxidised, making an excellent choice for the preparation of charge transfer salts with potentially novel conducting properties.[13]

The electrochemical measurements of these two manganese compounds showed that Mn(II)ODMAPz is electron rich and thus an extremely strong reductant. The ultraviolet-visible spectrum showed that H_2ODMAPz exhibits a Soret peak centered at 334 nm and two broad bands at 522 nm and 705 nm.[23] The insertion of manganese(III) into the porphyrazines caused striking changes in the absorption spectrum although the Soret band, matches that of a freebase. The next two peaks were blue-shifted and centred at 467 nm and 607 nm with a less intense shoulder near 765 nm. The utility of the dimethylamino groups as peripheral bidentate chelation sites was demonstrated by the coordination of four $PdCl_2$ units by NiODMAPz to give $[PdCl_2]_4$[NiODMAPz].[14] In contrast the spectrum of NiODMAPz was qualitatively similar to that of the freebase with a small shift (~20 nm) of all three bands.[16,23]

1.2.7 *Trans*-porphyrazines

Forsyth and his co-workers[8] studied the *trans*-heterofunctionalised porphyrazine derivatives, M[pz(A_2B_2) where (A= -Nme2, -Sr, -OR). These *trans*-macrocycles were studied using cyclic voltammetry, ultraviolet-visible spectra and X-ray crystallography. The *trans*-porphyrazines showed

electronic absorption spectra at 539 nm and 747 nm, 656 nm and 798 nm, 638 nm and 718 nm and 632 nm and 705 nm respectively. In addition, they all had split Q bands.[8]

The introduction of heteroatoms in the peripheral positions of these *trans*-porphyrazines may complicate the spectra by adding n-π^* transitions which broaden the Q bands split.[15] The propyl substituted compound has a split Q band and a shoulder at 450 nm. The oxygen substituted compound is similar except the Q bands are blue shifted and the sulphur substituted has a red shifted Q-band with a large splitting. The nitrogen substituted compound is less red shifted with a larger Q band split, this unusual breadth of Q bands is due to the n-π^* transitions of the dimethylamino nitrogen groups.[3,24]

1.2.8 Sandwiched porphyrazines

Montalban and his co-workers[25] also studied and characterised the lanthanide porphyrazine sandwiched type metal complexes. These sandwiched metal complexes are of great interest because of their unique physical, spectroscopic and electrochemical properties. Those studied include $[Ce(OPTAP)_2]$, $[Lu(OPTAP)_2]$, $[Eu(OPTAP)_2]$ and $[Eu_2(OPTAP)_3]$ where OPTAP = 2,3,7,8,12,13,17,18octa-propyltetraazaporphyrazinato.

The cerium structure was studied through X-ray crystallography. The ultraviolet-visible spectrums of the compounds were typical of sandwich type metal complexes. They displayed intense bands in the Soret region at 326 nm, 318 nm, 320 nm, and 329 nm respectively. These were due to the strong π-π^* interaction, thus resulting in a shift suggesting a D_{4h} symmetry as compared to the freebase (OPTAP). Single Q bands at 584 nm, 588 nm, 595 nm and 580 nm respectively were displayed. This was in contrast to the freebase, which shows a split Q band with peaks centered at 559 nm, and 626 nm consistent with a D_{2h} symmetry.[25]

1.2.9 Diverse porphyrazines

The Hoffman and Barret groups[20] carried out studies and characterisation of diverse porphyrazine derivatives consisting of heteroatom groups directly bonded to the macrocyclic core of the porphyrazine. Such species are exemplified by the porphyrazineoctathiolate $[pzS_2]_4^{8-}$ and the dithiolate $[(pzS_2)(pc)_3]^2$ species.

These porphyrazines showed unusual coordination chemistry through binding of metal ions both within the macrocyclic cavity and by the peripheral ligating groups. There was a clear possibility of metal ion binding either via the bidentate S-CH=CH-S units or within the meso pocket via

bonding to the S-N-S entities. Such electron rich porphyrazines showed unusual ultraviolet-visible spectra, electrochemistry and magnetic properties.[20]

1.2.10 Aquation of *trans*-$Cr(ox)_2(py.3COOEt)_2^-$

Kormoh and his co-workers[26] studied the kinetics of the aquation of *trans*-$Cr(ox)_2(py.3COOEt)_2^-$ using spectrophotometric methods in aqueous $HClO_4^-$ /$NaClO_4^-$ media.

The spectral changes revealed a band shift with an increase in the absorbance with aquation showing the formation of the *trans*-diaquo intermediate(*trans*-$Cr(ox)_2(OH_2)_2^-$) prior to the final product *cis*-$Cr(ox)_2(OH_2)_2^-$. The absorbance measurements showed the wavelengths at 415 nm and 555 nm which closely resemble the *trans*-$Cr(ox)_2(OH)_2^-$ compound, and that of *trans*-$Cr(ox)_2(py.3COOEt)_2^-$ at 395 nm and 540 nm. The *cis*-compounds closely resembled those mentioned in the literature.[27,28,29] The plots of $\ln(A-A_t)$ versus time exhibited good linearity up to three half-lives. The observed activation parameters for the *trans*-$Cr(ox)_2(py.3COOEt)_2^-$ are large and positive ΔH^* and a fairly large and negative ΔS^*. These correspond to values obtained for the isomerism study on the *trans*-$Cr(ox)_2(OH)_2^-$ complex.[29] These observations suggested a

similar mechanism involving the slow dissociation of one end of the oxalate ligand as the rate determining step.[26]

1.3 METALLATION ATTEMPTS

A range of different substituents provides porphyrazines with greatly enhanced organic solubility compared to their phthalocyanine counterparts.[20,22] Porphyrazines, especially when functionalized with peripheral heteroatoms, are quite soluble in diverse solvents from hexanes to methanol. The corresponding porphyrazines bearing hydroxyalkyl side chains are even soluble in water.[20]

Studies have been done on the central and peripheral metallation of various metal ions into the freebase porphyrazine ligand. The peripheral dimethylamino groups make the octakis(dimethylamino)porphyrazinato macrocycle extremely electron rich. This has been exploited by the peripheral coordination of four $PdCl_2$ and other metal ions such as tin(IV) or nickel(II) which resulted in compounds such as star-porphyrazines.[17,30] The octakis(dimethylamino)porphyrazinato macrocycle can also be oxidised either with air, under acidic conditions or with manganese dioxide to provide the corresponding *seco*-porphyrazine, with one pyrrole ring opened.[17,30]

1.4 KINETIC STUDIES INVOLVING METALLATION

Most of the work involving metallation has concentrated on examining the effect of the macrocycle nature on metal complexation[22] in different solvents.[31,32,33] Very little work has been done on the effect of changing the metal ions on the rate of complexation.[34]

During their studies, Goldberg and co-workers[22] found out through electrochemical measurement that Mn(ODMAPz) was extremely electron rich and could act as a strong reductant. It could therefore be used for the preparation of donor-acceptor molecule based magnets.[22]

Further work on metallation of porphyrazines has involved synthesis and characterization using infrared, NMR, ultraviolet-visible spectrophotometry.[8,10,13,20] Hence our interest of study is to synthesize the porphyrazine ligand and use its demetallated template for incorporating the chromium(III) ion and compare its insertion with the other coordinated central metal ions, using kinetic methods.

1.5 AIMS AND OBJECTIVES

The lack of any kinetic studies on metal ions insertion has motivated this investigation into the rate of insertion of chromium(III) ion into

octakis(propyl)porphyrazinemagnesium(II) complex. This is to be compared with similar studies in our group involving other cations.

(i) The first objective was to synthesise the octakis(propyl) porphyrazine magnesium(II) complex.

(ii) The second objective was to investigate the mechanism of formation of octakis(propyl)porphyrazinechromium(III) and the 2,3,9,10,16,17,23,24octa-substituted phthalocyanine complexes.

(iii) The third objective was to investigate the mechanism of reduction of the octakis(propyl)porphyrazinechromium(III) complex.

The specific questions to be answered in this research were:

(a) Did the introduction of chromium(III) ion into the octakis(propyl)porphyrazine ligand increase or decrease the stability of the porphyrazine?

(b) Did the introduction of chromium(III) ion affect the use of the application and uses of octakis(propyl)porphyrazine ligand in particular?

(c) How did the rate of reduction in chromium(III) compare with other macrocyclic ligands?

(d) Is the redox mechanism anomalous or in line with other similar chromium(III) macrocyclic compounds?

CHAPTER TWO

LITERATURE REVIEW

2.1 LITERATURE REVIEW

In general porphyrazines especially when functionalised with peripheral heteroatoms, are quite soluble in diverse solvents[20], for example the octakis(dimethylamino)porphyrazine is very soluble in common solvents from hexanes to methanol. The corresponding porphyrazines bearing hydroxyalkyl side chains are even more soluble in water.[10,17,20]

The synthesis of porphyrazine with maleonitrile derivatives allows for the direct preparation of functional groups attached to the β-position of the pyrrole rings. However, with these properties, it is possible to prepare compounds in which solubility, redox and electronic properties may be tuned.[1,2,25]

2.2 SYNTHESIS AND METALLATION STUDIES

2.2.1 Unsymmetrical porphyrazines

Montalban and co-workers[10,17] synthesised the unsymmetrical porphyrazines bearing 2,4,6(dimethylamino) functionalities. The synthetic strategy employed for the preparation of the unsymmetrical porphyrazines involved the co-cyclization of bis(dimethylamino)maleonitrile and 1,2-

dicyanobenzene about a magnesium template, in the molar ratio of 25:1 giving a product mixture of two compounds. These two compounds were separated by column chromatography over silica gel, using THF and hexane (1:4).[10,17]

2.2.2 Unsymmetrical porphyrazines with peripheral metallation

Lange and his co-workers[9] synthesised the unsymmetrical porphyrazine bearing a single bis(dimethylamino) functionality. $Mg[pz(NMe_2)_2(Pr)_6]$ was prepared by base-catalysed cross condensation of dipropyl maleonitrile (in excess) and with dimethylamino maleonitrile. The magnesium(II) ion was removed by treatment with trifluoroacetic acid to give the freebase ($H_2[pz(NMe_2)_2(Pr)_6]$). The reaction of the freebase with $Ni(OAc)_2.4H_2O$ in a mixture of DMF and chlorobenzene at 90°C gave the centrally metallated compound. The Cu(II) porphyrazine was obtained after the reaction of the freebase and copper(II) acetate in chloroform/acetonitrile (3/1) at 50°C. Manganese(II) was incorporated into the macrocyclic cavity, oxidising to manganese(III) during the reaction.[12,16] Treatment of the freebase with excess nickel(II) resulting in $Ni[pz(NMe_2)_2(Pr)_6]$, which was further treated with palladium(II) chloride in chloroform/acetonitrile solution(3:1) at reflux to give a bimetallic porphyrazine with peripherally coordinated $PdCl_2$.[9]

2.2.3 Unsymmetrical magnesium(II)porphyrazines

Nie and his co-workers[35] synthesised the porphyrazinehexamines and dinitroporphyrazines abbreviated as $M[pz(H_2)(R)_6]$, with three substituted pyrroles at the periphery and one substituted pyrrole ring. The 3,4 dipropylpyrroline-2,5-diimine was prepared from the dipropylmaleonitrile by passing ammonia through the methanol solution at reflux for 15 hours. The 2,5-diiminopyrrolidine was co-macrocyclised with bis(dimethylamino)maleonitrile using magnesium butoxide in butanol at reflux. These resulted in two unsymmetrical compounds $Mg[pz(H)_2(NMe_2)_6]$ and $Mg[pz(H)_2(NMe_2)_8]$.[35]

These two compounds were demetallated by trifluoroacetic acid under nitrogen atmosphere in the dark, yielding a freebase $H_2[pz(H)_2(NMe_2)_6]$ and $H_2[pz(H)_2(NMe_2)_8]$, which were separated by chromatography. The other synthesized compounds included unsymmetrical $Mg[pz(H)_2(Ar)_6]$ and symmetrical $Mg[pz(H)_2(Ar)_8]$. The freebases of these compounds were obtained by demetallating the magnesium complexes with trifluoroacetic acid. The freebase was metallated with nickel acetate in a mixture of chlorobenzene and dimethylformamide(3:1) at 100°C. The freebase in dichloromethane was also treated with a solution of nitrogen dioxide in hexane resulting in the formation of dinitroporphyrazine, which was isolated

in 90% yield. These two macrocycles have shown favourable solubility and an open site for possible peripheral functionalisation such as nitration, halogenation, hydroxylation and subsequent oxidation.[35]

2.2.4 Unsymmetrical bis(dimethylamino)porphyrazine

Barrets and his co-workers[9,13,14,15,16] designed a new class of macrocyclic molecules, porphyrazinehexaamines and dinitroporphyrazines. The synthesis of these compounds involved the macrocyclization of 2,5-diiminopyrrolidine with bis(dimethylamino)maleonitrile using $Mg(OBu)_2$ in butanol at reflux. This gave two unsymmetrical porphyrazines $Mg[pz(H_2)(NMe_2)_6]$ and $Mg[pz(NMe_2)_8]$.The compounds were demetallated using trifluoroacetic acid under nitrogen atmosphere yielding the freebase $H_2[pz(H_2)(NMe_2)_6]$ and $H_2[pz(NMe_2)_8]$ which were separated by column chromatography. They also synthesized unsymmetrical $Mg[pz(H_2)(Ar)_6]$ where Ar is (tert-butylphenyl) and symmetrical $Mg[pz(Ar)_8]$ which were separated by column chromatography. Treatment of the freebase ($H_2[pz(H_2)(NMe_2)_6]$) in dichloromethane with a solution of nitrogen dioxide in hexane resulted in the formation of dinitroporphyrazine, which was metallated by nickel(II) cation to give nickel(II)porphyrazine. [9,16]

2.2.5 Octakis(dimethylamino) porphyrazines magnesium(II) complex

Montalban and his co-workers[10,17,18,19] also synthesised octakis(dimethylamino)porphyrazinesmagnesium(II) complex. Linstead macrocyclization of tetramethyl derivative using magnesium propoxide in propanol gave octakis(dimethylamino)porphyrazinemagnesium(II) complex (mgODMAPz) up to 48% yield.[17] The demetallation of the magnesium complex with trifluoroacetic acid under an inert atmosphere gave the expected freebase porphyrazine only in 21% yield. With glacial acetic acid, however, the desired product was obtained in 69% yield. The demetallation of porphyrazine using trifluoroacetic acid in the presence of air gave freebase porphyrazine with one of the pyrrole rings opened giving a *seco*-porphyrazine in 62% yield.[10,17]

2.2.6 *Trans*-porphyrazines

Forsyth and co-workers[8] studied the *trans*-heterofunctionalised porphyrazine derivatives. The synthesis of *trans*-director started with alkylation of inexpensive 2,3-dicyanohydroquinone by 2-bromopropane. The resulting hydroquinone diisopropylether was unreactive under normal Linstead macrocyclization conditions. This compound was converted to 1,3-diiminoisoindoline by bubbling ammonia through a solution of ethylene

glycol at 140-150°C that was previously treated with a catalytic amount of sodium for 4-5 hours. The 1,3-diiminoisoindoline was then macrocyclised with bis(dimethylamino)maleonitrile, 2,3-bis(benzylthio)maleonitrile, diprolpylmaleonitrile and dispiromaleonitrile. In each case the product containing Mg[pz(A_2B_{4-n}), was treated with trifluoroacetic acid to form a freebase 2H[pz(A_2B_{4-n}) and then chromatographed to give the desired *trans*-[pz(A_2B_2). Magnesium templated cyclisation of bisdimethylamino maleonitrile and a 3 fold excess diiminoisoindoline produced three pigments Mg[pz(A_1B_3), *cis*-Mg[pz(A_2B_2) and *trans*-Mg[pz(A_2B_2) which were simpler to purify and to separate.[8]

2.2.7 Manganese(III)porphyrazines with peripheral metallation

Goldberg and co-workers[22] synthesised two manganese porphyrazine (tetraazaporphyrin) complexes, [Mn(Et_2dtc)ODMAPz)] (Et_2dtc = diethyl-dithiocarbamato) and [Mn(cl)ODMAPz] (ODMAPz = octakis(dimethylamino)porphyrazinato).

[Mn(Et_2dtc)ODMAPz)] was prepared by adding a sample of Mn(Et_2dtc)$_2$ to a purple suspension of H_2ODMAPz, which formed a dark blue solution and this mixture was stirred for 12 hours. [Mn(cl)ODMAPz] was prepared by adding a sample of $MnBr_2$ to a purple suspension of H_2ODMAPz in DMF,

and the mixture was heated at 80°C for 24 hours under nitrogen. The peripheral metallation of four units of $PdCl_2$ into the Ni(ODMAPz), was achieved by combining Ni(ODMAPz) and $PdCl_2$ in $CH_3CN/CHCl_3$ (3:1). The mixture was heated for 4 hours at 100°C, and stirred for additional 12 hours at 60°C to give $[PdCl_2]_4$[NiODMAPz].[10,14,22]

2.2.8 Lanthanide sandwiched porphyrazines

Montalban and his co-workers[25] further synthesised the lanthanide porphyrazine sandwiched type metal complexes. They synthesized bis[2,3,7,8,12,13,17,18octa-propylporphyrazinato]cerium(IV), by adding a octakispropylporphyrazine in 1,2,4-trichlorobenzene to $Ce(acac)_3.H_2O$, and heated to reflux for 24 hours. Bis[2,3,7,8,12,13,17,18-octakispropylporphyrazinato]lutetium(III) was prepared from the addition of octakispropylporphyrazine in dry redistilled hexanol to $Lu(OAc)_3.H_2O$, followed by refluxing the mixture for 24 hours. Bis[2,3,7,8,12,13,17,18-octakispropylporphyrazinato]-europium(III) and tris[2,3,7,8,17,18-octapropylporphyrazinato]-dieuropium(III) were also synthesized by adding various metal salts.[25]

2.3 CHEMISTRY OF PORPHYRAZINES

2.3.1 Porphyrazine ligands and metallation with metal ions

Porphyrazine ligands are prepared from the corresponding functionalised maleonitriles using a Linstead magnesium alkoxide templated macrocyclization reaction in an alcohol solvent under reflux. The reactions were followed by conversions of derivatives of 2,4- dimercapto-, 2,3 diamino-, and 2,3 dihydroxy-maleonitrile to provide the corresponding porphyrazine-octathiols, -octaamines, and -octaols. In each case the magnesium ion template was removed under acid conditions and replaced with representative diamagnetic ions, Ni(II) or Zn(II), or representative paramagnetic ions, Cu(II) or Mn(II), as shown in Figure 2.1.[20]

2.3.2 Star porphyrazines

Dissolving the metal reduced octabenzylthioporphyrazinatonickel(II) gave an intense purple, air sensitive and water soluble pigment that was presumably the corresponding octathiolate. This air sensitive pigment was smoothly condensed with di-tert-butyltin dinitrate to produce the corresponding star porphyrazine as air stable green-black crystals[20], as shown in Figure 2.2.

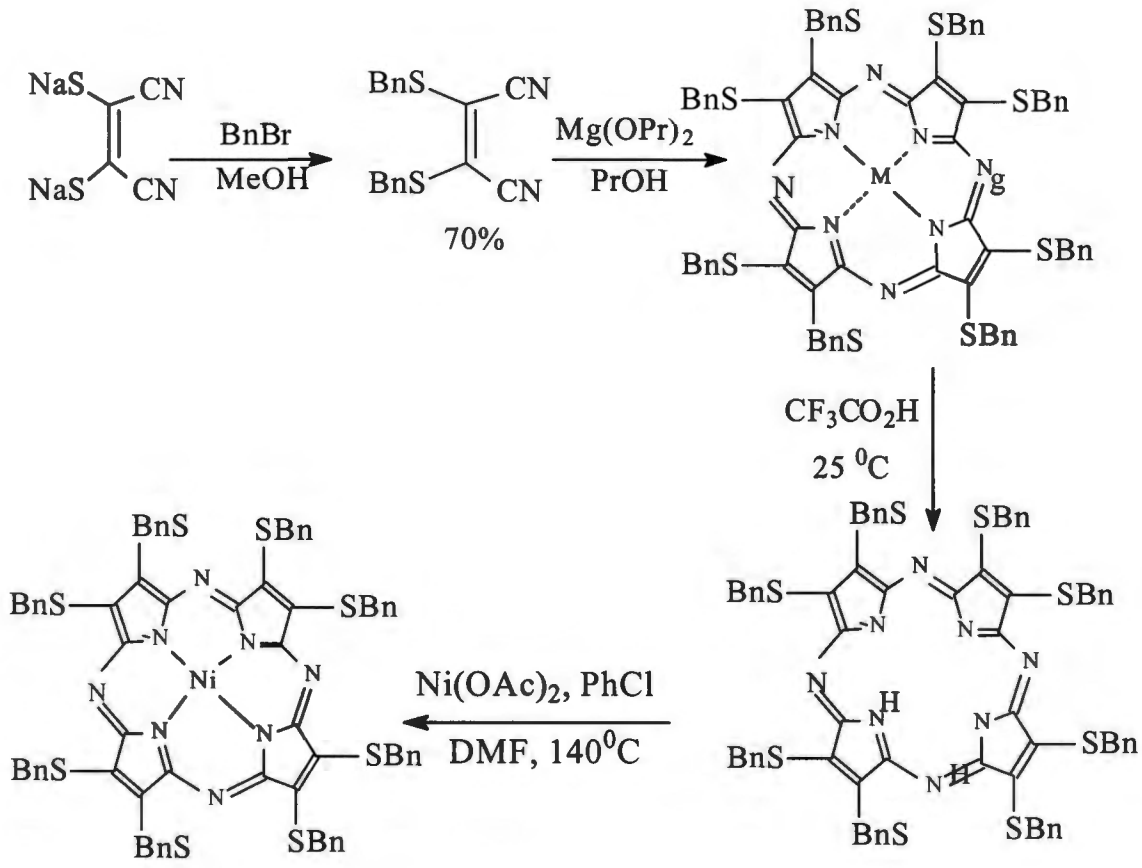

Figure 2.1

2.3.3 Formation of multimetallic porphyrazines

The *tetra*-tin star porphyrazine is a convenient starting material for the preparation of other multimetallic arrays. The reaction of the green macrocycle in Figure 2.2 with (diphos)$NiCl_2$ and related salts gave the corresponding *tetra*-nickel star porphyrazines as shown in Figure 2.3. This methatic exchange of metals is important giving the ease of handling of the *tetra*-tin star porphyrazine compared with its precursor, the air sensitive porphyrazine octathiolate.[20]

2.3.4 Peripheral metallation

More recently, there has been increased effort in preparing porphyrazine molecules with the substituents linked directly to the β-carbon atoms of the pyrrole rings, including those that provide metal binding site on the periphery, as shown in Figure 2.4 by Mn(III) core coordination and Pd(II) peripheral coordination.[11,12,22,36]

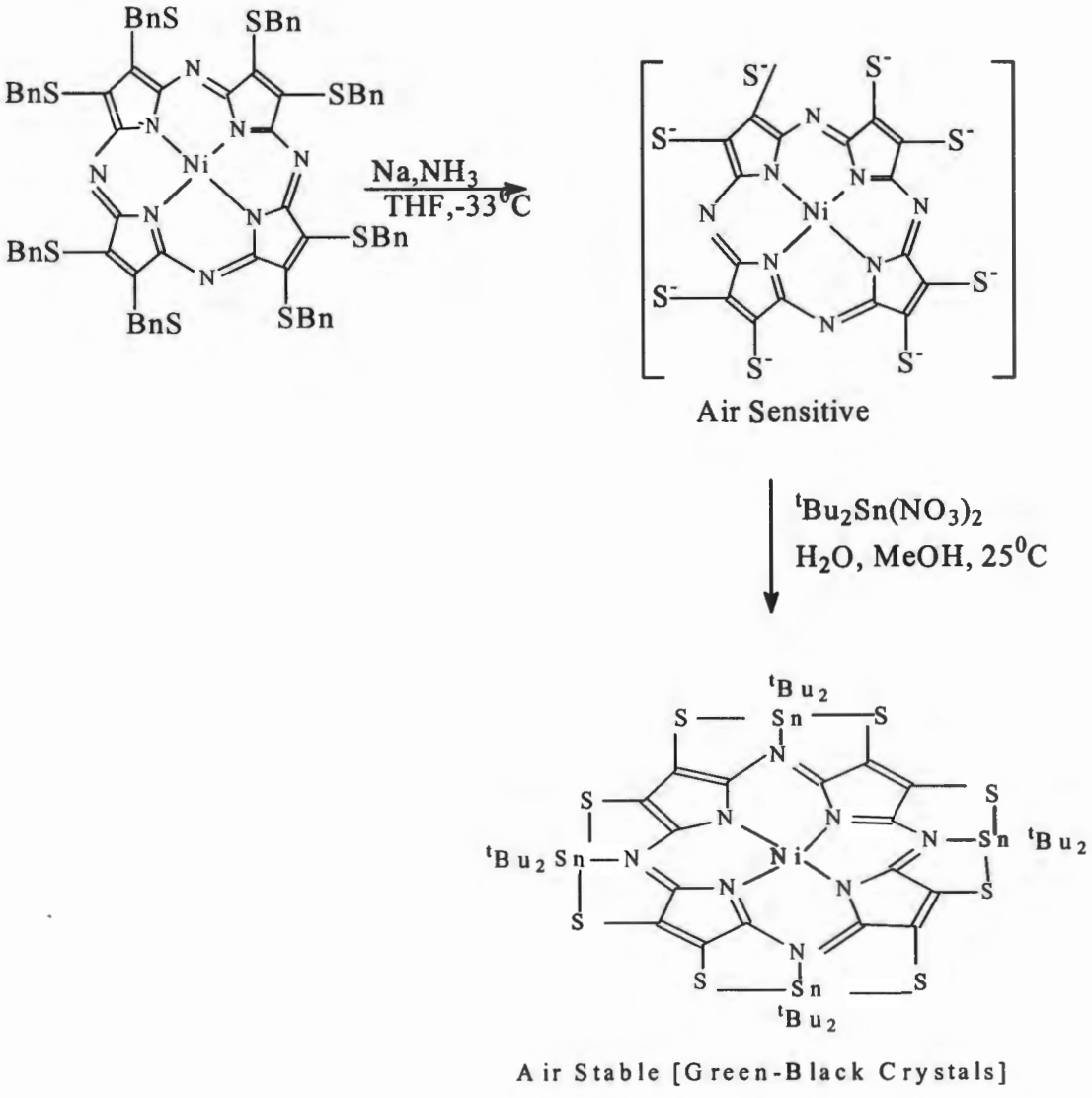

Figure 2.2

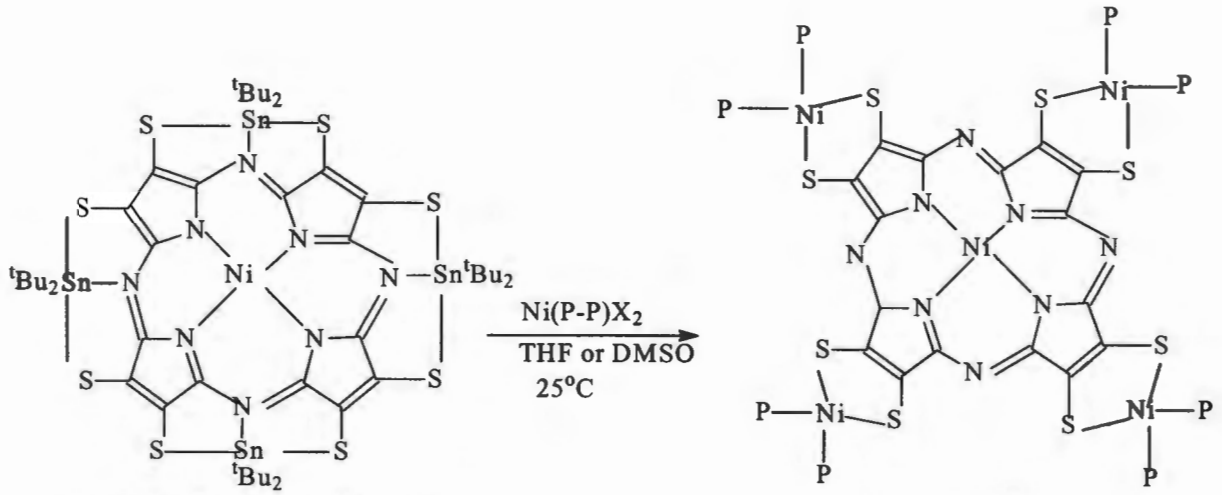

Air stable, Green Black Crystals

Purple Black Crystals

Figure 2.3.

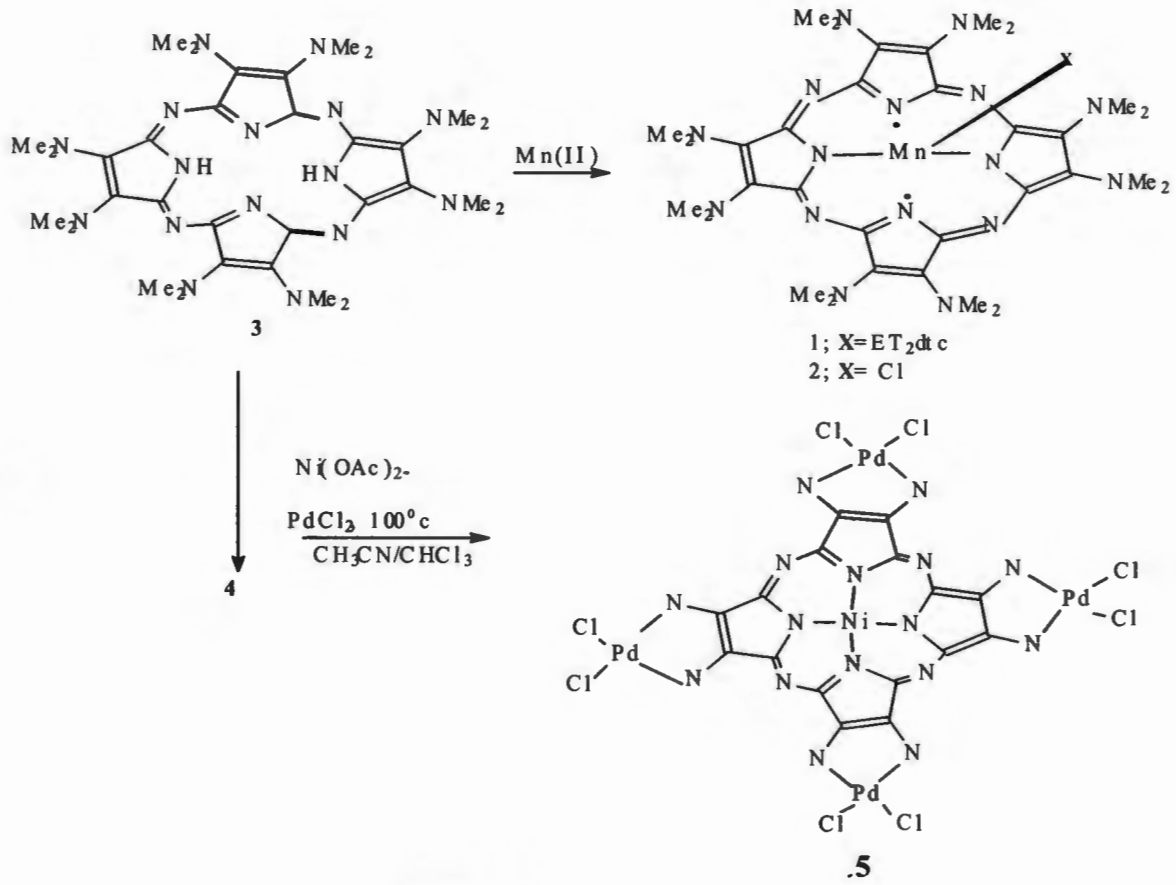

3

1; X=ET2dtc
2; X= Cl

4

.5

Figure 2.4

2.3.5 *Trans*-porphyrazines

Hydroquinone diisopropyl ether was the main *trans*-director for the formation of *trans*-M[pz(A_2:B_2), which is unreactive under normal Linstead macrocyclization conditions. When adding a suspension of magnesium butoxide in refluxing butanol to hydroquinone diisopropyl ether, the 1,3-diiminoisoindoline **(3)** was formed.[8] 1,3-Diiminoisoindoline **(3)** was microcyclized with bis(benzylthio)maleonitrile, 2,3-bis(benzylthio)maleonitrile, dipropylmaleonitrile and dispiromaleonitrile. In each case the product formed contains Mg[pz(A_2;B_2)]. Mg[pz(A_2;B_2)] was treated with trifluoroacetic acid to form a freebase H_2[pz(A_2;B_2)], and then chromatographed to give the desired *trans*-[pz(A_2B_2)], as shown in Figure 2.5.[8]

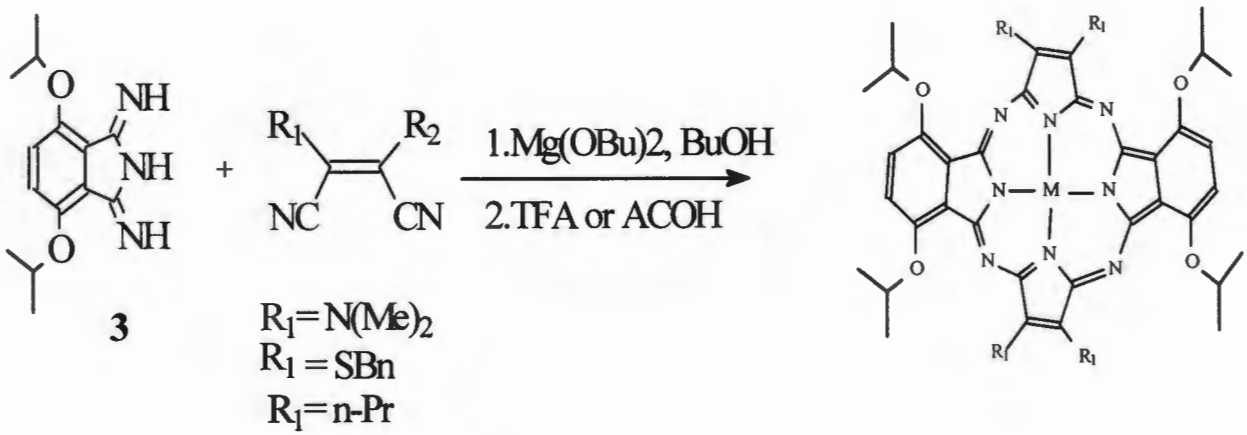

Figure 2.5

2.3.6 Demetallation of magnesium(II)porphyrazines

Demetallation of the magnesium(II) complex with trifluoroacetic acid under an inert atmosphere gave the expected freebase porphyrazine in 21% yield. The yield however improved to 69% if glacial acetic acid is used. The demetallation of magnesium(II)porphyrazine using trifluoroacetic acid in the presence of air gave freebase porphyrazine with one of the pyrrole rings opened, as shown in Figure 2.6.[13,,37]

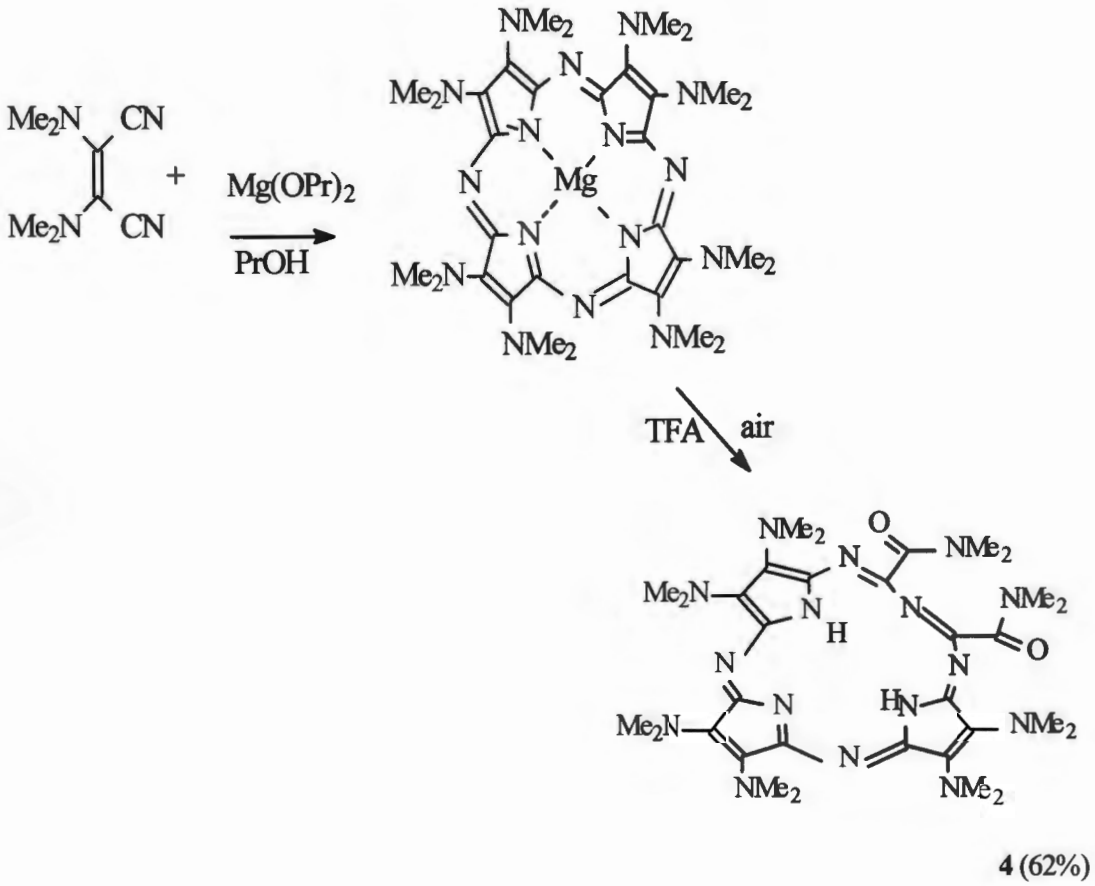

4 (62%)

Figure 2.6

2.3.7 *Seco*-porphyrazines

The zinc(II)porphyrazine was formed by the reaction of the freebase (**4**) (as in Figure 2.6), with zinc(II) acetate. The synthesis of *seco*-porphyrazine was obtained by the oxidation of zinc(II)porphyrazine in potassium permanganate[18,19,38], as shown in Figure 2.7

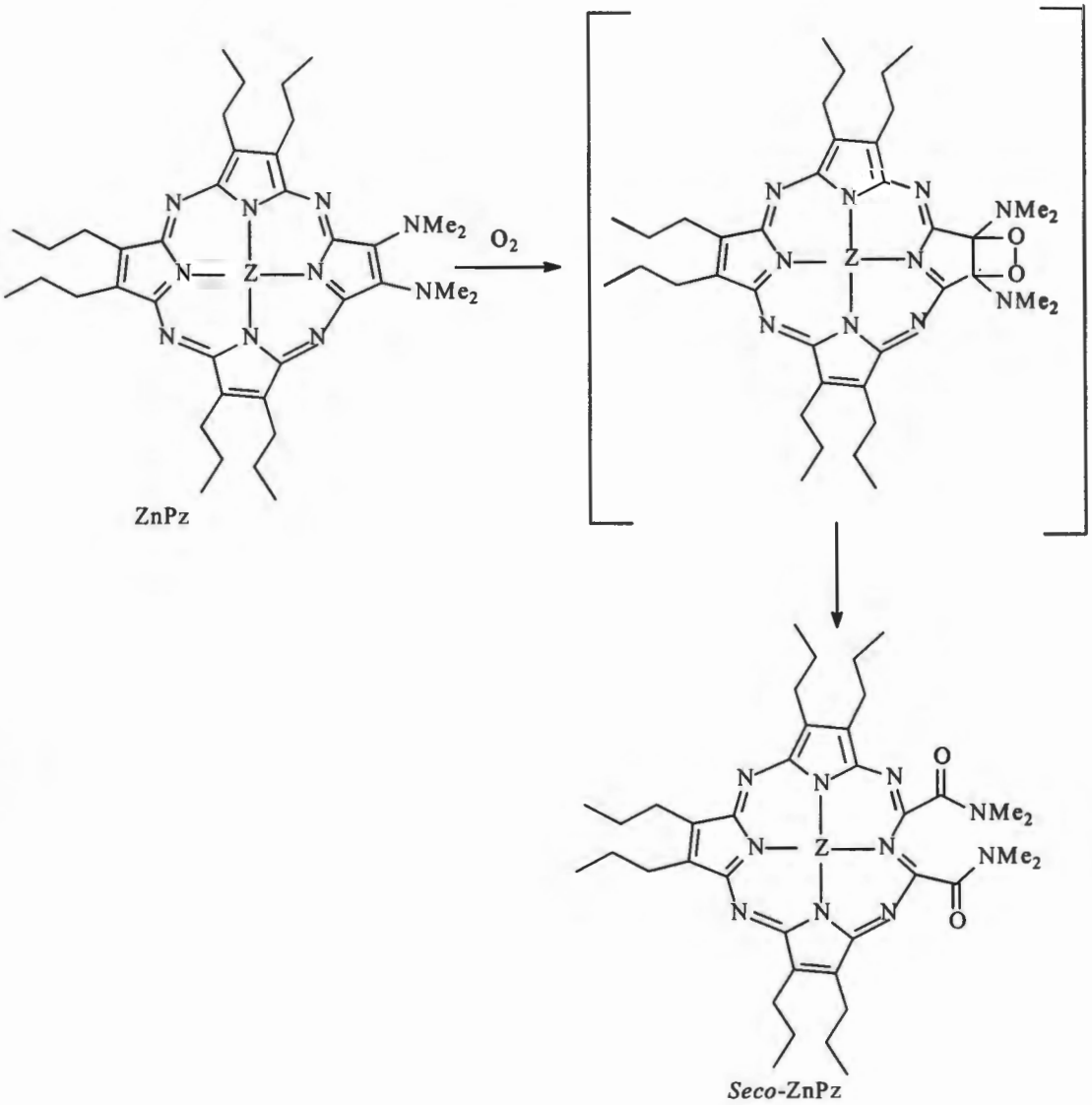

Figure 2.7

2.3.8 Porphyrazinediols

Mixed Linstead macrocyclization of maleonitrile (a) with a 7-fold excess of 2,3-dipropylmaleonitrile (b) in the presence of magnesium butoxide gave porphyrazine (c) in 60% yield. The removal of magnesium ion was cleanly achieved by the reaction with glacial acetic acid, which gave the freebase (d). The cleavage of the ketal unit of metal free porphyrazine (d) was accomplished using aqueous trifluoroacetic acid (95%) at room temperature, giving the expected more stable octaol derivative (e) as in Figure 2.8 [39]

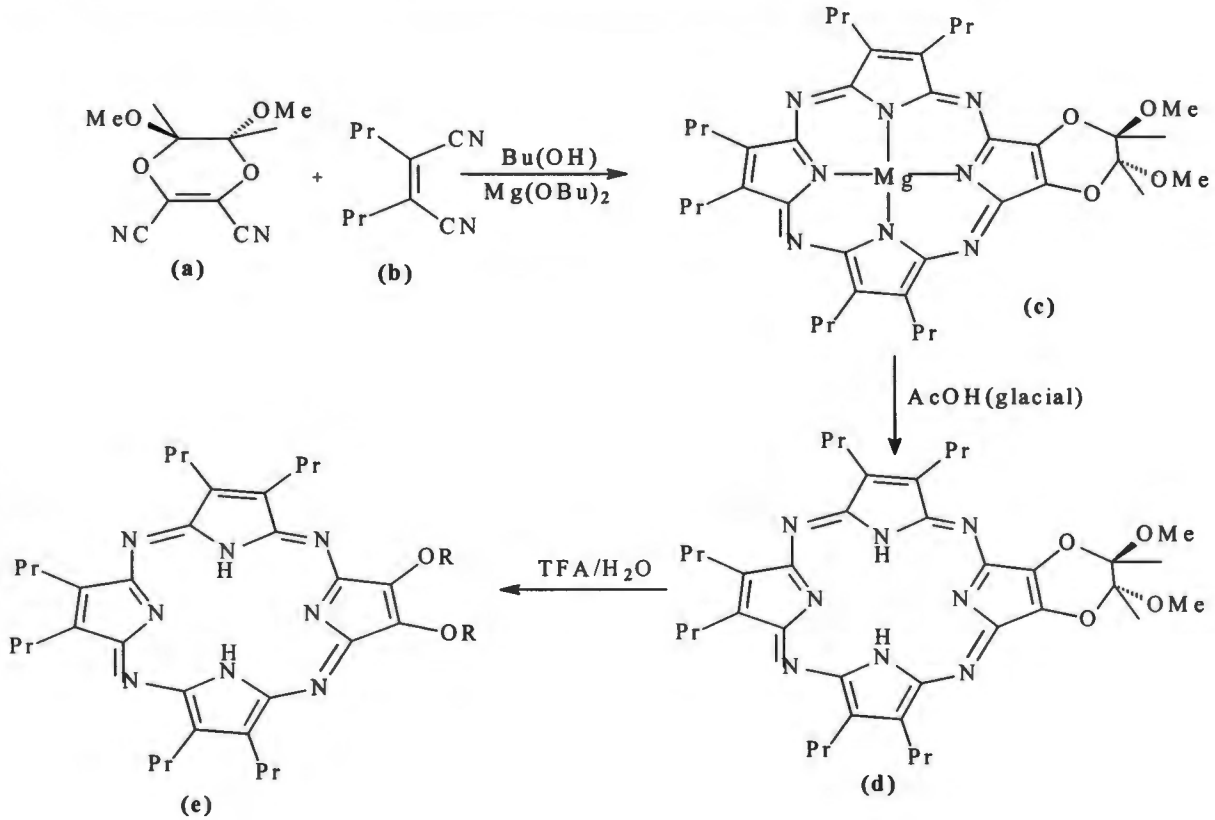

Figure 2.8

2.3.9 Benzo-fused porphyrazine

Mixed Linstead macrocyclisation of benzobis(1,3diiminopyrroline) (a) with an excess of bis(dimethylamino)maleonitrile (b) using magnesium butoxide gave a mixture of porphyrazines that were mostly separated after the demetallation with trifluoro acetic acid, and flash chromatography to give the desired benzo-fused porphyrazine dimer (c) as in Figure 2.9 This compound has showed three distinct N-methyl resonances in the ^{1}H and ^{13}C NMR spectra.[10]

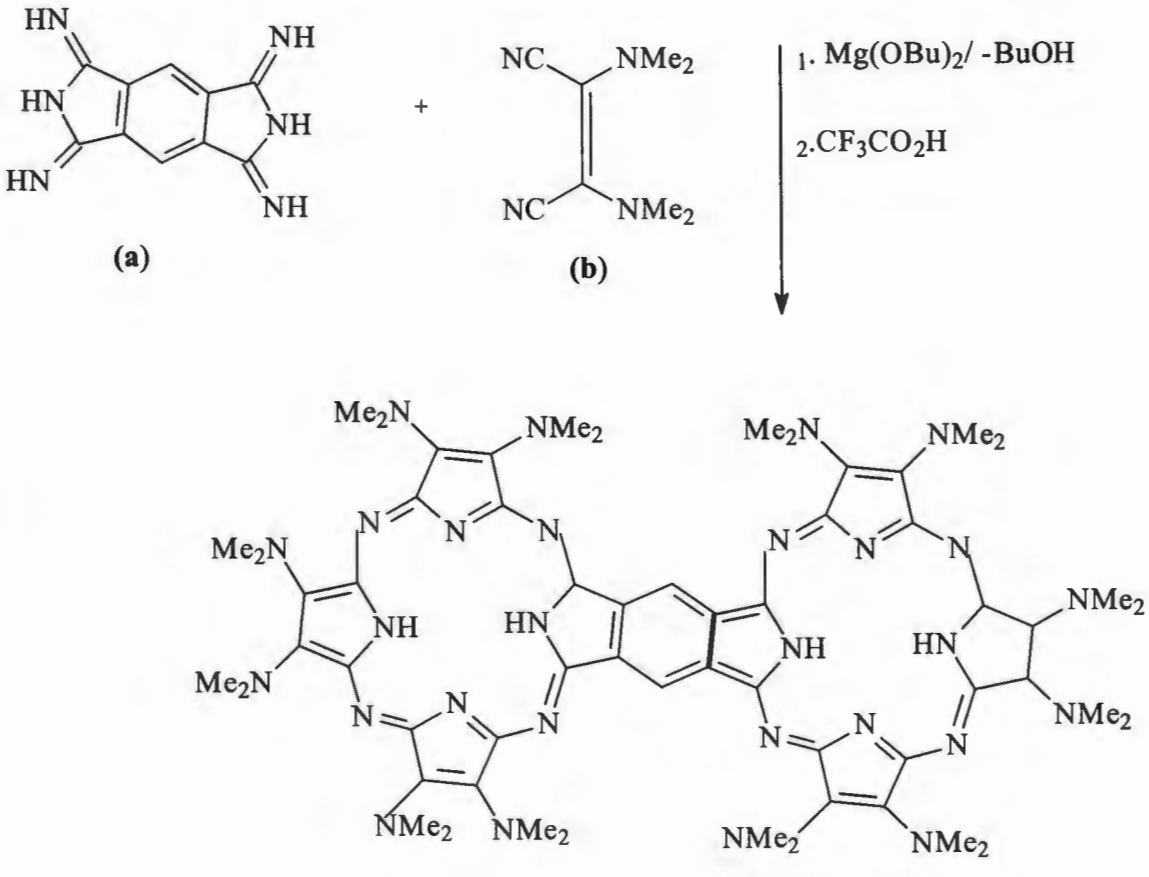

Figure 2.9

2.3.10 Solitaire porphyrazines

Solitaire porphyrazines have been prepared by cocyclization of 1,2 dicyanobenzene (a) and bis(dimethylamino) (b) at a ratio of 1:25, giving a product mixture of compound 1 and 2 as shown in Figure 2.10. They were separated by using column chromatography over silica gel and by ^{1}H NMR.[10]

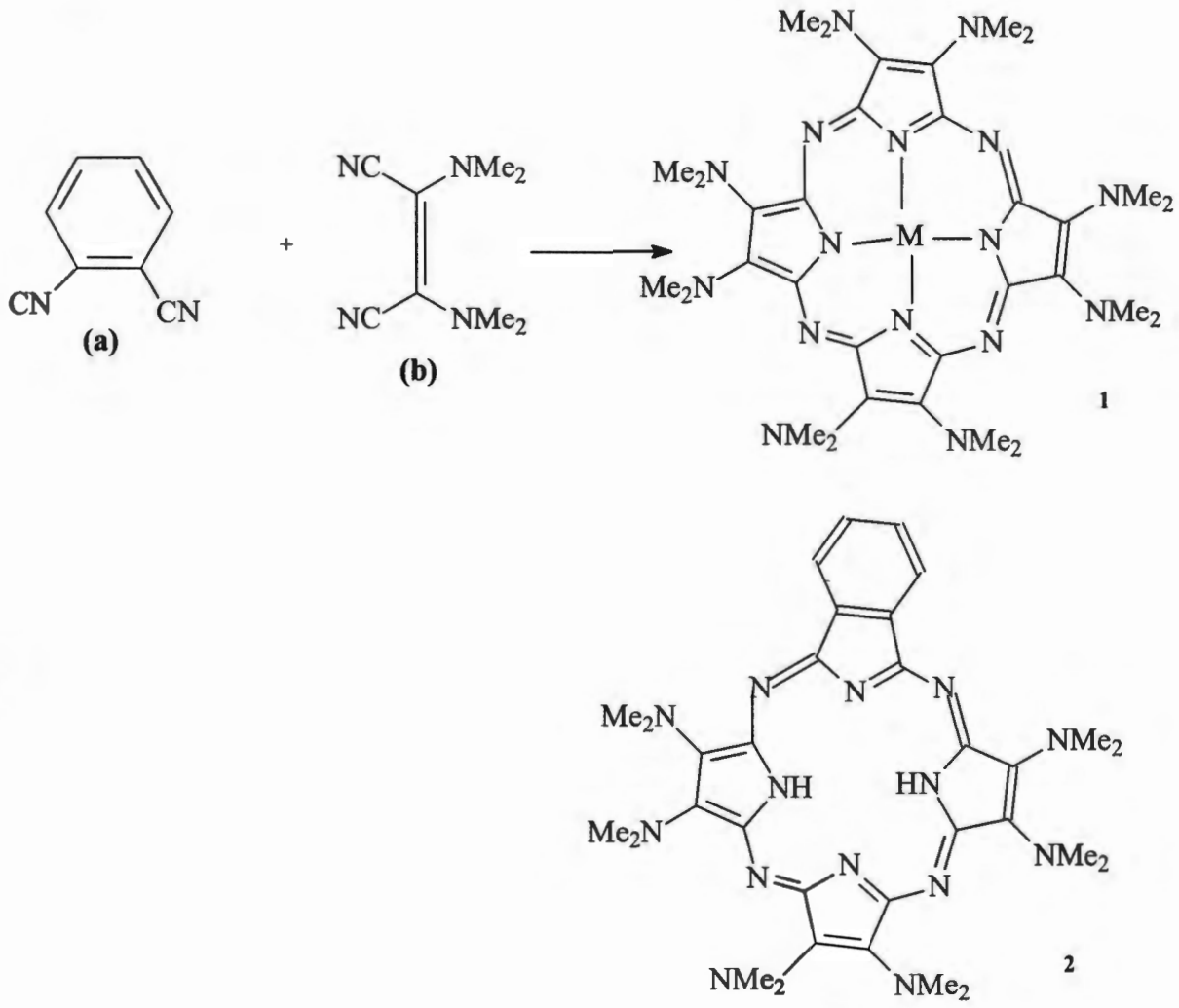

Figure 2.10

2.4 RELATED MACROCYCLES TO PORPHYRAZINES

2.4.1 Phthalocyanines

Phthalocyanine comes from the Greek word "naphtha" (rock oil) and cyanine (dark blue). Phthalocyanines are macrocyclic compounds having alternating nitrogen and carbon atoms. They are large flat, aromatic systems related to naturally occurring porphyrinic compounds. The pyrrole groups in the phthalocyanines are conjugated to benzene rings and bridged by aza nitrogens rather than methane carbons, as shown in Figures 2.11 and 2.12. The ability of the phthalocyanine macrocycle to coordinate several metal ions into its central core, has resulted into the synthesis of a variety of phthalocyanine complexes.[40,41]

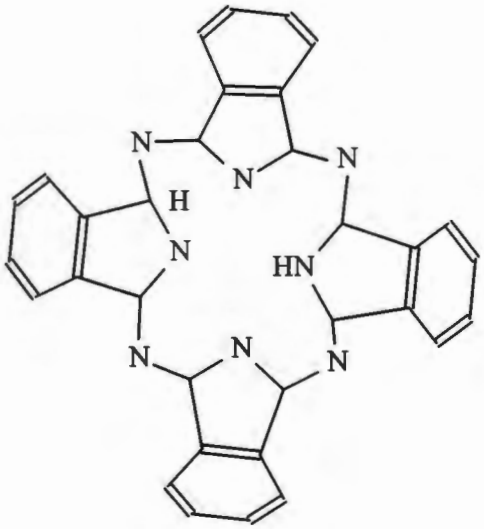

Figure 2.11

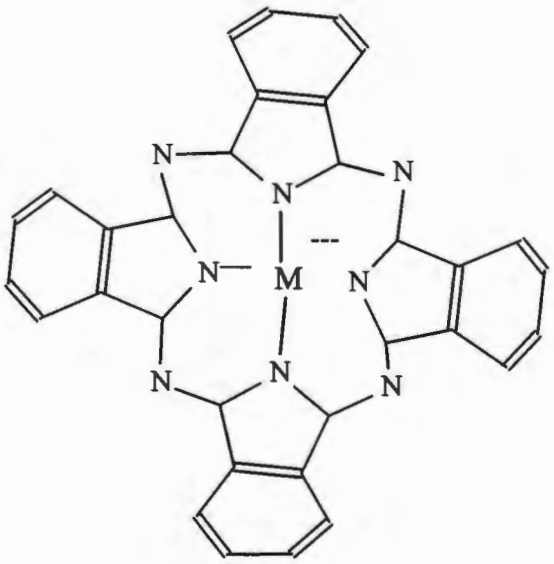

Figure 2.12

2.4.2 Porphyrins

Porphyrins are very interesting and a unique class of terapyrrole compounds. A porphyrin is a heterolytic macrocycle made from three pyrrole subunits and one pyrroline subunit and linked on opposite sides through four methane bridges as shown in Figure 2.13. The macrocycle is therefore more aromatic than the related corrins or chlorins, and this conjugated system makes the compound chromatic, hence the name "porhyrin" which came from the "Greek" word purple.[17,40]

Considerable success has been achieved in both porphyrin synthesis and investigation of their physico-chemical properties.[40,42] The introduction of additional exocyclic rings into natural porphyrins and chlorins as well as their derivatives results in substantial changes in physical, chemical and biological properties of initial compounds. This is unlike natural pigments which retain their five- and seven-membered cycles. The majority of the chemical modification is connected with the formation of six-membered cycles.[20,40]

Interactions of porphyrins with transition metal salt results ultimately in the formation of metalloporphyrins, which are very stable coordination compounds. Porphyrins have definite solubility in non-aqueous solvents and are insoluble in water because of the high stability of their crystal lattices.

Introduction of bulky substituents that loosen the crystal lattice can increase porphyrin solubility in non-aqueous media.[41,43]

Some iron containing porphyrins are called heme, and heme-containing proteins or hemoproteins such as haemoglobin are found extensively in biochemistry. If one of the three pyrrole subunits is reduced to pyrroline a chlorin is produced, which has a ring structure similar to the one found in chlorophyll.[40]

Porphyrins can be considered as amphoteric compounds having both acidic (N-H acids) and basic (N-base) properties. Nitrogen atoms of imine type (-N=) are able to accept surplus protons, whereas pyrrole type nitrogen atoms (N-H) simply donate protons.[42]

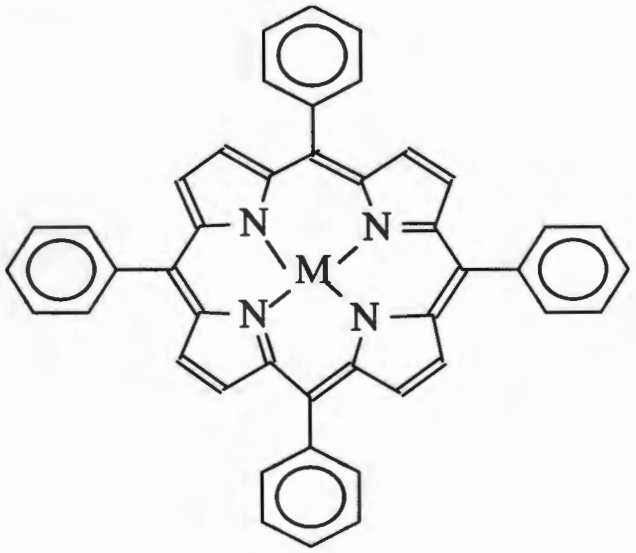

Figure 2.13 Substituted porphyrin

2.5 USES OF PORPHYRAZINES AND RELATED COMPOUNDS

2.5.1 Uses of Porphyrazines

Peripherally functionalised tetraazaporphyrazines are used for the development of porphyrinic macrocycles, which are used in areas such as catalysis, photodynamic therapy, chemical sensors, non-linear optics, fabrication of molecular electronic or magnetic devices that are precursors to new conducting materials.[15,16]

Porphyrazine metal(II) complexes are potential photosynthesizers due to their effective absorbance in the blue region of the visible spectrum. Star porphyrazines are used as novel magnetic, optical, imaging materials and as therapeutic agents in the photodynamic therapy (PDT).[8,9,17] The *trans*-porphyrazines have a split Q band and due to this it absorbs at long wavelength. As light, at this wavelength, can effectively penetrate mammalian tissue, they are used as potential biomedical agents.[8]

2.5.2 Uses of porphyrins

Large aromatic systems such as phthalocyanines and porphyrins are of substantial interest for the development of electro-optical devices, ion complexation and biological redox reactions.[20,43,44,45] Among the large number of synthetic porphyrin derivatives, water soluble ones are of

particular interest. They are used in industry, medicine and biology as drugs, catalysts, inhibitors and sensitizers for different reactions. The distribution of porphyrin in the human body, transport and accumulation in tissues as well as the pathways and yields of energy deactivation depend on the micro environmental properties such as hydrophobicity, ionic strength and others.[17] Polymer-connected porphyrins, such as important natural complexes as the haemoglobin found in blood and the cytochromes, represent a vast and unique group of inter-complex compounds that perform major biological, photochemical and fermentative functions in nature.[40,41]

The incorporation of metalloporphyrin molecules in a polymer matrix causes improvements of the main properties of polymers and appearance of new properties. Polymer-connected porphyrins are unique bipolar models that provide many opportunities for construction of effective catalysts for redox processes and a new generation of photosensitizers.[42]

2.5.3 Uses of phthalocyanines

Phthalocyanines are macrocyclic compounds that are highly important commercial commodities. The annual output of about 45 000 is largely used as industrial blue-green colourants. Phthalocyanines have important optoelectronic, photophysical conducting and photoconducting properties.

These properties have attracted many groups worldwide who use them as functional materials for the emerging technologies associated with molecular electronics.[41]

Pthalocyanines and other related compounds containing nitrogen have been successfully used as active components of ion selective electrodes.[20]

Phthalocyanato metal complexes are effective second generation photosensitizers for photodynamic therapy (PDT) with platinum based complexes, as the most popular antitumor drugs.[20] Photogem was the first domestically produced photosynthesizer for photodynamic therapy of cancer. It was obtained using original methodology based on natural hematoporphyrin. Research showed that this drug had good therapeutic effects and low-side phototoxicity.[20,40,42]

Bis(phthalocyaninato)-lutetium(III), a sandwich-type complex, was the first intrinsic semiconductor in thin films and one of the most promising electrochromic display materials. These characteristic features result from of strong π-π interactions due to close proximity by which two macrocycles are held together through the metal ion.[25]

2.6 KINETIC AND MECHANISTIC STUDIES

Metal complex formation reactions or ligand substitution reactions with simple ligands generally occur very rapidly in aqueous solution. Macrocyclic ligands form highly selective and kinetically labile complexes with a wide range of cations, including alkali metals and alkaline earth metal cations. Complexation reactions of simple monodentate ligands have formation rate constants that are high and remarkably insensitive to ligand structures. These formation rate constants tend to decrease with an increasing charge density of the cation. The dissociation rate constants directly reflect the changes in complex stabilities within a related series of cations and over a wide range of ligand structures and solvents.[44]

The wide range of complexation and decomplexation rates occurring across the range of macrocycles and cations has prompted the use of a large number of different kinetic techniques. The most common techniques are stopped-flow and chemical relaxation methods. NMR methods, however, are becoming increasingly popular and are used for kinetic studies involving a variety of nuclei including ^{1}H, ^{7}Li, ^{13}C, ^{23}Na. Stationary methods, particularly ultrasonic absorption, which allow measurement of relaxation times as low as few nanoseconds, have been particularly valuable for

studying rapid conformational changes in ligands and crown ether complexation reactions.[44]

CHAPTER THREE

EXPERIMENTAL

3.1 REAGENTS

3.1.1 All reagents used were obtained from UnivAR, Saarchem, Merck Chemicals (Pty) Ltd, and solvents were distilled prior to use: dichloromethane:calcium hydride (CaH_2); dimethylformamide (pre-dried from barium oxide) distilled in alumina; tetrahydrofuran (THF) in sodium benzophenone ketyl; butanol and methanol (in magnesium).

3.1.2 Chromatography

TLC was carried out on E. Merck precoated silica gel 60 F_{254} plates. Flash chromatography was on E. Merck silica gel 60, 40-60 μm.

3.1.3 Other reagents

All other reagents were used as commercially supplied.

3.2 SYNTHESIS OF COMPOUNDS

3.2.1 Octakis(propyl)porphyrazinemagnesium(II) complex

Figure 3.1 summarises the overall reaction for the preparation of octakis(propyl)porphyrazinemagnesium(II) complex. Treatment of terminal alkyne **1** with one equivalent of bromine in the presence of bromide ion, produced *trans*-dibromoalkene **2**. The vinylic dibromide was converted to fumaronitrile **3**, via the Rosenmund-von Braun reaction, which was further

photoisomerised to the corresponding maleonitrile **4**, using a modified form of the procedure of Turro[1]. Mixed Linstead macrocyclisation of maleonitrile **4**, in the presence of magnesium butoxide gave the desired porphyrazine **5**.

3.2.2 4,5-dibromo-4E-octene(2)

A solution of bromine (46.6 ml, 0.91 mol) in acetic acid (250 ml) was added dropwise to 4-octyne dissolved in an equal amount of acetic acid (250 ml) at such a rate as not to develop an orange colour in the flask. After the addition was complete, the solution was stirred for an additional 30 minutes and then poured into ice water (2 l). A yellow oil separated under the aqueous layer and was collected. This was followed by extraction with dichloromethane (300 ml x 4) and the dichloromethane extract was washed with sodium hydrogen carbonate (300 ml x 3) followed by water (300 ml x 3). The extract was then dried with magnesium sulphate (anhydrous) and filtered. The solvent was removed by rotary evaporation to yield a yellow crude oil (220 g, 90%), which was used without further purification.

3.2.3 Fumaronitrile (3)

A suspension of copper cyanide (23.664 g, 0.268 mol) in a dry anhydrous DMF (250 ml) was heated to 145°C for approximately one hour, or until the

solution turned clear with some white solids adhered to the sides of the flask. The solution was cooled to 130°C, and 4,5-dibromo-4E-octene (23.120 g, 0.088 mol) was added all at once. The solution turned dark brown, and heating with stirring was continued for at least 12 hours but not longer than 18 hours. After this time the solution was allowed to cool to room temperature and carefully poured into concentrated ammonium hydroxide (600 ml). The resulting solution was stirred for approximately 30 minutes, and washed several times with diethyl ether in a separating funnel. The ether portions were combined and washed once with water (3 x 200 ml) and once with a saturated aqueous solution of sodium chloride (2 x 200 ml). The organic layer was dried with anhydrous magnesium sulphate. The resulting brown oil was purified by vacuum distillation to give clear oil (5.240 g, 40%).

3.2.4 Maleonitrile (4)

The fumaronitrile (6.335 g, 0.043 mol) was dissolved in acetonitrile (1 l) in a quartz round-bottom flask and sealed with a septum. Nitrogen was bubbled through the solution for a minimum of 20 minutes before the flask was placed in a Rayonet photochemical reactor fitted with magnetic stirrer. The solution was irradiated with light (λ_{max} = 253nm) for 30 hours, during that

time the reaction temperature rose to approximately 40°C from the heat given off by the reactor lamps. After approximately 30 hours the reaction reached a photostationary state and was stopped. The solvent was removed by rotary evaporation, and the *cis*- and *trans*-isomers were separated by fractional distillation under high vacuum. The *trans*-isomer distilled first, at about 40°C lower than the desired *cis*-isomer. The yield was (2.2 g, 34 %).

3.2.5 Octakis(propyl)porphyrazinemagnesium(II) complex (5)

Iodine (2.61 g, 10 mmol) was added to a suspension of magnesium (0.50 g, 20 mmol) in dry butanol (25ml). This mixture was heated overnight at reflux under nitrogen until all the magnesium metal has been consumed. The resulting solution was allowed to cool at room temperature and diethyl-maleonitrile (2.75 g, 20 mmol) was added and the mixture was heated again under reflux for 18 hours. The solution was allowed to cool and the resulting mass was dissolved in ethanol (200 ml). The solution was poured into water (800 ml) resulting in the precipitation of crude octakis(propyl) porphyrazinemagnesium(II) complex. Octakis(propyl)porphyrazine magnesium(II) complex was separated from the soluble tar by soxhlet extraction in chloroform (250 ml). The solvent was removed and the resulting residue was collected by chromatography with (TLC; 10 x 4 cm)

using a mixture of dichloromethane and diethyl ether (10:1) as eluent, yielding (0.58 g, 21%) octakis(propyl)porphyrazinemagnesium(II) complex. The overall synthesis is shown in Figure 3.1.

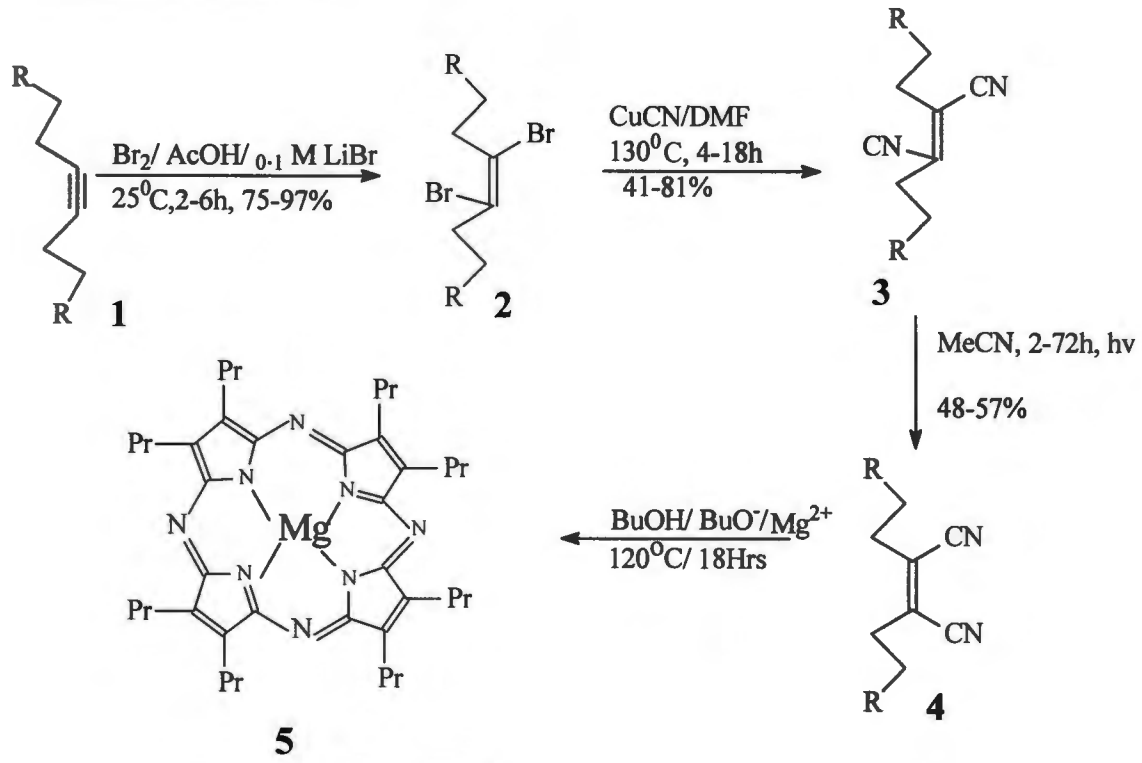

Figure 3.1

3.3 Demetallation of octakis(propyl)porphyrazinemagnesium(II) complex

Magnesium(II)porphyrazine (0.88 g, 31%) was demetallated under reflux at 25°C in trifluoroacetic (30-50 ml) acid for one-hour using inert conditions, as shown in Figure 3.2. The solution was cooled and poured into 200 ml water, and made basic by adding sodium hydroxide (NaOH). The organic layer was separated, washed once with 10% sodium hydroxide (50 ml)

solution and dried with sodium sulphate (Na_2SO_4) and then filtered. The freebase ligand was adsorbed onto silica gel by suspending TLC grade silica gel (30.0 g) in the filtrate, and coated silica gel was loaded onto a column and eluted with a solution of dichloromethane in hexane with a 1:1 ratio. Slow evaporation of the solvent gave a microcrystalline solid, which was recrystallized by slow diffusion of benzene into a chloroform solution of the tetraazaporphyrazine, yielding (0.55 g, 20%) product.

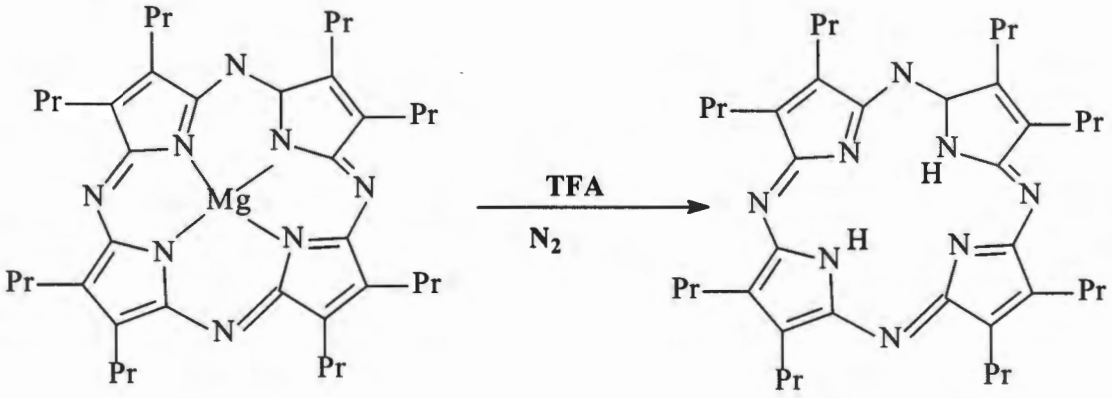

Figure 3.2

3.4 Synthesis of 2,3,9,10,16,17,23,24octa-substituted phthalocyanine

The synthesis of 2,3,9,10,16,17,23,24octa-substituted phthalocyanine was done as shown in Figure 3.3. A solution of 4-nitrophthalonitrile **(14)** was reacted with phenol **(15)**, in the presence of tetrahydrofuran, at lower temperatures to form 1,2-diisocyano-4-phenoxybenzene **(16)**. Compound **16** was further reacted with 1.8 diazabicyclo[5.4.0]-undec-7-ene, in the

presence of methanol, to give 2,3,9,10,16,17,23,24octa-substituted phthalocyanine **(17).**

3.4.1 1,2-diisocyano-4-phenoxybenzene

A solution of phenol **(15)** (0.353 g, 0.0375 mol) in THF was mixed with sodium hydride (0.15 g), and 4-nitrophthalonitrile **(14)** (0.50 g, 0.0028 mol) in THF was added to the solution and the reaction was allowed to run for 8 hours as in Figure 3.3. The resulting 1,2-diisocyano-4-phenoxybenzene (16) was filtered and the solid washed with ethyl acetate and both the filtrate and the washings were mixed and evaporated under reduced pressure. The resulting white precipitate was purified by flash column chromatography using ethyl acetate:hexane as a solvent in the ratio 1:4

Yield = (0.737 g, 40%) R_f = 0.36 (ethyl acetate: hexane, 1:4)

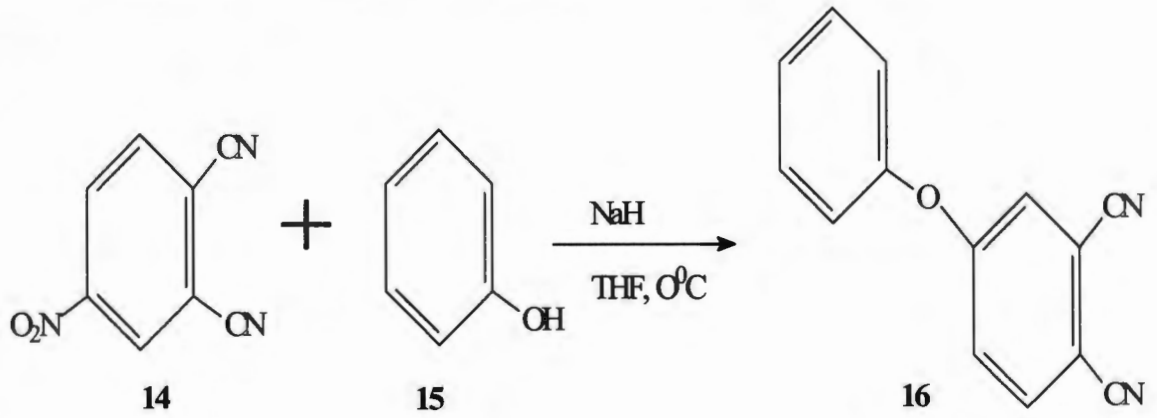

14 **15** **16**

Figure 3.3

3.4.2 2,3,9,10,16,17,23,24octa-substituted phthalocyanine

1,2-diisocyano-4-phenoxybenzene **(16)** (0.300 g, 1.36 x 10^{-3} mol) was refluxed in 1-pentanol (14 ml) in the presence of 1 mol 1,8-diazabicyclo[5.4.0]-undec-7-ene (0.21 g, 1.36 x 10^{-3} mol) for 16 hours. Methanol (20 ml) was added and the precipitate filtered off, soxhlet extracted with methanol and acetone and dried at 60^0C, resulting in 2,3,9,10,16,17,23,24octa-substituted phthalocyanine **(17)** as shown in Figure 3.4. Yield = 0.294 g, 98% R_f = 0.23

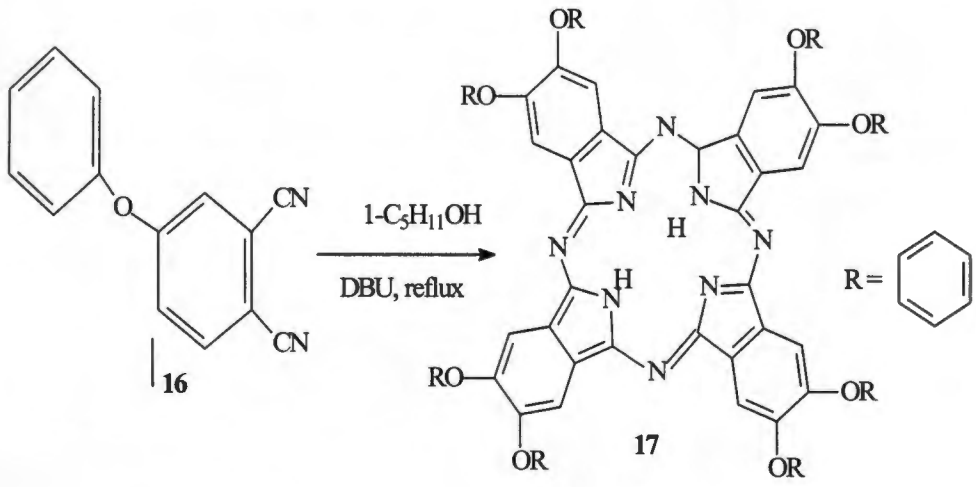

Figure 3.4

3.5 Insertion of metal ions into the octakis(propyl)porhpyrazine ligand

3.5.1 Chromium(III) insertion

Chromium(III) chloride (2.7 g, 0.01 mol) was dissolved in ethanol to make a concentration 0.1 M in a 100 ml volumetric flask. The chromium(III) ion solution was mixed with the freebase ligand (1.14 x 10^{-5} M in

dichloromethane) until a uniform solution was attained. This mixture was heated for 30 minutes to make sure that all the chromium is consumed under nitrogen controlled conditions. The solvent was removed by a rotary evaporator at a controlled temperature of 110°C. A dark green residue was collected and washed with chloroform (250 ml). The solvent was removed by a rotary evaporator giving a dark green oil, with a (1.53 g, 56%) yield.

3.5.2 Cobalt(II) insertion

Cobalt(II) nitrate (2.9 g, 0.01 mol) was dissolved in ethanol to make a 0.1 M solution in a 100 ml volumetric flask. The cobalt(II) solution was mixed with the freebase ligand (1.14×10^{-5} M in dichloromethane) until a uniform solution was attained. The mixture was heated for 60 minutes to make sure that all the cobalt was consumed under nitrogen controlled conditions. The solvent was removed by rotary evaporation at a controlled temperature of 110°C. The compound was used without further purification.

3.6 CHARACTERISATION OF COMPOUNDS

3.6.1 ^{1}H and ^{13}C NMR spectra

The proton and ^{13}C NMR spectra of the compounds were recorded on a Varian-Gemini-300 (300 MHz) spectrometer. The spectra are shown in

Figures 4.1.1 to 4.1.10, while Table 4.1.1a to Table 4.1.5a summarise the ^{1}H and ^{13}C NMR spectra of the compounds.

3.6.2 Ultraviolet-visible spectra

Ultraviolet-visible electronic absorption spectra of freshly prepared solutions of the compounds in appropriate solvents were measured in 1 cm quartz cell using a Varian Cary 50 Conc. ultraviolet-visible spectrophotometer in the range of 300-800 nm (λ_{max}). The relevant spectra of the compounds are shown in Figures 4.2.1 to 4.2.8

3.6.3 Infrared spectra

The infrared spectrum of nujol mulls of all compounds between sodium chloride windows were measured with an FTIR Impact 410 spectrometer in the range between 500 cm^{-1} and 4000 cm^{-1}. The relevant spectra are collected in Figures 4.3.1 and 4.3.2

3.7 PROCEDURE FOR KINETIC STUDIES

3.7.1 Insertion of chromium(III) into octakis(propyl)porphyrazine ligand

A spectrophotometric procedure was used for following the kinetics of metallation of octakis(propyl)porphyrazine ligand. A chromium(III) chloride

(1.00×10^{-1} M) solution in ethanol was added to the freebase porphyrazine ligand solution (1.13×10^{-5} M) until a uniform solution was attained. The ultraviolet-visible spectrum of the resulting solution was then scanned at 10 minutes intervals at 15°C. A set of isosbestic points that were maintained throughout the entire reaction indicated the possibility of a simple reaction. The procedure was repeated for various temperature ranges from 17-35°C. The spectral change is indicated in Figure 4.4.1.1

3.7.2 Direct insertion of chromium(III) into octakis(propyl) porphyrazinemagnesium(II) complex

Octakis(propyl)porphyrazinemagnesium(II) complex (1.43×10^{-5} M) in dichloromethane was added to a chromium(III) (1.00×10^{-1} M) in ethanol. A spectrophotometric procedure was used for following the kinetics of insertion of chromium(III) into the octakis(propyl)porphyrazine magnesium(II) complex. A set of isosbestic points were maintained throughout the entire reaction at various temperature ranges. The relevant spectral change is indicated in Figure 4.4.1.2

3.7.3 Insertion of Cr(III) ion into 2,3,9,10,16,17,23,24octa-substituted phthalocyanine

2,3,9,10,16,17,23,24octa-substituted phthalocyanine ($1.43x10^{-5}$ M) complex in chloroform was added to a chromium(III) ($1.00x10^{-1}$ M) solution dissolved in ethanol. A spectrophotometric procedure was used for following the kinetics of insertion of chromium(III) into the 2,3,9,10,16,17,23,24octa-substituted phthalocyanine. A set of isosbestic points that were maintained throughout the entire indicated a simple reaction. These were followed at various temperature ranges from 15-35°C. The relevant spectral changes are indicated in Figure 4.4.1.3

3.7.4 Reduction of octakis(propyl)porphyrazinechromium(III) complex with octakis(propyl)porphyrazinecobalt(II) complex

A freshly prepared solution of chromium(III)porphyrazine(0.1M) in ethanol was mixed with a solution of cobalt(II)porphyrazine(0.01M) in ethanol at the various ratios, at different time intervals. The reaction was then followed spectrophotometrically by observing the change in absorption spectra over the range of 300-800nm, at various temperature ranges. The relevant spectral changes are indicated in Figure 4.4.2

3.8 COMPUTATION OF RATE CONSTANTS

The observed rate constants were obtained from plots of ln $(A-A_\infty)$ versus time (min), where

A is the absorbance at time t

A_∞ is the absorbance at time infinity.

The activation energy (E) was obtained from the Arrhenius equation,

$K = Ae^{-E/RT}$

where k is the rate constant

A is the pre-exponential factor

E is the activation energy

R is the gas constant

T is the temperature in kelvin

The plot of ln k versus 1/T was used to determine the activation energy of the reaction, using the Arrhenius equation $k = Ae^{-E/RT}$, whereby the slope E/R was obtained from the graph.

3.8.1 Insertion of Cr(III) into octakis(propyl)porphyrazine ligand

The data for ln $(A-A_\infty)$ versus time (min) are compiled in Tables 4.5.1 to 4.5.6. while the plots of ln $(A-A_\infty)$ versus time (min) are plotted in Figures 4.5.1 to 4.5.6.

3.8.2 Direct insertion of Cr(III) into octakis(propyl)magnesium(II) complex

The data of ln ($A-A_\infty$) versus time (min) are compiled in Tables 4.5.7 to 4.5.12 while plots of ln ($A-A_\infty$) versus time (min) are plotted in Figures 4.5.7 to 4.5.12.

3.8.3 Insertion of Cr(III) into 2,3,9,10,16,17,23,24octa-substituted phthalocyanine

The data of ln ($A-A_\infty$) versus time (min) are compiled in Tables 4.5.13 to 4.5.18 while plots of ln ($A-A_\infty$) versus time (min) are plotted in Figures 4.5.13 to 4.5.18.

3.8.4 Reduction of octakis(propyl)porphyrazinechromium(III) complex with octakis(propyl)porphyrazinecobalt(II) complex

The data of ln ($A-A_\infty$) versus time (min) are compiled in Tables 4.5.19 to 4.5.24 while plots of ln ($A-A_\infty$) versus time (min) are plotted in Figures 4.5.19 to 4.5.24.

3.8.5 Calculation of the activation energy

The individual rates constants for each reaction are summarised in Tables 4.6.1 to 4.6.4 while the plots of ln k versus 1/T for each reaction are shown on Figures 4.6.1 to 4.6.4, which were used to determine the activation energy.

CHAPTER FOUR

RESULTS

4. Characterisation of Compounds

4.1 ^{1}H and ^{13}C NMR Spectrum

Tables 4.1.1a to 4.1.5a summarises the ^{1}H and ^{13}C NMR shifts of the compounds, while their spectra are shown in Figures 4.1.1 to 4.1.10

4.1.1 ^{1}H and ^{13}C spectra of 4,5-dibromo-4E-octene

4,5-dibromo-4E-octene	^{1}H NMR (δ)	^{13}C NMR (δ) $CDCl_3$
	0.973 (t, 4H)	13.09, 21.24, 35.67
	1.64 (m, 4H)	115.35, 129.101
	2.52 (t, 6H)	

Table 4.1.1a summarises the proton and carbon shifts of 4,5-dibromo-4E-octene

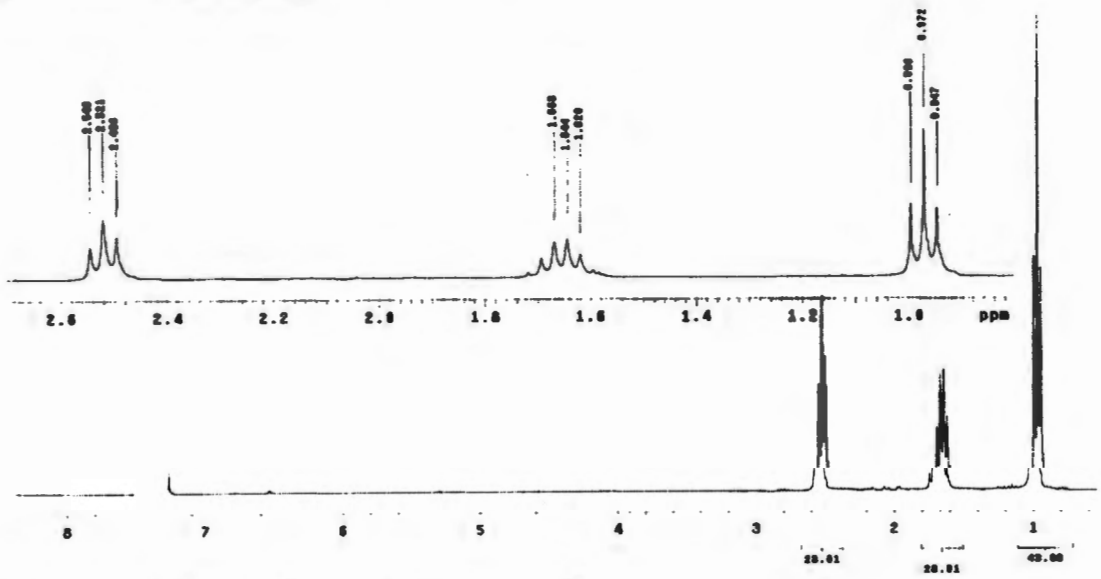

Figure 4.1.1 ^{1}H NMR of 4,5-dibromo-4E-octene

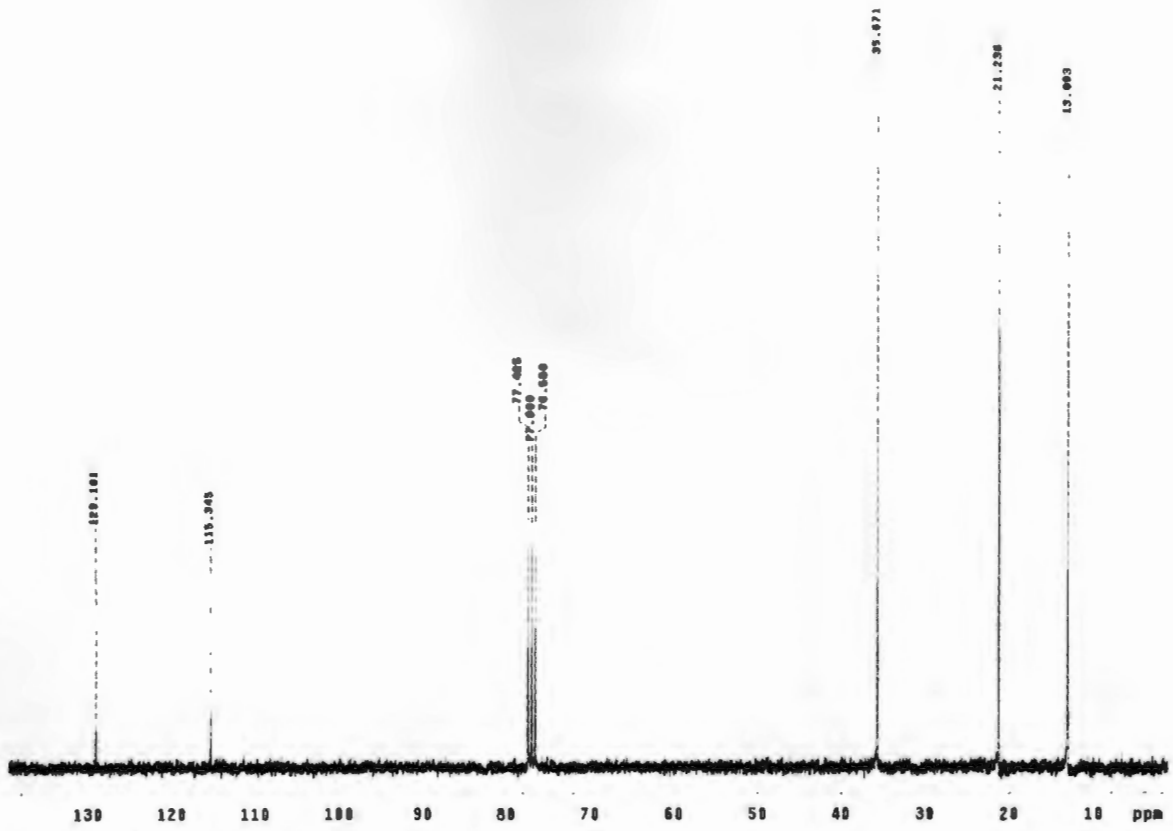

Figure 4.1.2 ^{13}C of 4,5-dibromo-4E-octene

4.1.2 ^{1}H and ^{13}C spectra of fumaronitrile

Fumaronitrile	^{1}H NMR (δ)	^{13}C NMR (δ) $CDCl_3$
	0.89 (t, 4H)	12.59, 20.77, 35.19
	1.58 (m, 4H)	114.94, 128.70
	2.437 (t, 6H)	

Table 4.1.2a summarises the proton and carbon shifts of fumaronitrile

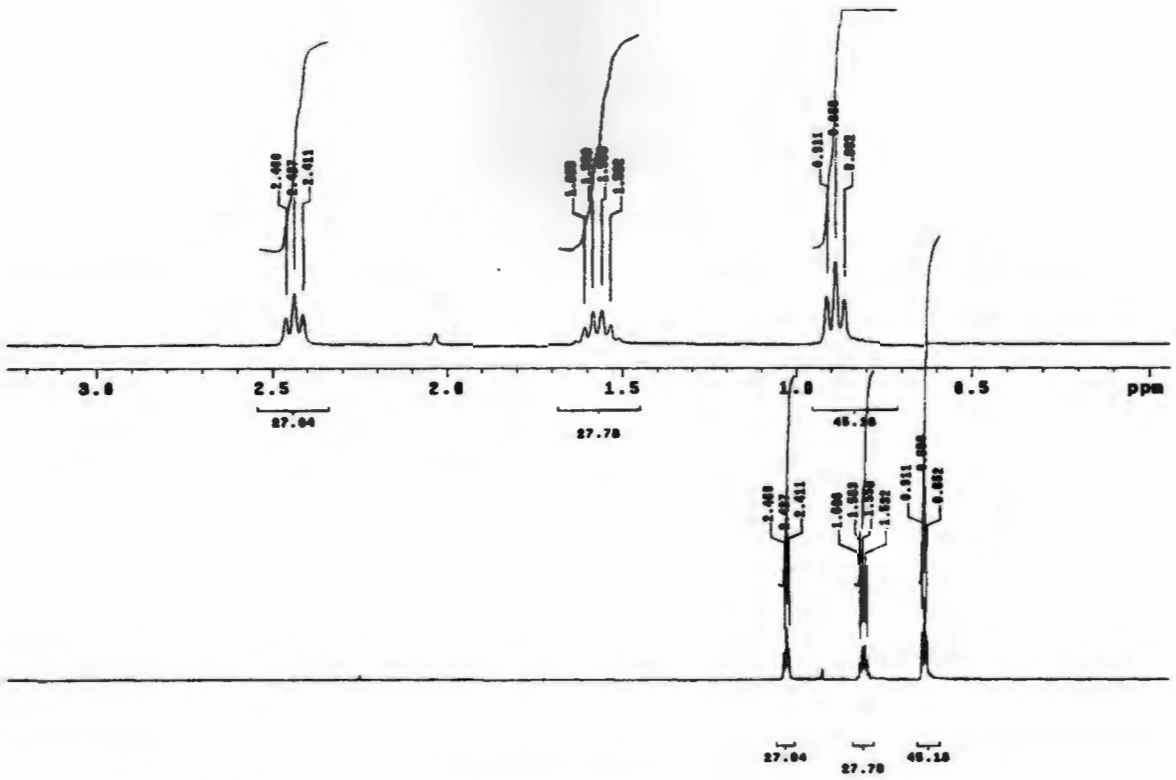

Figure 4.1.3 ^{1}H NMR of *trans*-CN octene (fumaronitrile)

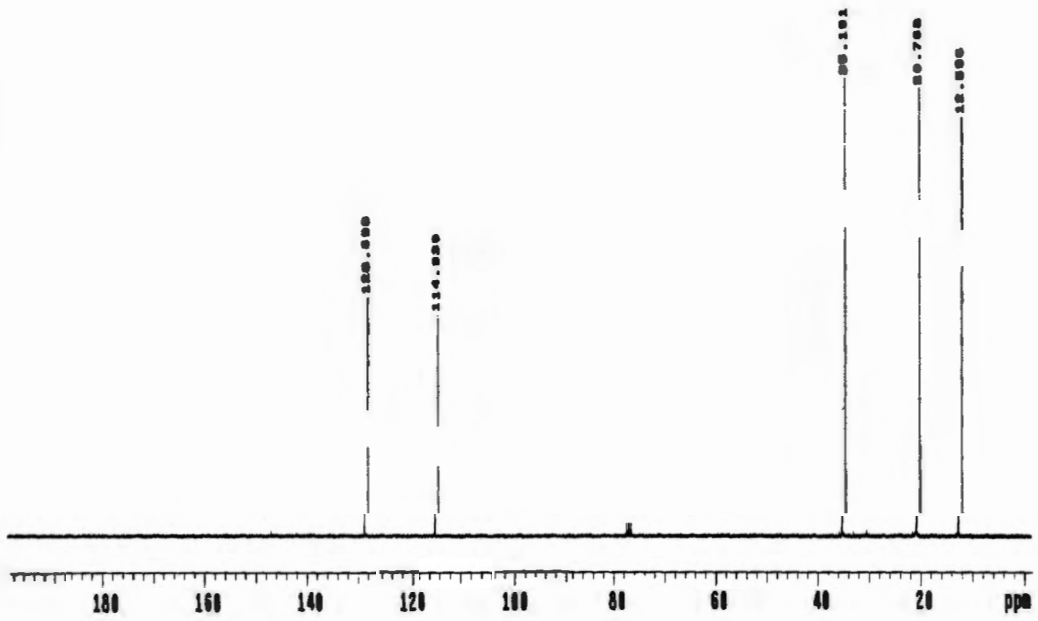

Figure 4.1.4 ^{13}C NMR of *trans*-CN octene (fumaronitrile)

4.1.3 ^{1}H and ^{13}C spectra of maleonitrile

Maleonitrile	^{1}H NMR (δ)	^{13}C NMR (δ) $CDCl_3$
	1.65 (t, 4H)	12.97, 20.73, 31.76
	2.32 (m, 4H)	116.02, 128,88
	3.03 (t, 6H)	

Table 4.1.3a summarises the proton and carbon shifts of maleonitrile

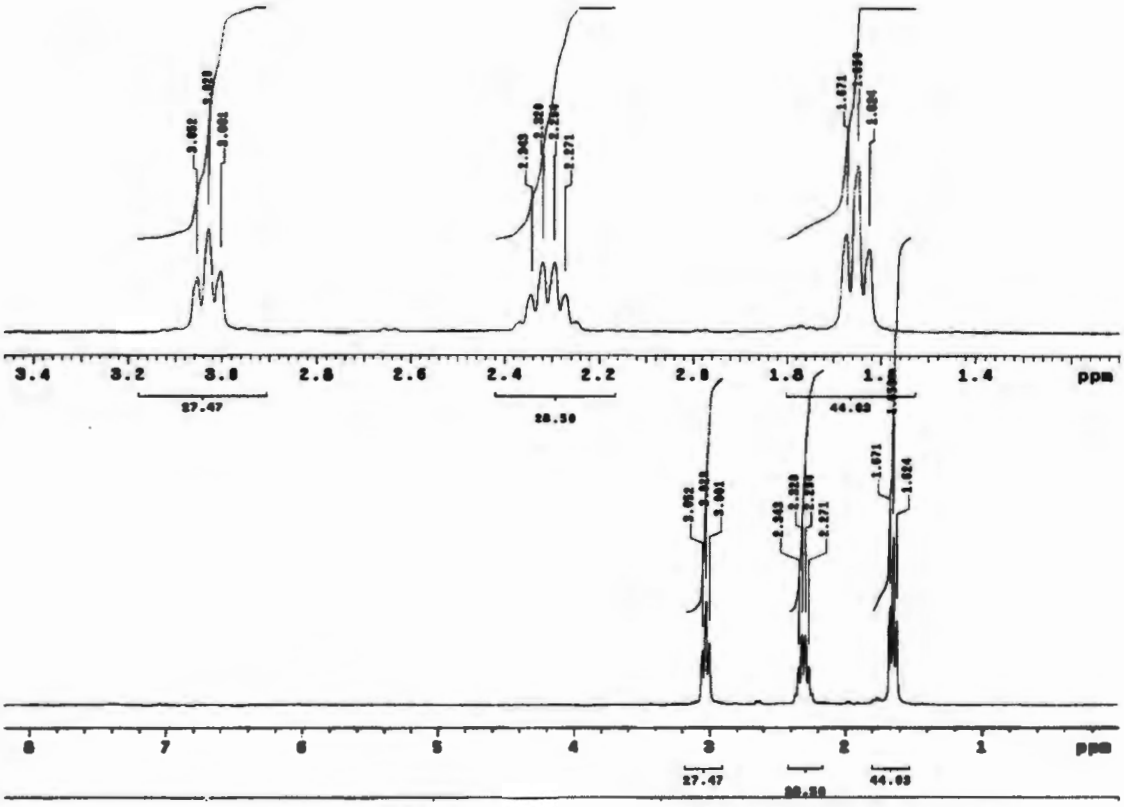

Figure 4.1.5 ^{1}H NMR *cis*- CN (maleonitrile)

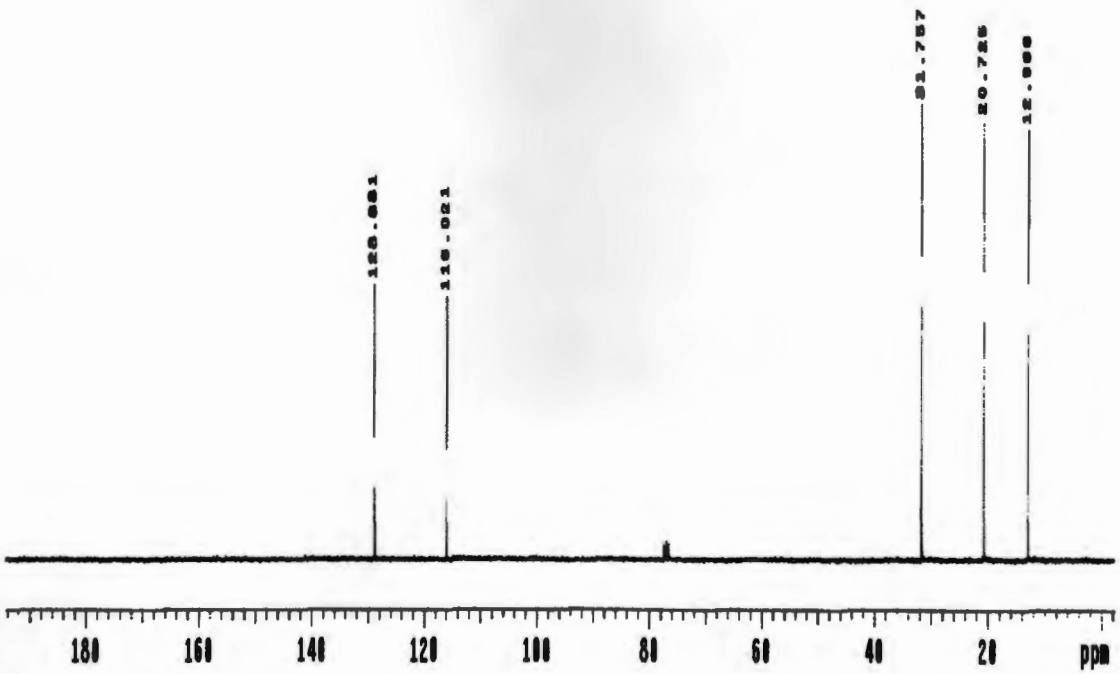

Figure 4.1.6 ^{13}C NMR *cis*-CN (maleonitrile)

4.1.4 ^{1}H and ^{13}C NMR spectra of 1,2 diisocyano-4-phenoxybenzene

1,2 diisocyano-4 -phenoxybenzene	^{1}H NMR (δ)	^{13}C NMR (δ) $CDCl_3$
	7.058	71.017
	7.085	76.996
	7.152	117.459
	7.224	119.698
	7.509	128.941
	7.539	135.201

Table 4.1.4a summarises the proton and carbon shifts of 1,2 diisocyano-4-phenoxybenzene.

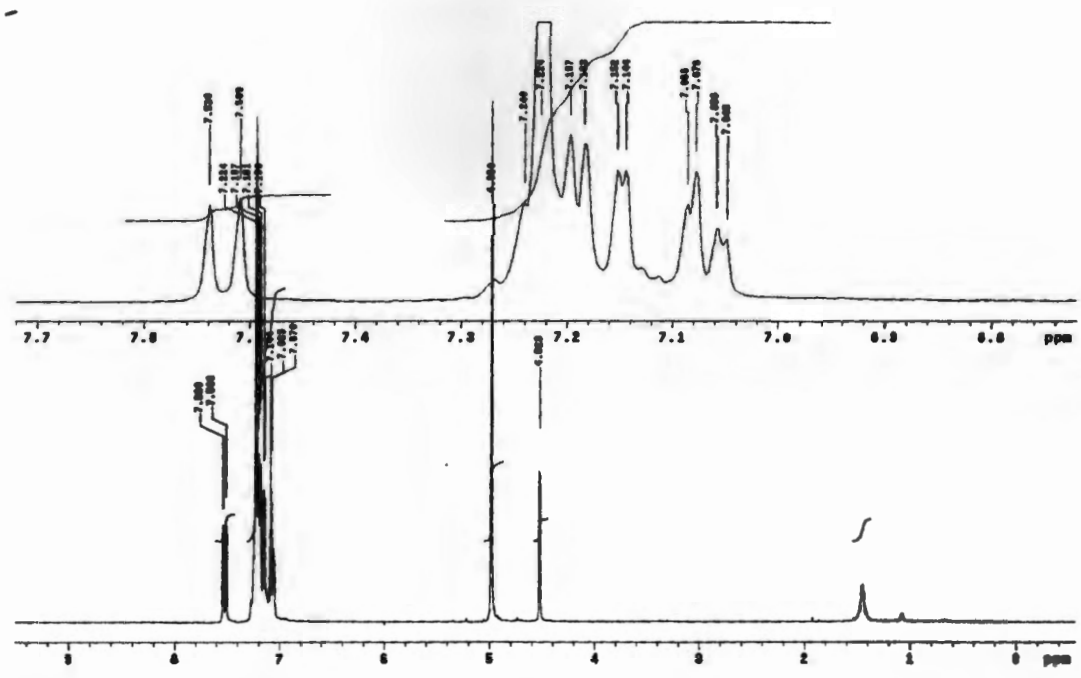

Figure 4.1.7 ^{1}H NMR spectra 1.2 diisocyano-4-phenoxybenzene

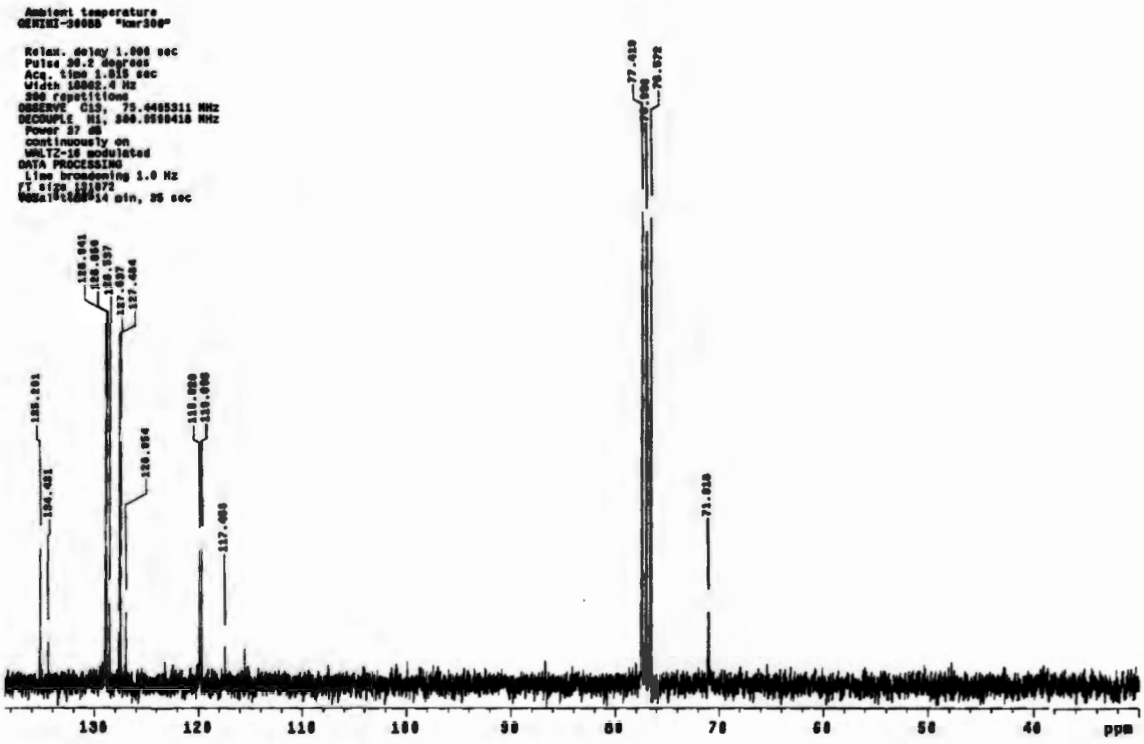

Figure 4.1.8 ^{13}C NMR spectra of 1,2 diisocyano-4-phenoxybenzene

4.1.5 ^{1}H and ^{13}C spectra of 2,3,9,10,16,17,23,24octa-substituted phthalocyanine

2,3,9,10,16,17,23,24 octa-substituted phthlocyanine	^{1}H NMR (δ)	^{13}C NMR (δ) $CDCl_3$
	1.1	77.403
	1.4	115.403, 117.584
	6.8	120.594, 121.353
	7.2	126.278, 130.649
	7.4	135.334, 153.458
	7.7	157.065, 161.743

Table 4.1.5a summarises the proton and carbon shifts of 2,3,9,10,16,17,23,24octa-substituted phthalocyanine

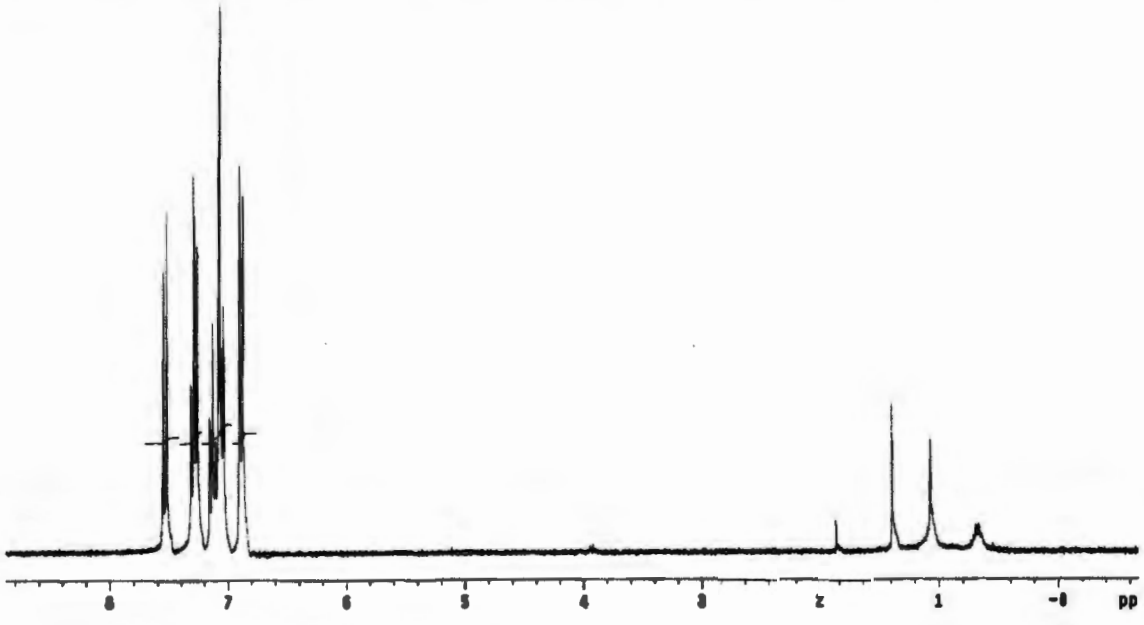

Figure 4.1.9 ^{1}H NMR spectra 2,3,9,10,16,17,23,24octa-substituted phthalocyanine

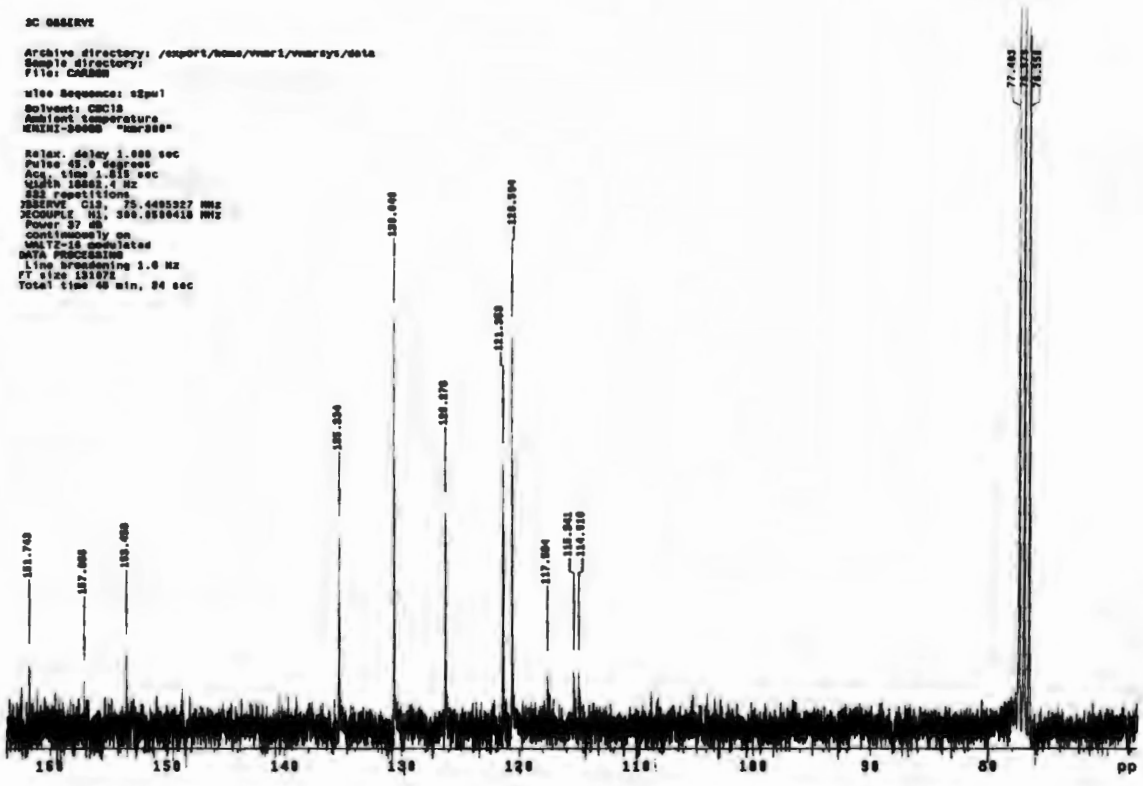

Figure 4.1.10 ^{13}C NMR spectra of 2,3,9,10,16,17,23,24octa-substituted phthalocyanine

4.2 ULTRAVIOLET-VISIBLE SPECTRUM

A summary of the wavelengths of maximum absorption and the absorbances at these wavelengths for the compounds are summarised in Tables 4.2.1a to 4.2.8a, while the spectra of these compounds are compiled in Figures 4.2.1 to 4.2.8

4.2.1 Ultraviolet-visible spectra of mg(II)porphyrazine

Wavelength (λ_{max})(nm)	345.9	599.5	547.79	638.5
Absorbance (log ε)	0.694(4.69)	0.817(4.76)	0.1686(4.07)	0.168(4.06)

Table 4.2.1a Absorption bands in the mg(II)-pz

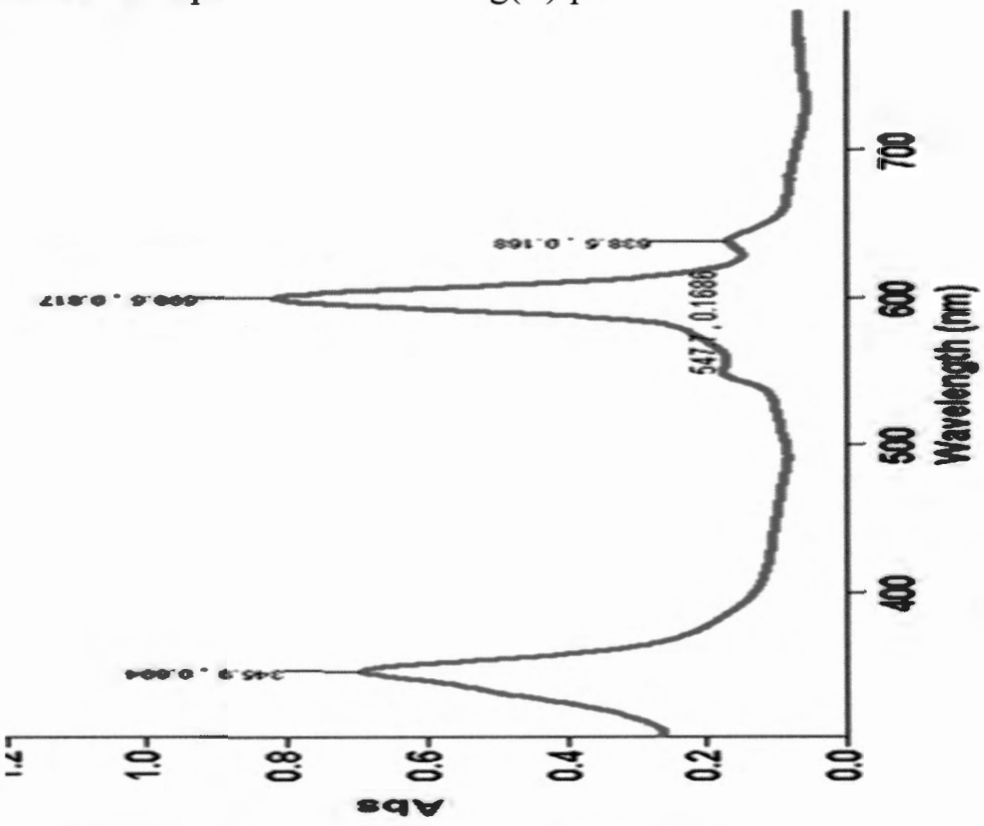

Figure 4.2.1 Ultraviolet-visible spectrum of mg(II)-pz

4.2.2 Ultraviolet-visible spectra of freebase ligand

Wavelength (λ_{max})(nm)	340.0	558.0	598	626.1
Absorbance(log ε)	1.363(5.08)	0.783(4.84)	0.234(4.32)	1.244(5.04)

Table 4.2.2a Absorption bands of the freebase ligand

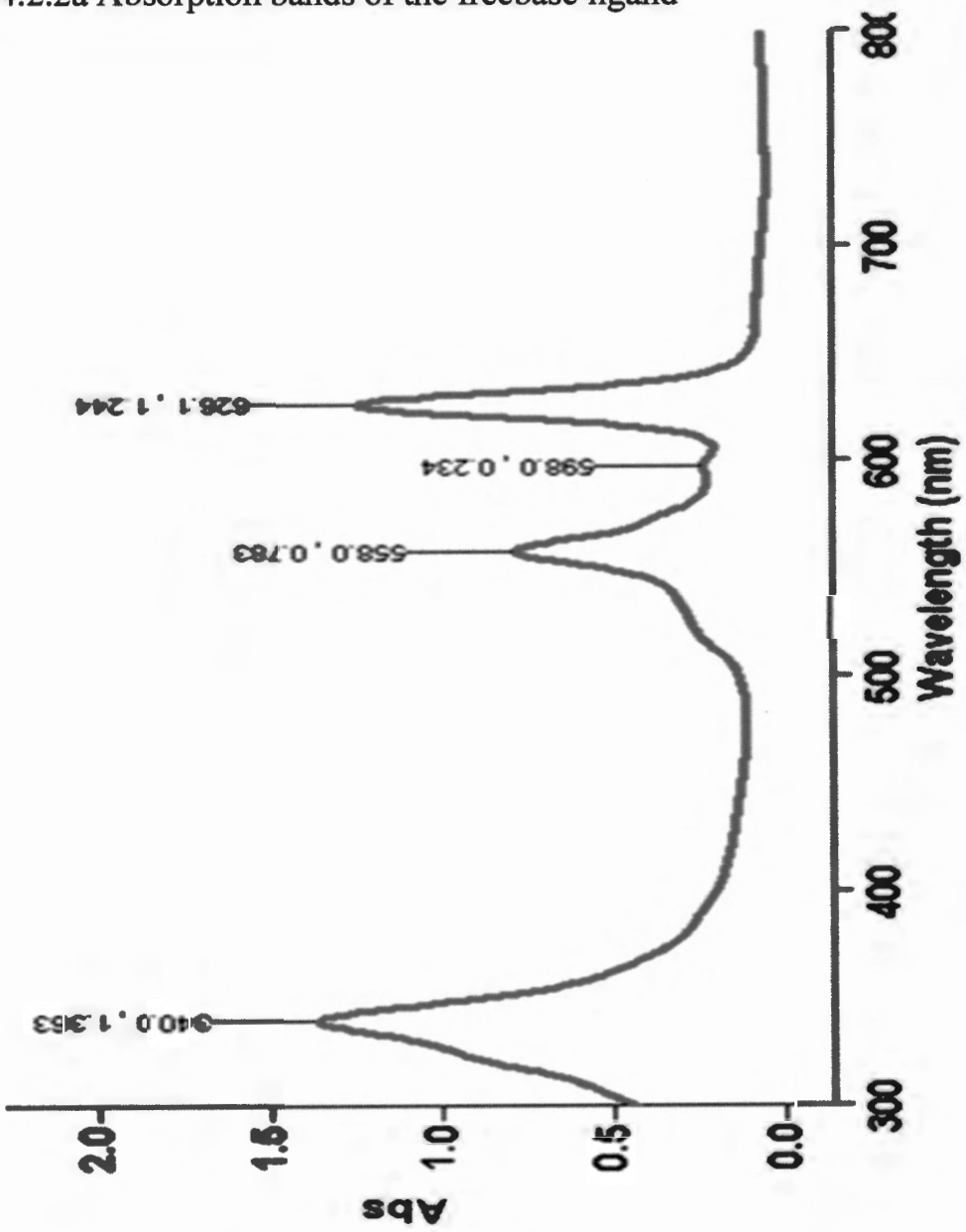

Figure 4.2.2 Ultraviolet-visible spectrum of freebase

4.2.3 Ultraviolet-visible spectra of $CrCl_3.6H_20$ in ethanol

Wavelength (λ_{max})(nm)	458.4	640.7
Absorbance (log ε)	2.6778 (1.43)	1.9945(1.30)

Table 4.2.3a Absorption bands in the $CrCl_3.6H_20$ in ethanol

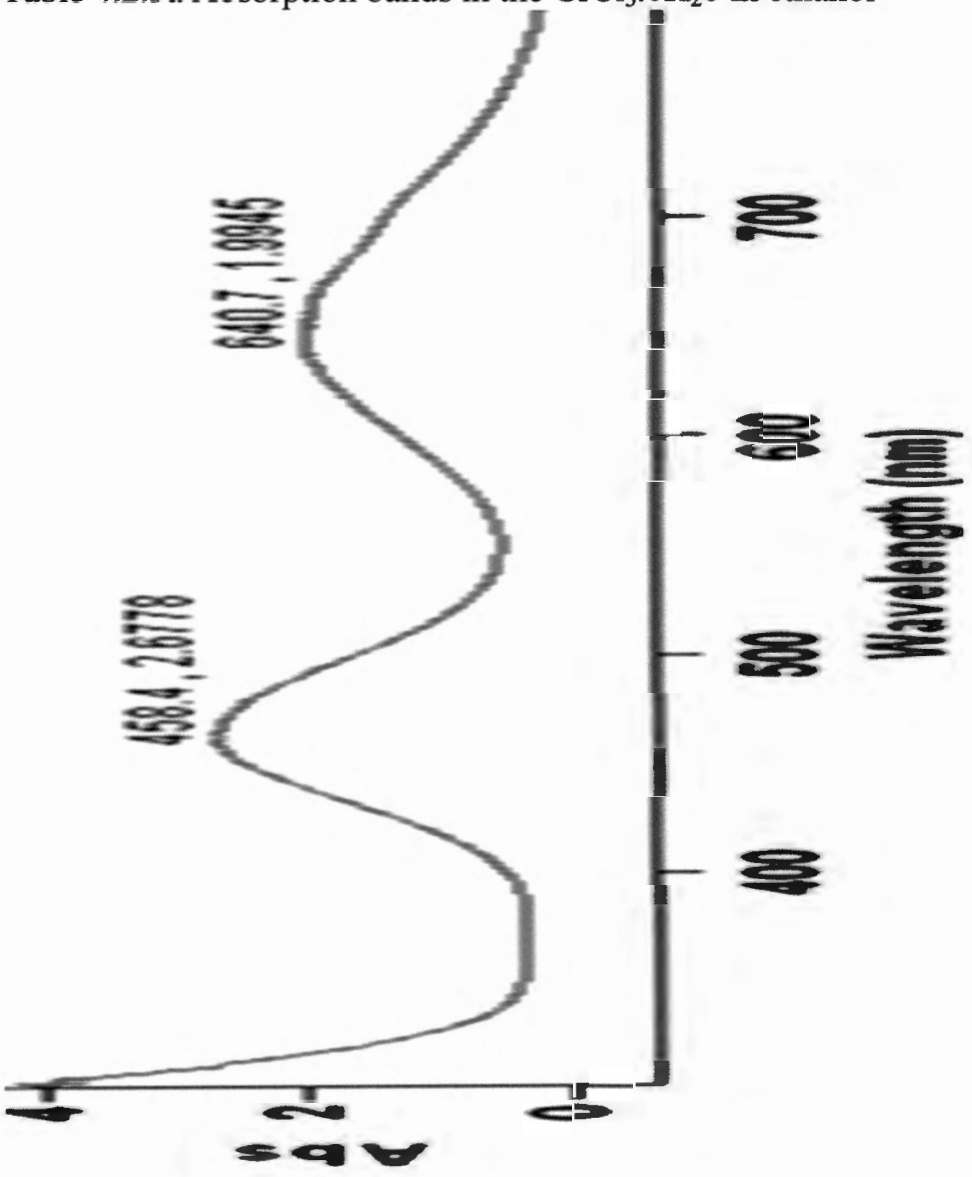

Figure 4.2.3 Ultraviolet-visible Spectrum of chromium(III) in ethanol

4.2.4 Ultraviolet-visible spectra of $Co(NO_3)_2.6H_2O$ in ethanol

Wavelength (λ_{max})(nm)	519.5
Absorbance (log ε)	0.947 (0.97)

Table 4.2.4a Absorption bands of $Co(NO_3)_2.6H_2O$ in ethanol

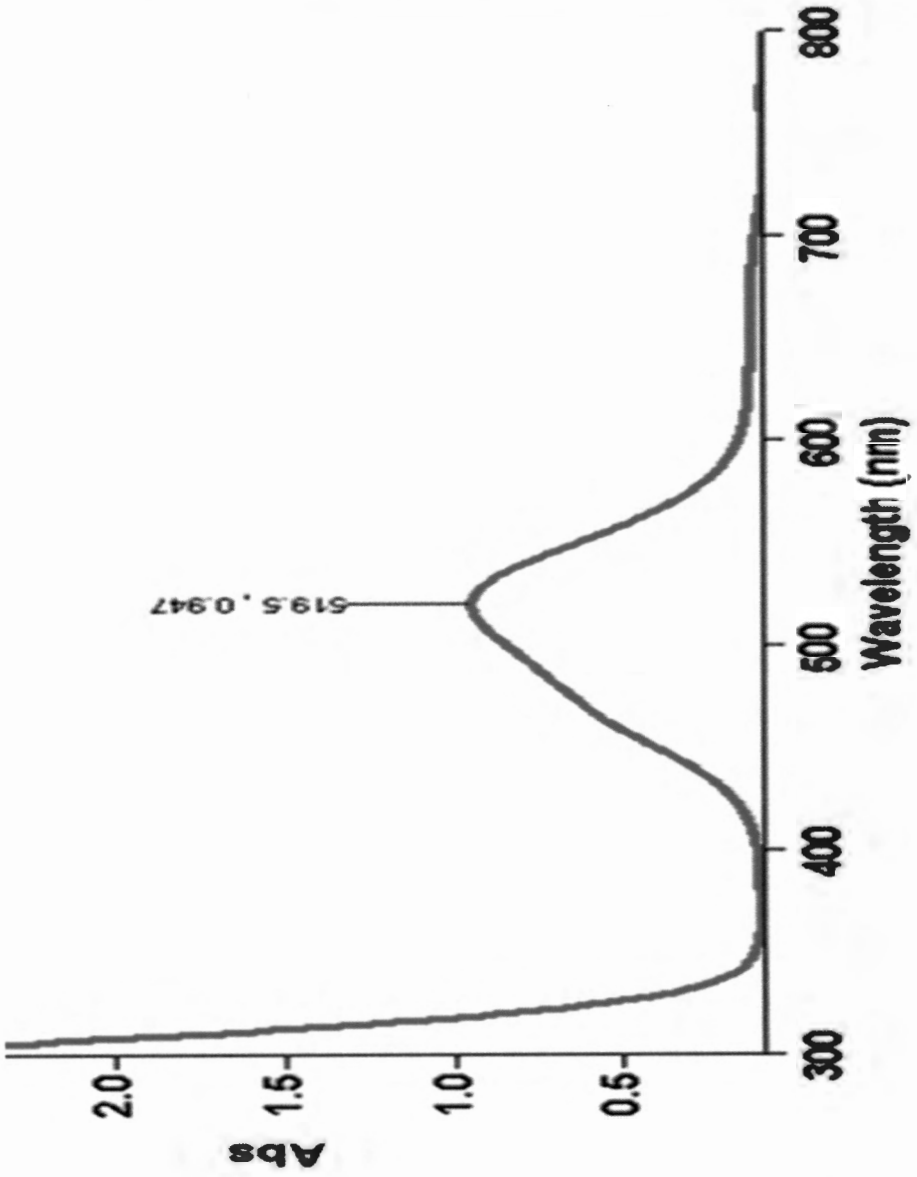

Figure 4.2.4 Ultraviolet-visible spectrum of cobalt(II) in ethanol

4.2.5 Ultraviolet-visible spectra of Co(II)-pz

Wavelength (λ_{max})(nm)	345.1	550.0	600.0
Absorbance (log ε)	3.320(1.52)	0.672 (0.83)	3.401(1.53)

Table 4.2.5a Absorption bands in the Co(II)-pz

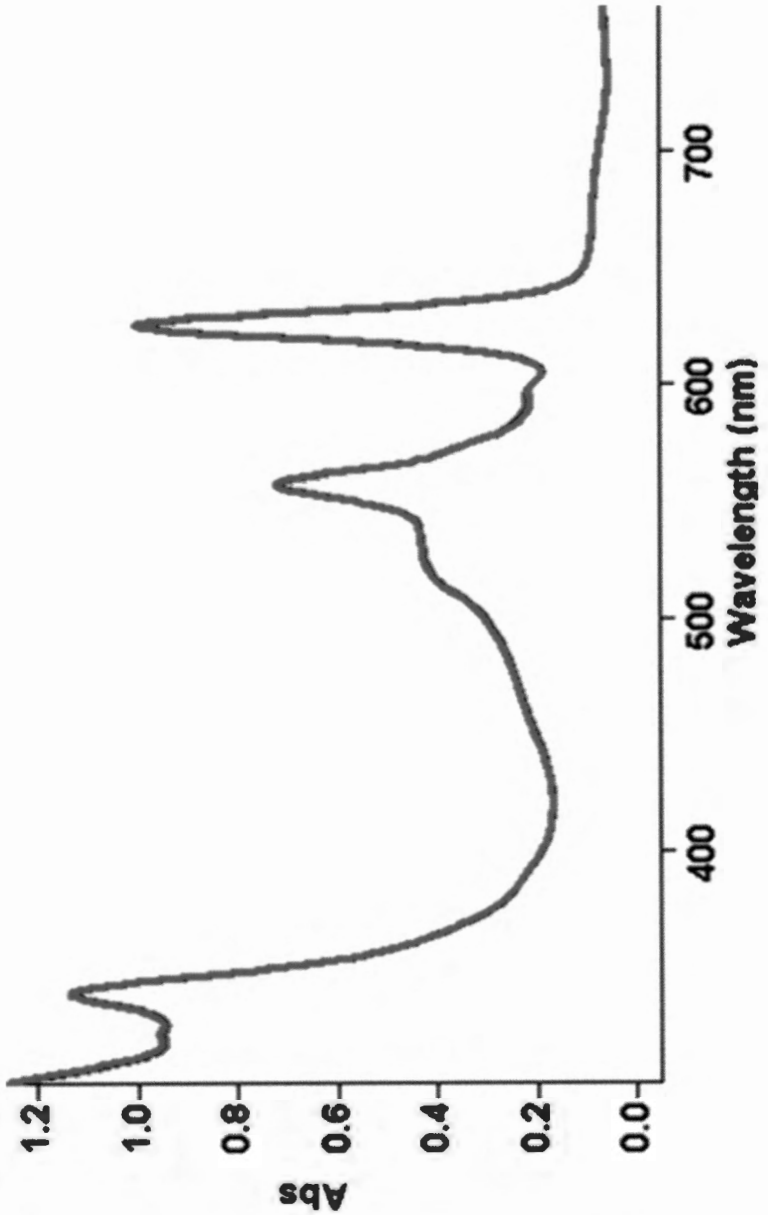

Figure 4.2.5 Ultraviolet-visible spectrum of Co(II)-pz

4.2.6 Ultraviolet-visible spectra of Cr(III)-pz

Wavelength (λ_{max})(nm)	337.6	462.0	557.5	625.0
Absorbance (log ε)	1.207(1.08)	0.939(0.97)	0.776(0.89)	1.409(1.15)

Table 4.2.6a Absorption bands in the Cr(III)-pz

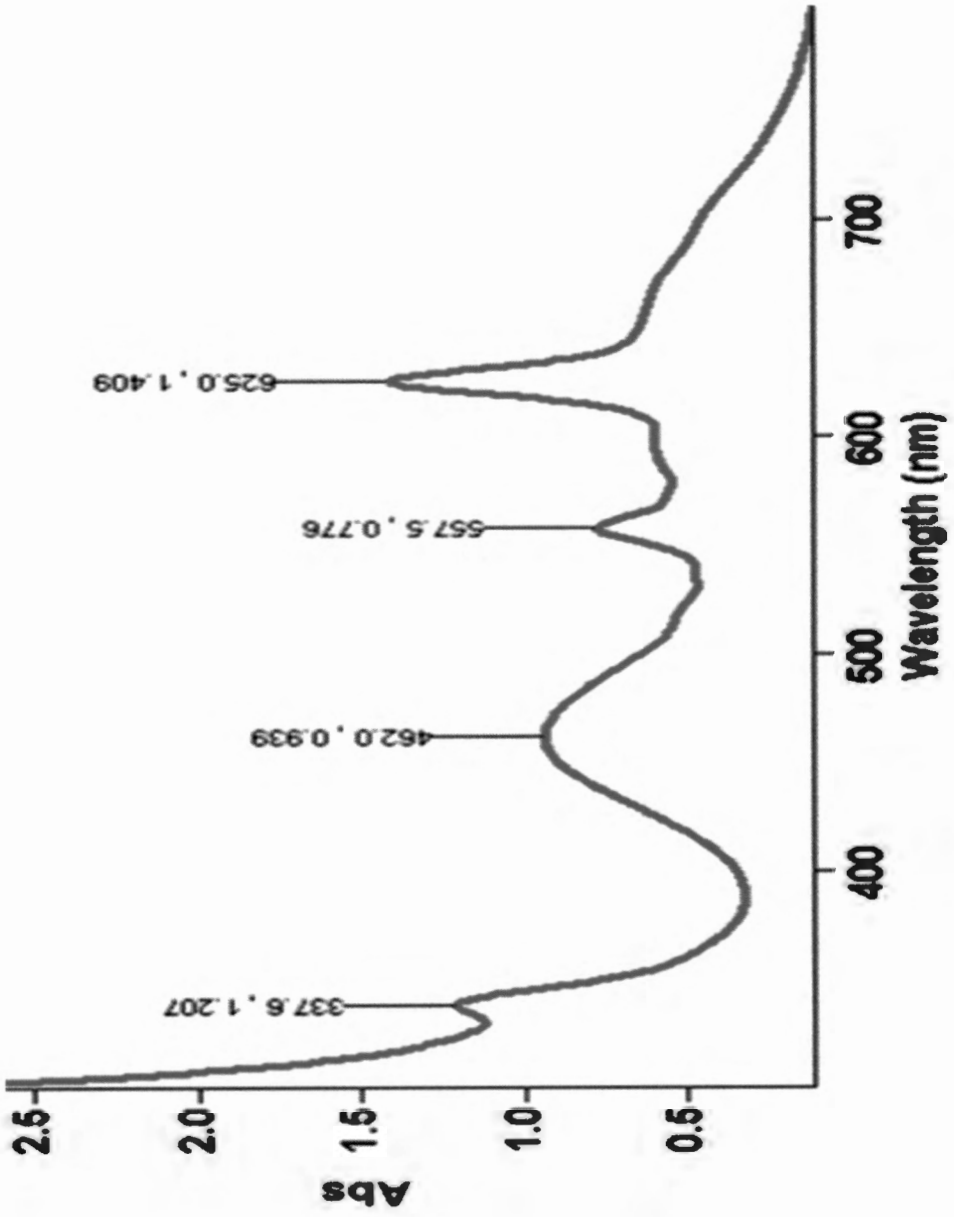

Figure 4.2.6 Ultraviolet-visible spectrum of Cr(III)-pz

4.2.7 Ultraviolet-visible spectra of direct insertion of Cr(III) ion into mg(II)-pz

Wavelength (λ_{max})(nm)	470.4	557.0	627.5
Absorbance(log ε)	0.957(0.98)	0.388(0.59)	0.782(0.89)

Table 4.2.7a Absorption bands for the direct insertion of the Cr(III) ion into mg(II)-pz

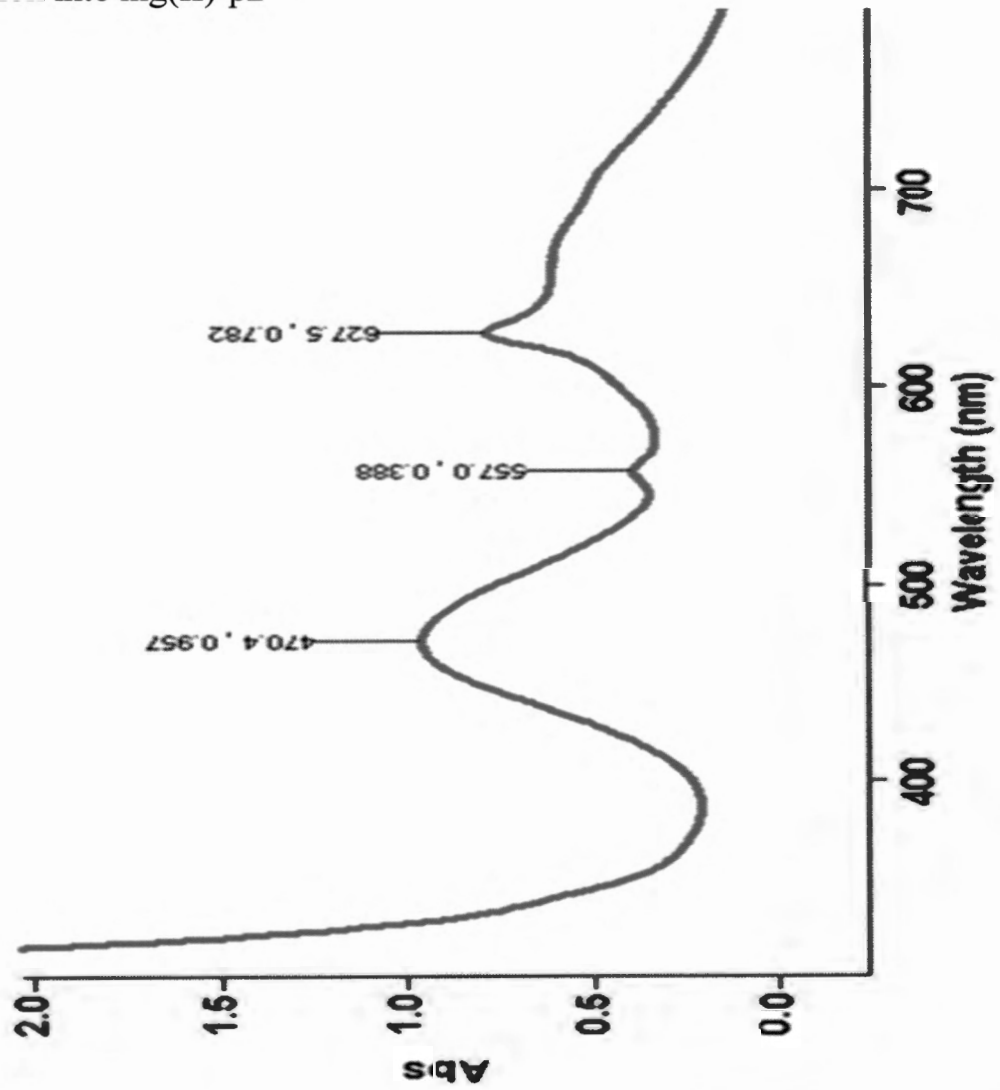

Figure 4.2.7 Ultraviolet-visible spectrum for the direct insertion of Cr(III) ion into mg(II)-pz

4.2.8 Ultraviolet-visible spectra of 2,3,9,10,16,17,23,24octa-sustituted phthalocyanine

Wavelength (λ_{max})(nm)	325.9	668.0	704.6
Absorbance (log ε)	1.8832(5.12)	1.048(4.87)	1.124(4.89)

Table 4.2.8a Absorption bands in the 2,3,9,10,16,17,23,24octa-substituted phthalocyanine

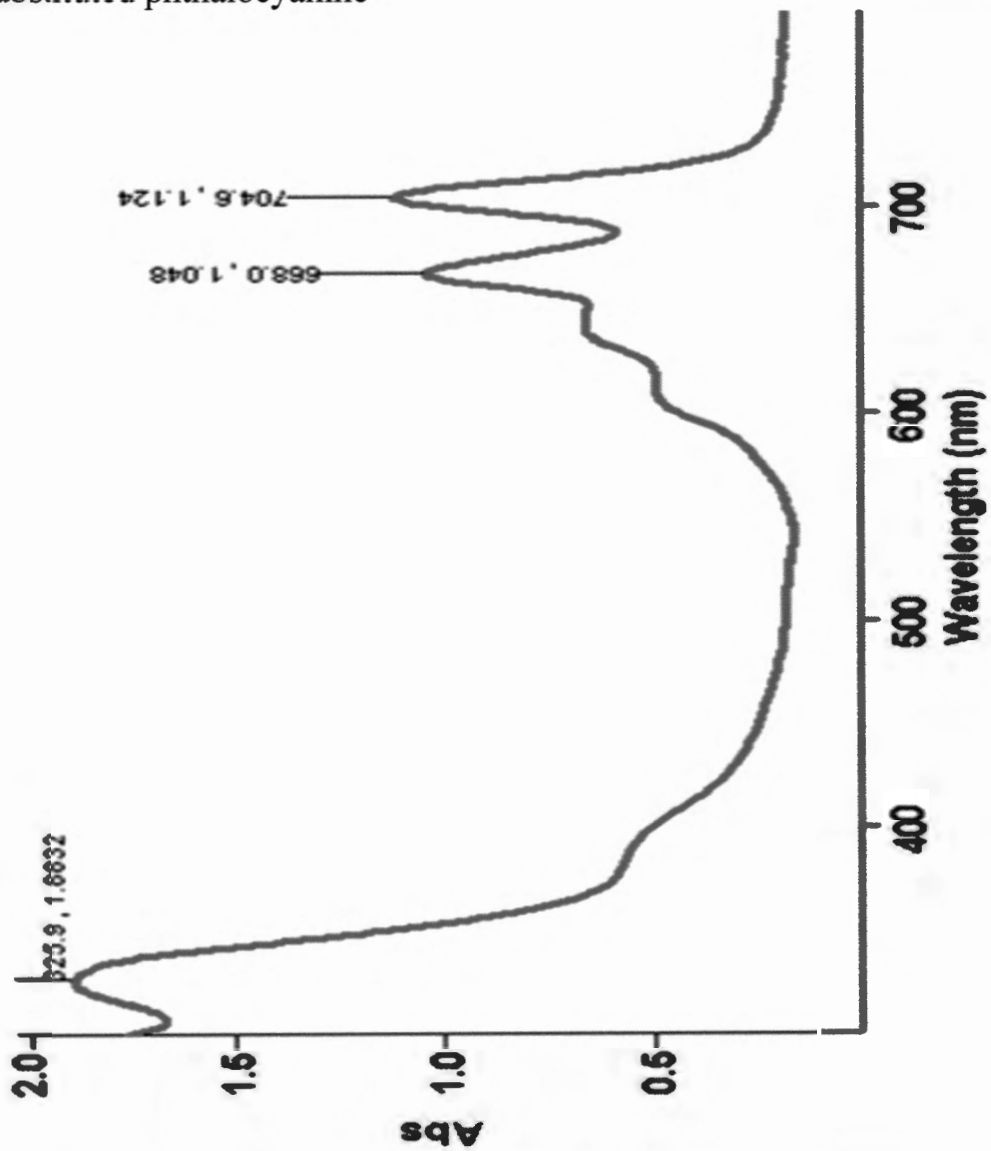

Figure 4.2.8 Ultraviolet-visible spectrum of 2,3,9,10,16,17,23,24octa-substituted phthalocyanine

4.3 INFRARED SPECTRUM

4.3.1 Ihe infrared spectra of mg(II)-pz is shown in Figure 4.3.1

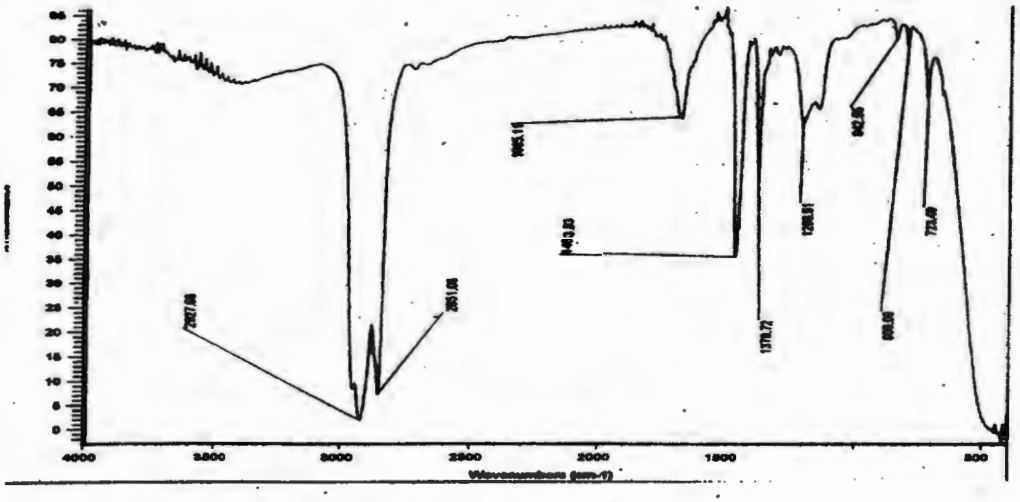

Figure 4.3.1 IR spectrum of mg(II)-pz

4.3.2 Infrared spectra of freebase is shown in figure 4.3.2

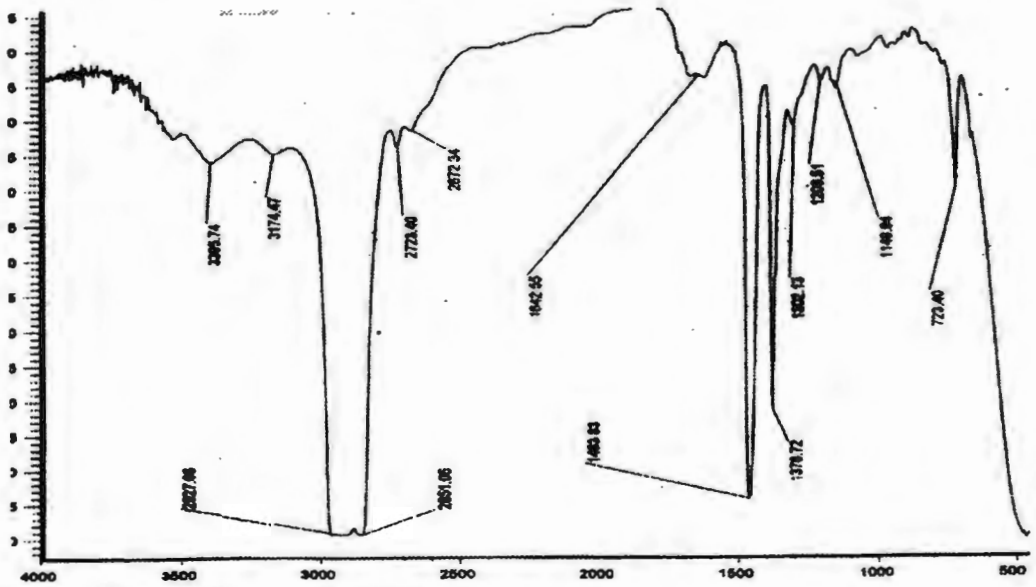

Figure 4.3.2 IR spectrum of freebase

4.4 KINETIC STUDIES

4.4.1 Kinetics of metallation of compounds

Preliminary repetitive scanning of the ultraviolet-visible spectral region during the insertion of Cr(III) in octakis(propyl)porphyrazine ligand, octakis(propyl)porphyrazinemagnesium(II) complex and 2,3,9,10,16,17,23,24octa-substituted pthalocyanine, gave well defined isosbestic points for over two half-lives of various reactions. Typical spectral changes for these reactions are compiled in Figures 4.4.1.1 to 4.4.1.3

4.4.2 Kinetics of reduction of Cr(III) porphyrazine

Preliminary repetitive scanning of the ultraviolet-visible spectral region during the reduction of Cr(III) in octakis(propyl)porphyrazinechromium(III) complex to chromium(II) with octakis(propyl)porphyrazinecobalt(II) complex, gave well defined isosbestic points for over two half-lives of various reactions. Typical spectral changes for the reaction are compiled in Figure 4.4.2

4.4.1.1 Spectral changes of Cr(III) insertion into octakis(propyl)porphyrazine ligand.

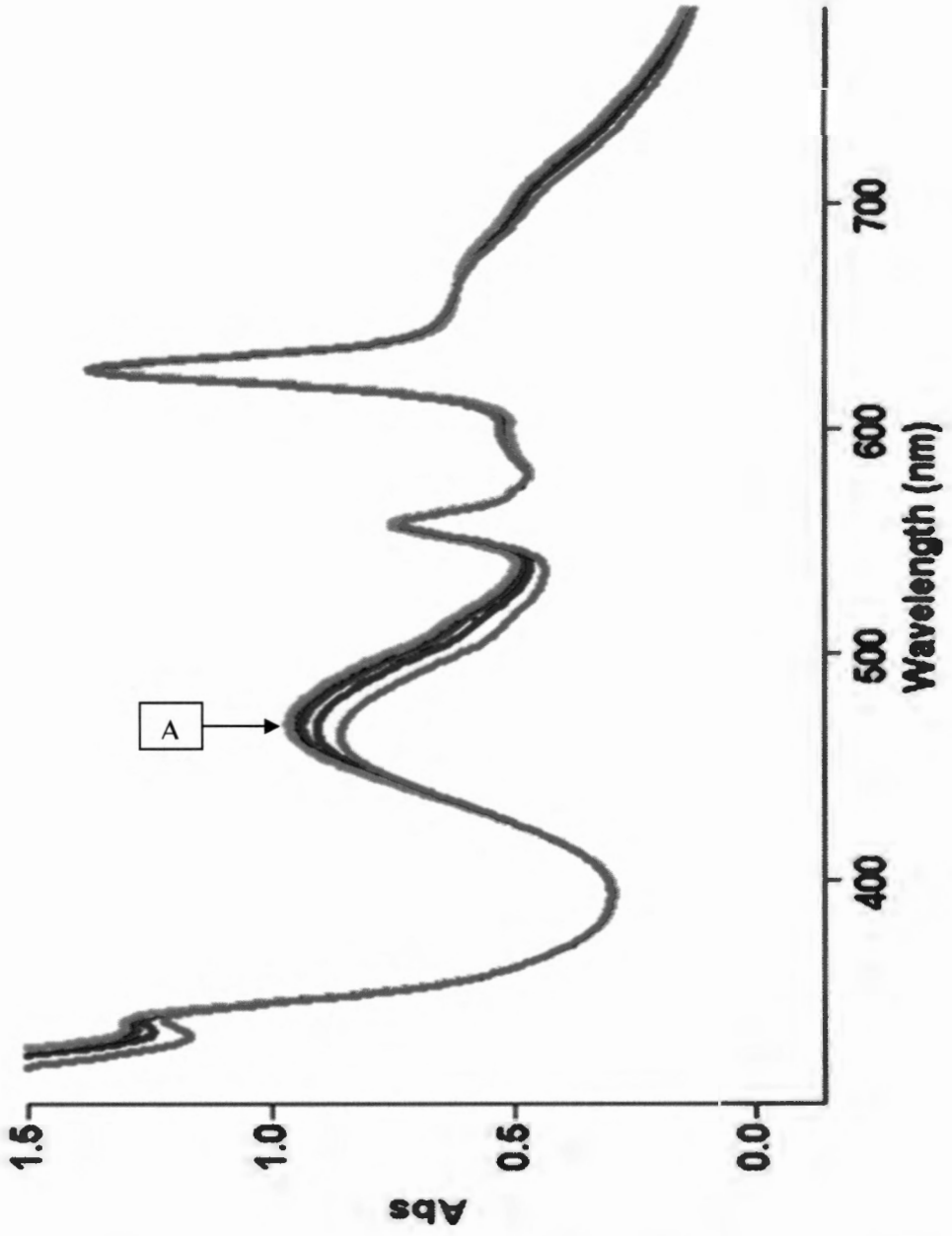

Figure 4.4.1.1 Spectral changes during insertion of Cr(III) into the octakis(propyl)porphyrazine at 25°C, A is the initial trace followed successively by traces at 4 minutes intervals

4.4.1.2 Spectral changes of direct insertion of Cr(III) ion into octakis(propyl)poprhyrazinemagnesium(II) complex

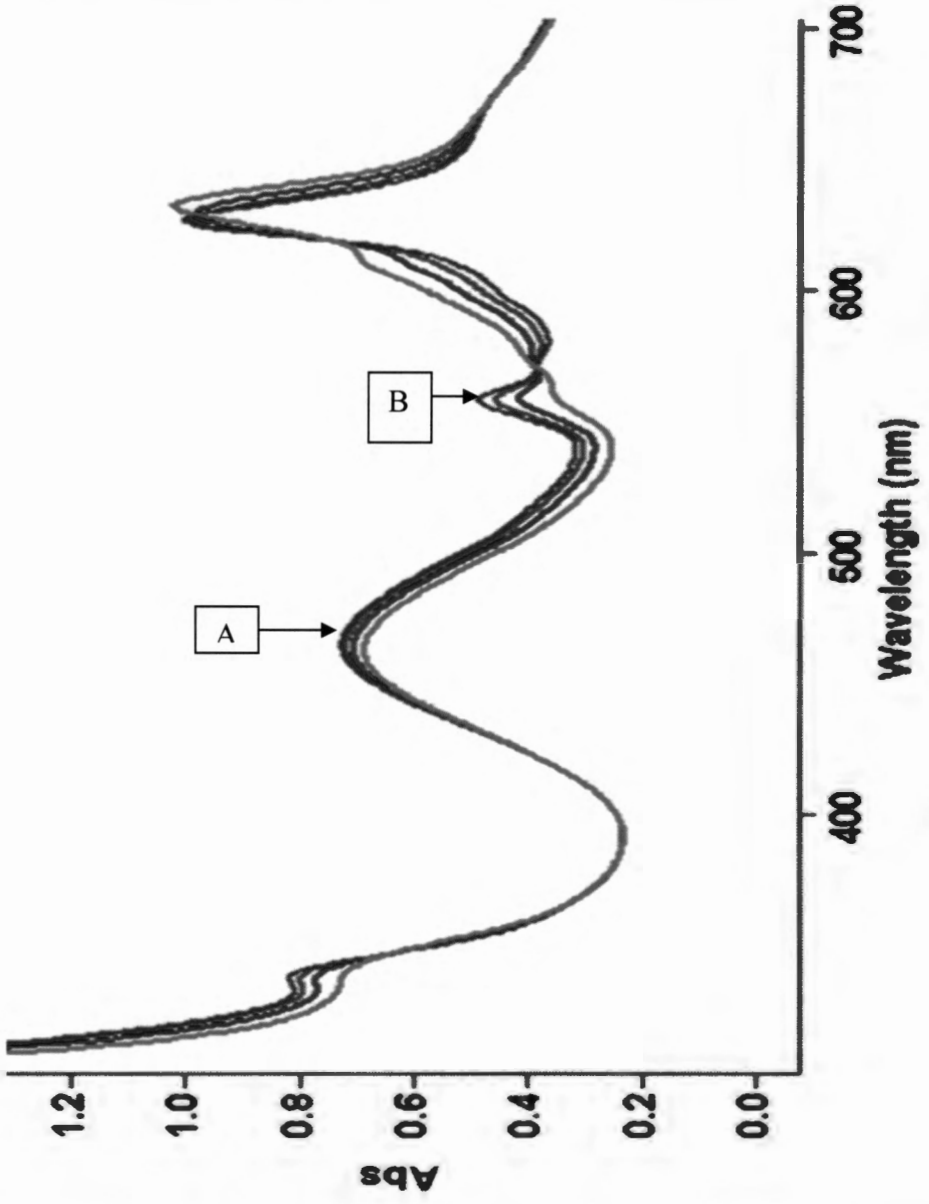

Figure 4.4.1.2 Spectral changes during direct insertion of Cr(III) into octakis(propyl)porphyrazinemagnesium(II) complex at 17°C, A and B are the initial traces followed successively by traces at 8 minutes intervals

4.4.1.3 Spectral changes of insertion of Cr(III) ion into 2,3,9,10,16,17,23,24octa-substituted phthlocyanine

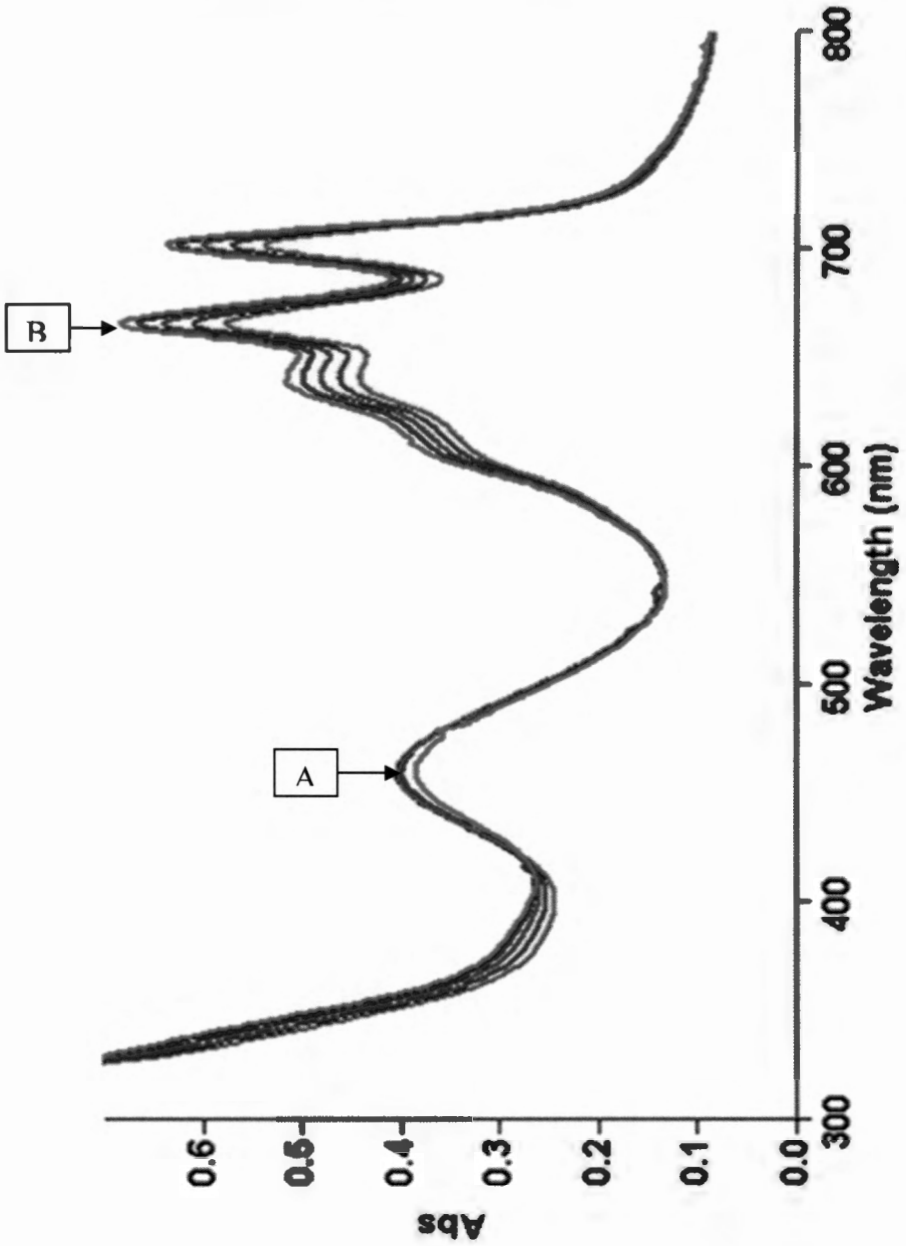

Figure 4.4.1.3 Spectral changes during insertion of Cr(III) into 2,3,9,10,16,17,23,24octa-substituted phthlocyanine 25°C, A and B are initial traces followed successively by traces at 5 minutes intervals

4.4.2 Spectral changes of reduction of octakis(propyl)porphyrazinechromium(III) complex with octakis(propyl)porphyrazinecobalt(II) complex

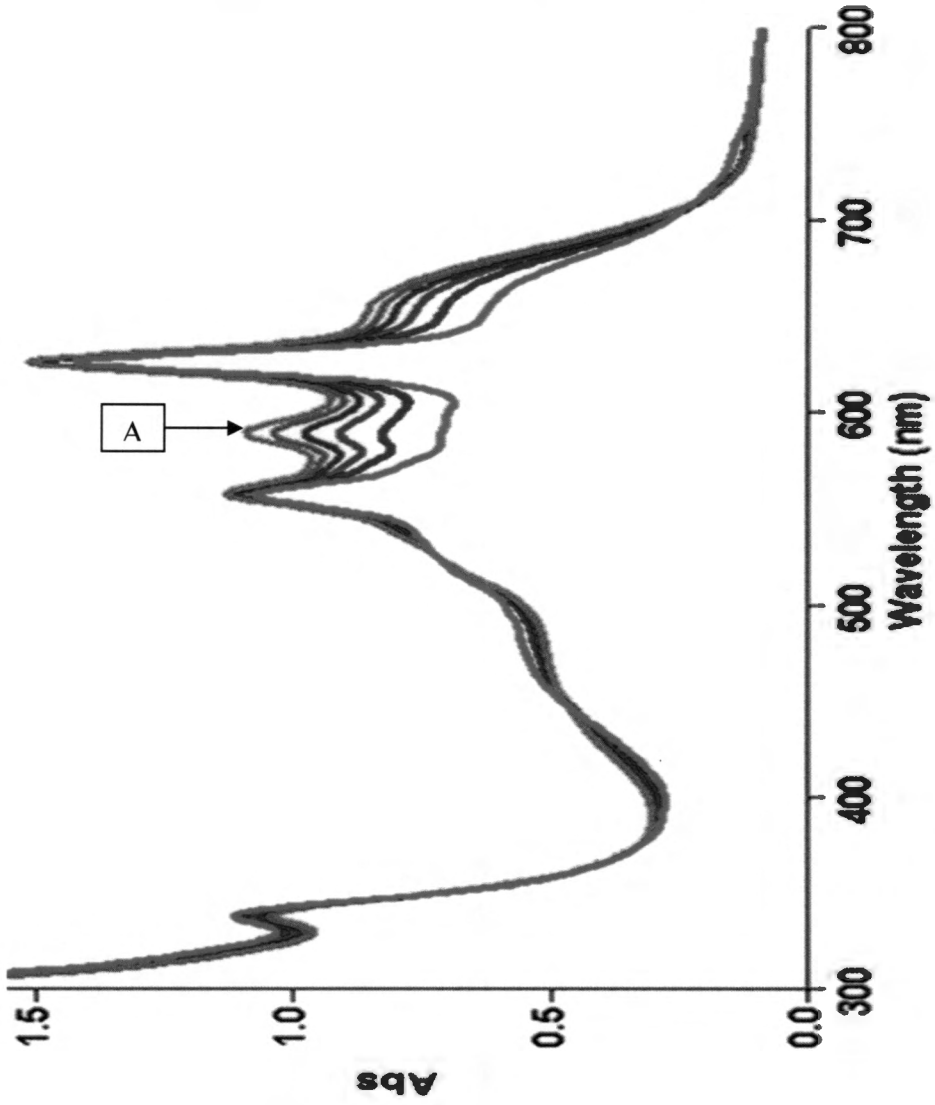

Figure 4.4.2 Spectral changes for reduction of octakis(propyl) porphyrazinechromium(III) complex with octakis(propyl) porphyrazinecobalt(II) complex at 20°C, where A is the initial trace followed successively by traces at 6 minutes intervals

4.5 CALCULATION OF RATE CONSTANTS

The kinetics of the reactions were then followed at fixed wavelength over a range of temperatures. The individual reaction conditions for the reactions are summarized in Tables 4.5.1a and 4.5.1b, followed by Tables 4.5.1 to 4.5.24 of rates constants at different temperatures and Figures 4.5.1 to 4.5.24 illustrating typical first order kinetic plots for the reactions.

Reaction	Positionof isosbestic points (nm)	Wavelength at which the reaction was followed (nm)
Cr(III) + Freebase	465	466
Cr(III) + Mg(II)-Pz	467.5	468
Cr(III) + Octa-phthalo	664.5	666

Table 4.5.1a Individual reaction conditions for insertion of Cr(III) into listed compounds

Reaction	Position of isosbestic points (nm)	Wavelength at which the reaction was followed (nm)
Reduction of Cr(III) by Co(II)	586	588

Table 4.5.1b Reaction conditions for reduction reaction listed.

4.5.1 Tables and various plots of absorbance versus time for direct insertion of Cr(III) ion into octakis(propyl)porphyrazine ligand, at various temperatures.

Time (min)	10	20	30	40	50	60	70	80
Ln ($A-A_\infty$)	-2.62	-3.0662	-3.5247	-4.332	-4.8911	-5.5728	-6.3771	-7.152

Table 4.5.1 Absorbance measurements for Cr(III) insertion into octakis(propyl)porphyrazine ligand at 15°C

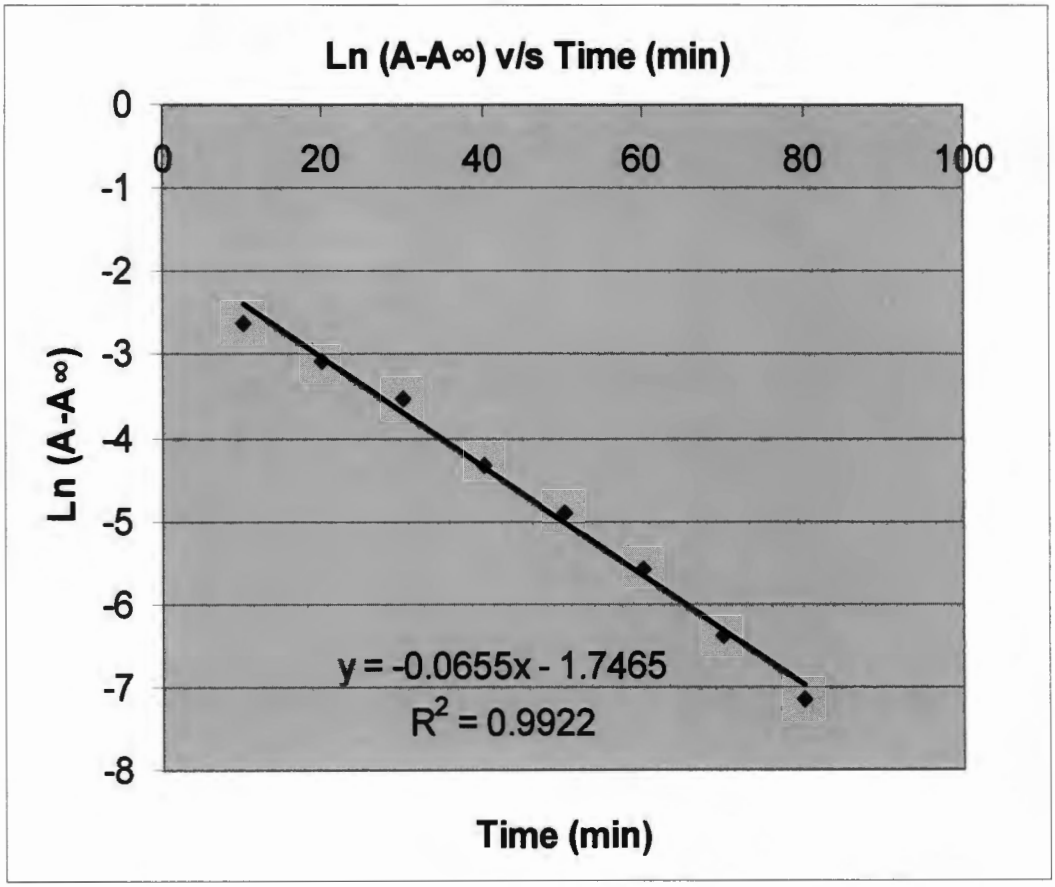

Figure 4.5.1 A plot of ln ($A-A_\infty$) vs time (min) at 15°C

Time (min)	8	16	24	32	40	48	56	64
ln ($A-A_\infty$)	-2.4853	-2.9469	-3.4514	-3.9686	-4.612	-5.1199	-5.9145	-7.0099

Table 4.5.2 Absorbance measurements for Cr(III) insertion into octakis(propyl)porphyrazine ligand at 17°C

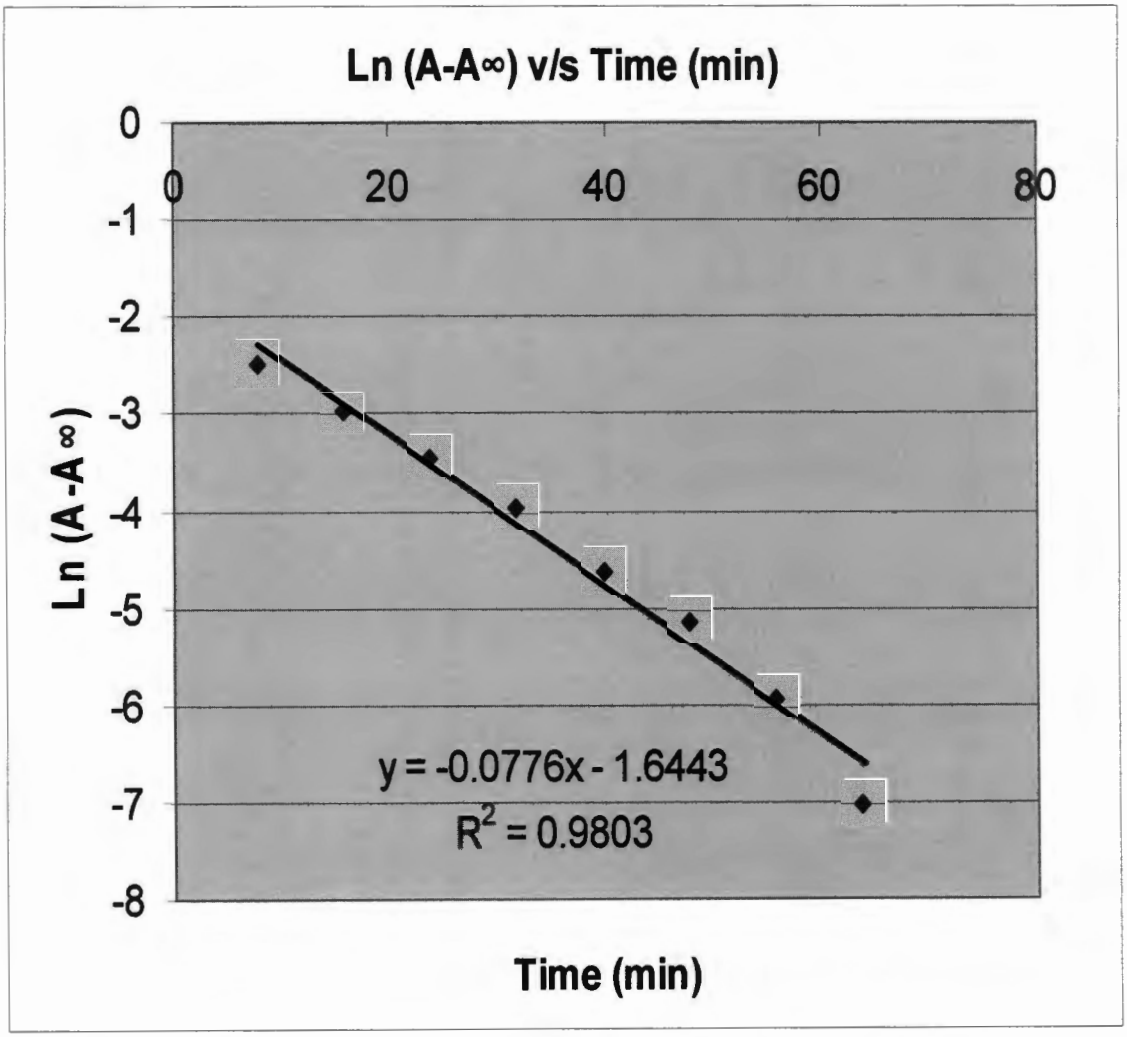

Figure 4.5.2 A plot of ln ($A-A_\infty$) vs time (min) at 17°C

Time (min)	5	10	15	20	25	30	35
Ln ($A-A_\infty$)	-3.6268	-4.0456	-4.4741	-4.9063	-5.3602	-5.9653	-6.5433

Table 4.5.3 Absorbance measurements for Cr(III) insertion into octakis(propyl)porphyrazine ligand at 20°C

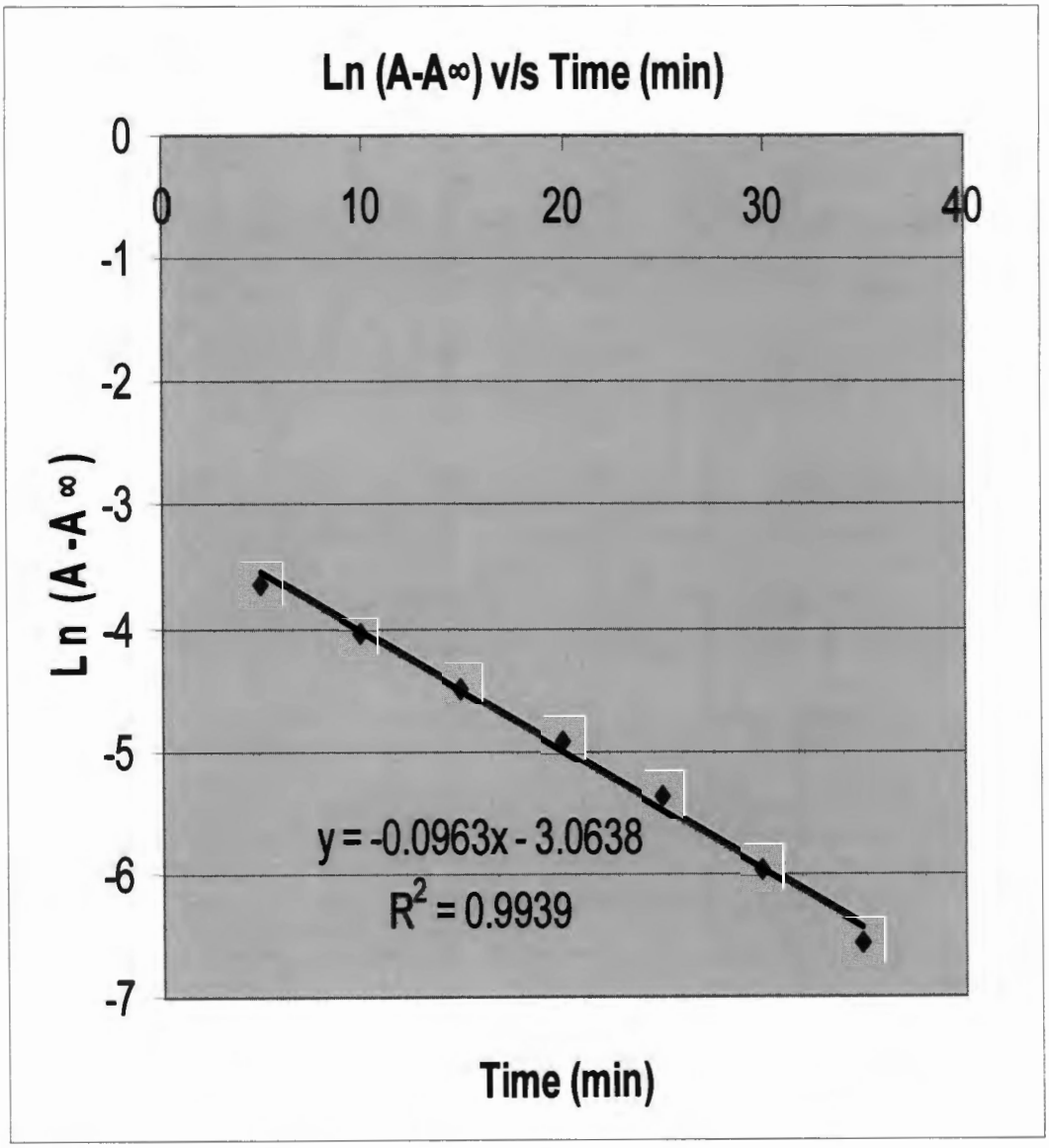

Figure 4.5.3 A plot of ln ($A-A_\infty$) vs time (min) at 20°C

Time (min)	4	8	12	16	20	24	28
Ln ($A-A_\infty$)	-1.9022	-2.4345	-2.9584	-3.5791	-4.2904	-5.1499	-6.1144

Table 4.5.4 Absorbance measurements for Cr(III) insertion into octakis(propyl)porphyrazine ligand at 25°C

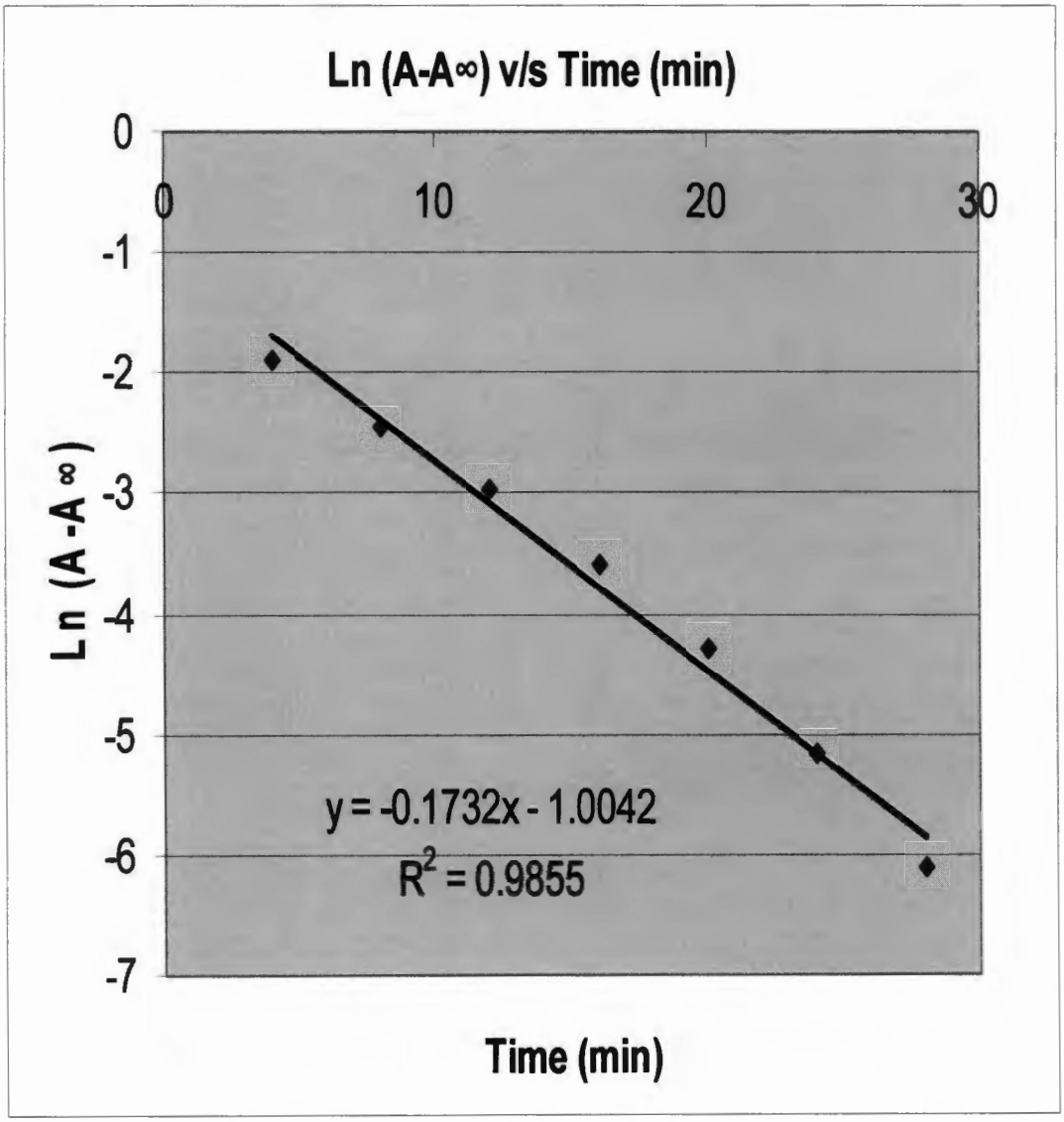

Figure 4.5.4 A plot of ln ($A-A_\infty$) vs time (min) at 25° C

Time (min)	3	6	9	12	15	18	21	24
Ln ($A-A_\infty$)	-1.9968	-2.5072	-3.0944	-3.7636	-4.5282	-5.1817	-5.7662	-6.4581

Table 4.5.5 Absorbance measurements for Cr(III) insertion into octakis(propyl)porphyrazine ligand at 30°C

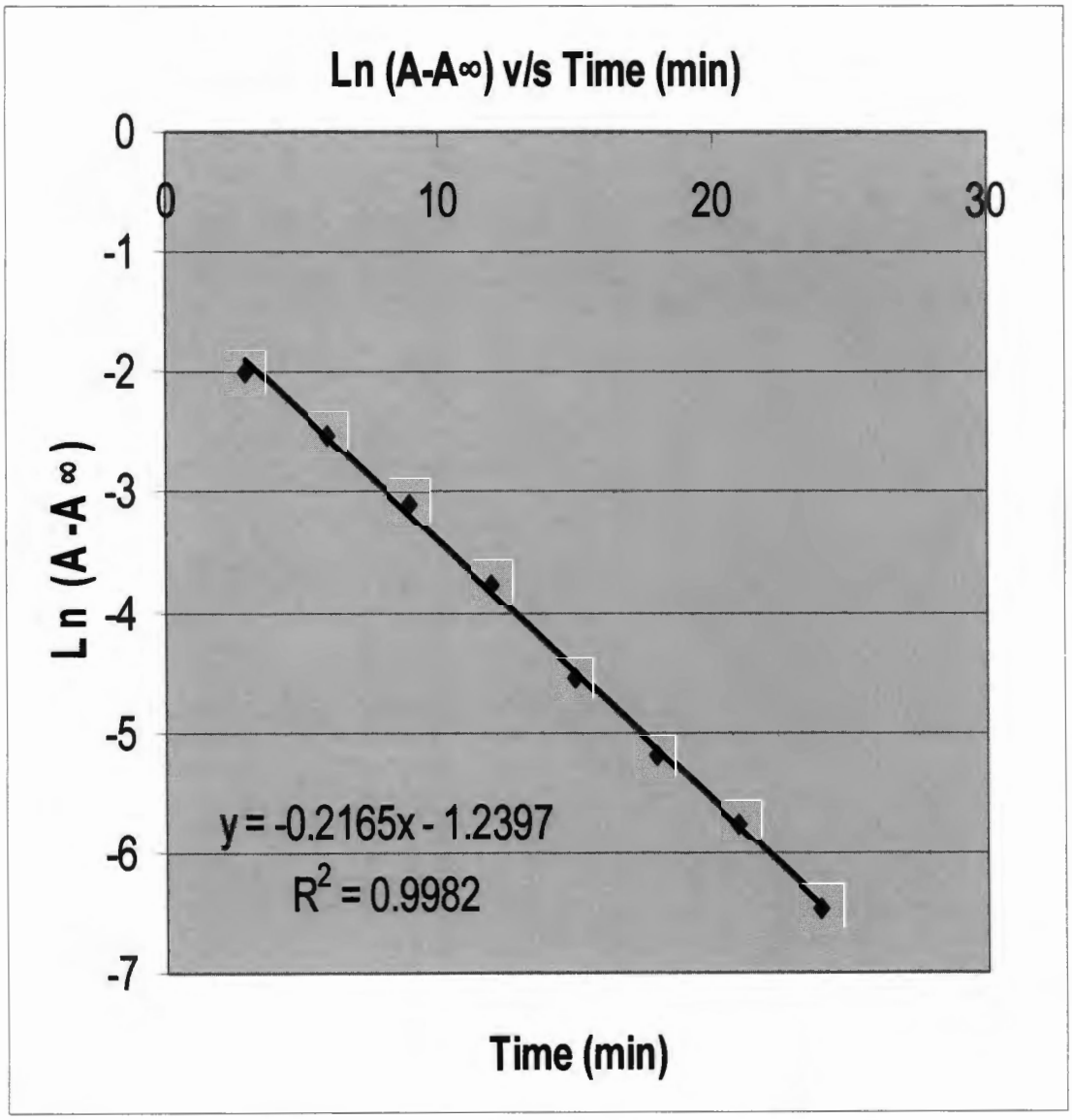

Figure 4.5.5 A plot of ln ($A-A_\infty$) vs time (min) at 30° C

Time (min)	2	4	6	8	10	12	14	16
Ln ($A-A_\infty$)	-2.0449	-2.6679	-3.0628	-3.6215	-4.4203	-4.9982	-5.6899	-6.2231

Table 4.5.6 Absorbance measurements for Cr(III) insertion into octakis(propyl)porphyrazine ligand at 35°C

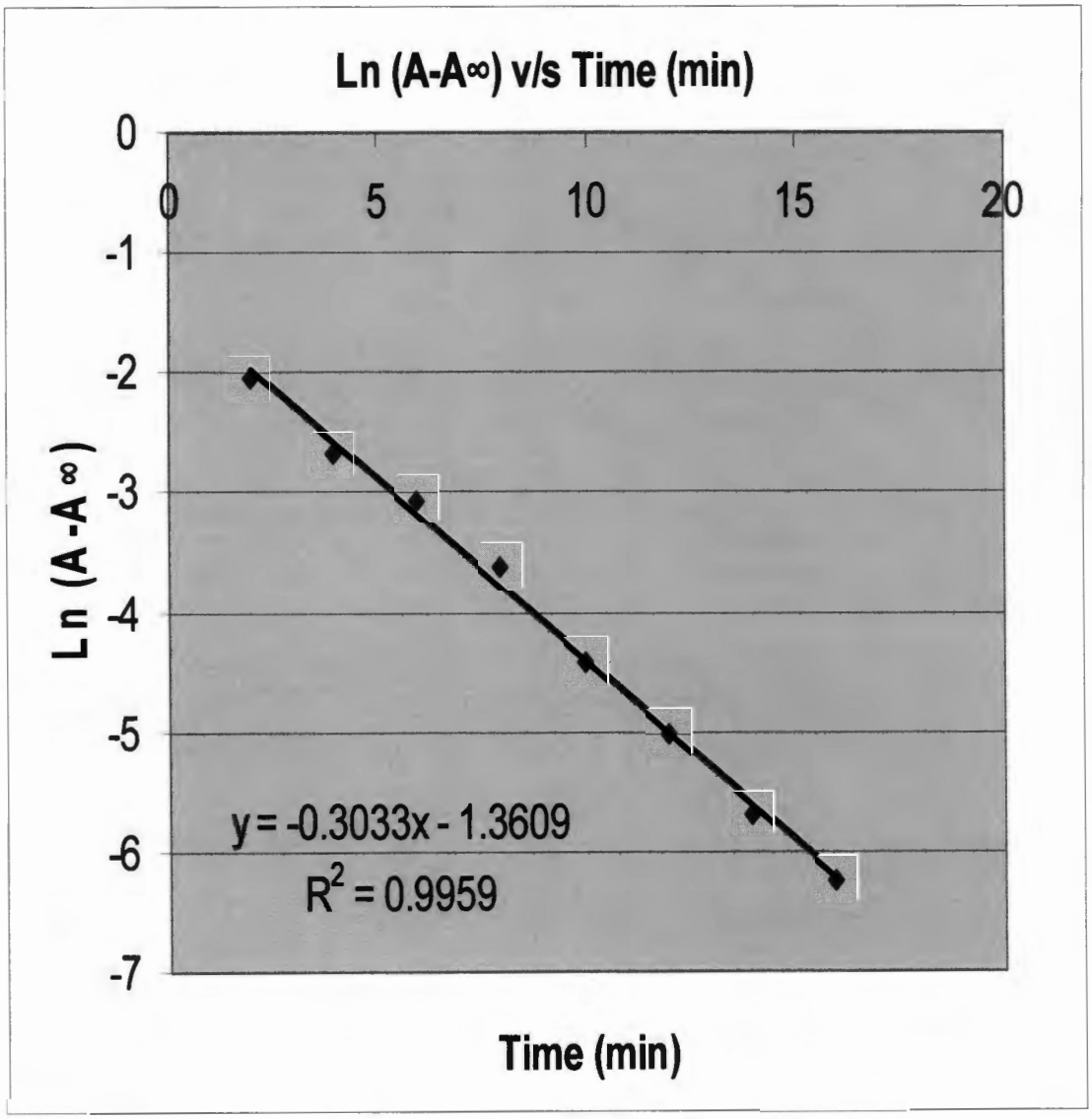

Figure 4.5.6 A plot of ln ($A-A_\infty$) vs time (min)at 35° C

4.5.2 Table and plots of absorbance versus time of direct insertion of Cr(III) ion into octakis(propyl)porphyrazine magnesium(II) complex at various temperatures

Time (min)	10	20	30	40	50	60	70	80
Ln ($A-A_\infty$)	-1.5828	-2.2346	-2.9898	-3.4262	-3.9665	-4.4752	-5.4232	-6.2756

Table 4.5.7 Absorbance measurement for Cr(III) insertion into mg(II)-pz at 15°C

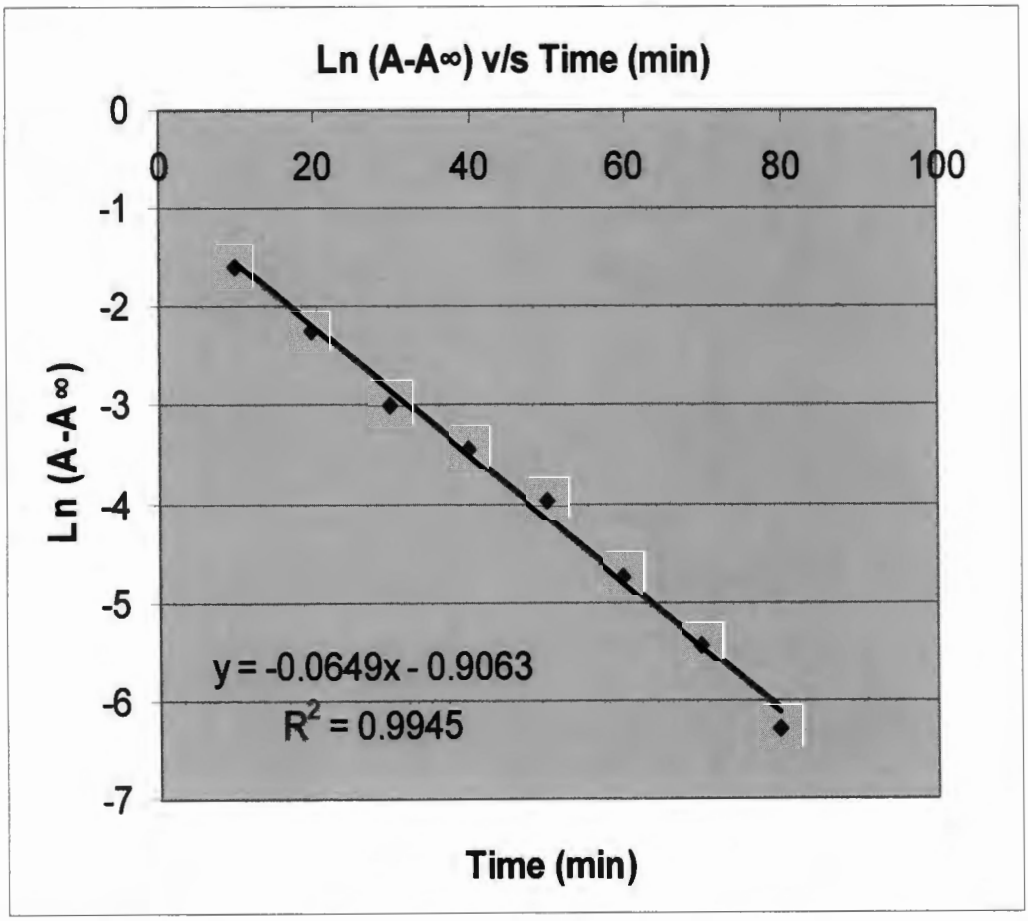

Figure 4.5.7 A plot for direct insertion of Cr(III) into mg(II)-pz at 15°C

Time (min)	8	16	24	32	40	48	56	64
Ln ($A-A_\infty$)	-1.6446	-2.2214	-2.8968	-3.6009	-4.1669	-4.836	-5.4223	-5.8225

Table 4.5.8 Absorbance measurement for Cr(III) insertion into mg(II)-pz at 17°C

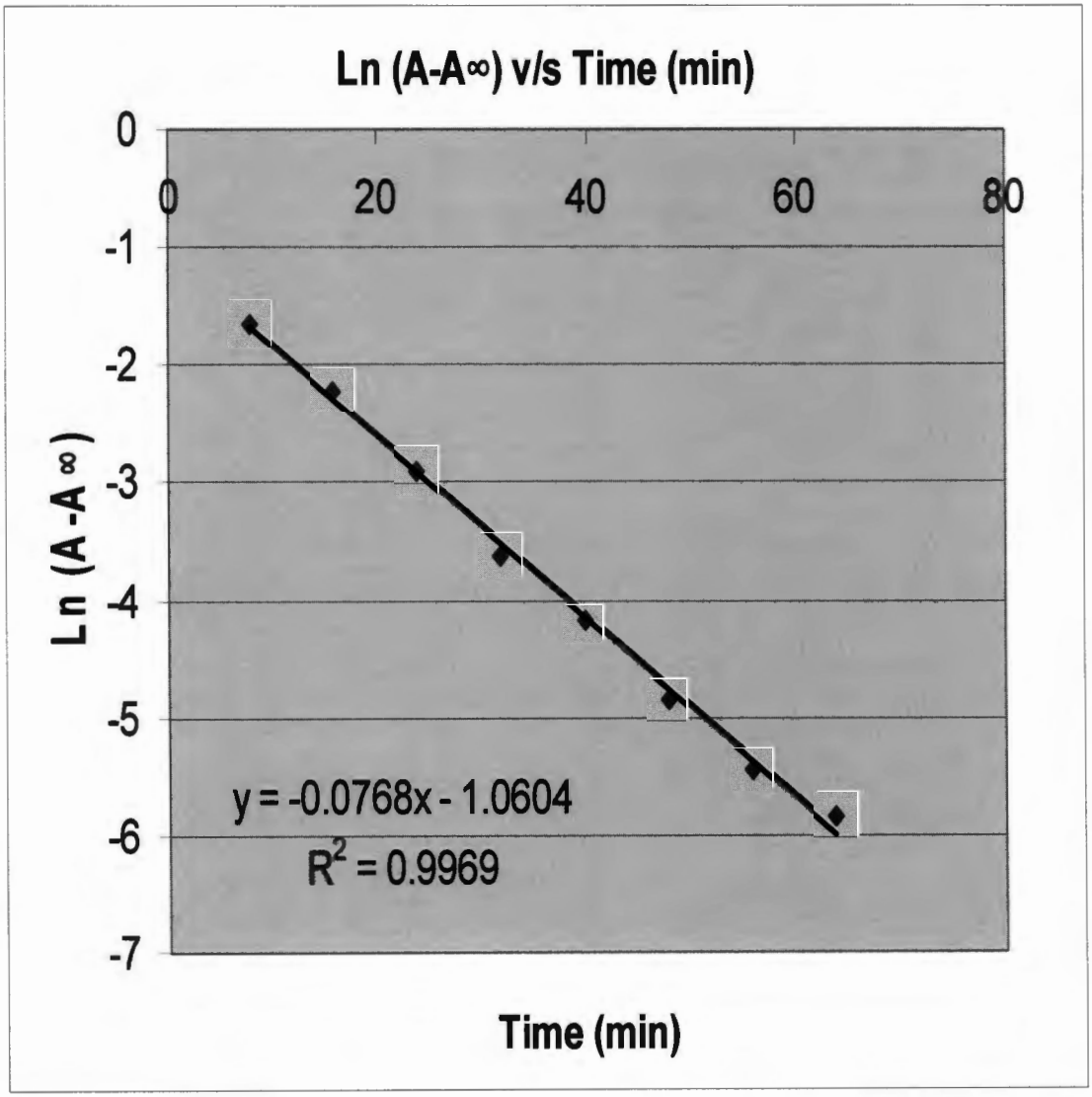

Figure 4.5.8 A plot for direct insertion of Cr(III) into mg(II)-pz at 17°C

Time (min)	5	10	15	20	25	30	35
Ln ($A-A_\infty$)	-1.5944	-2.1568	-2.6644	-3.1168	-3.6045	-3.9922	-4.5623

Table 4.5.9 Absorbance measurement for Cr(III) insertion into mg(II)-pz 20°C

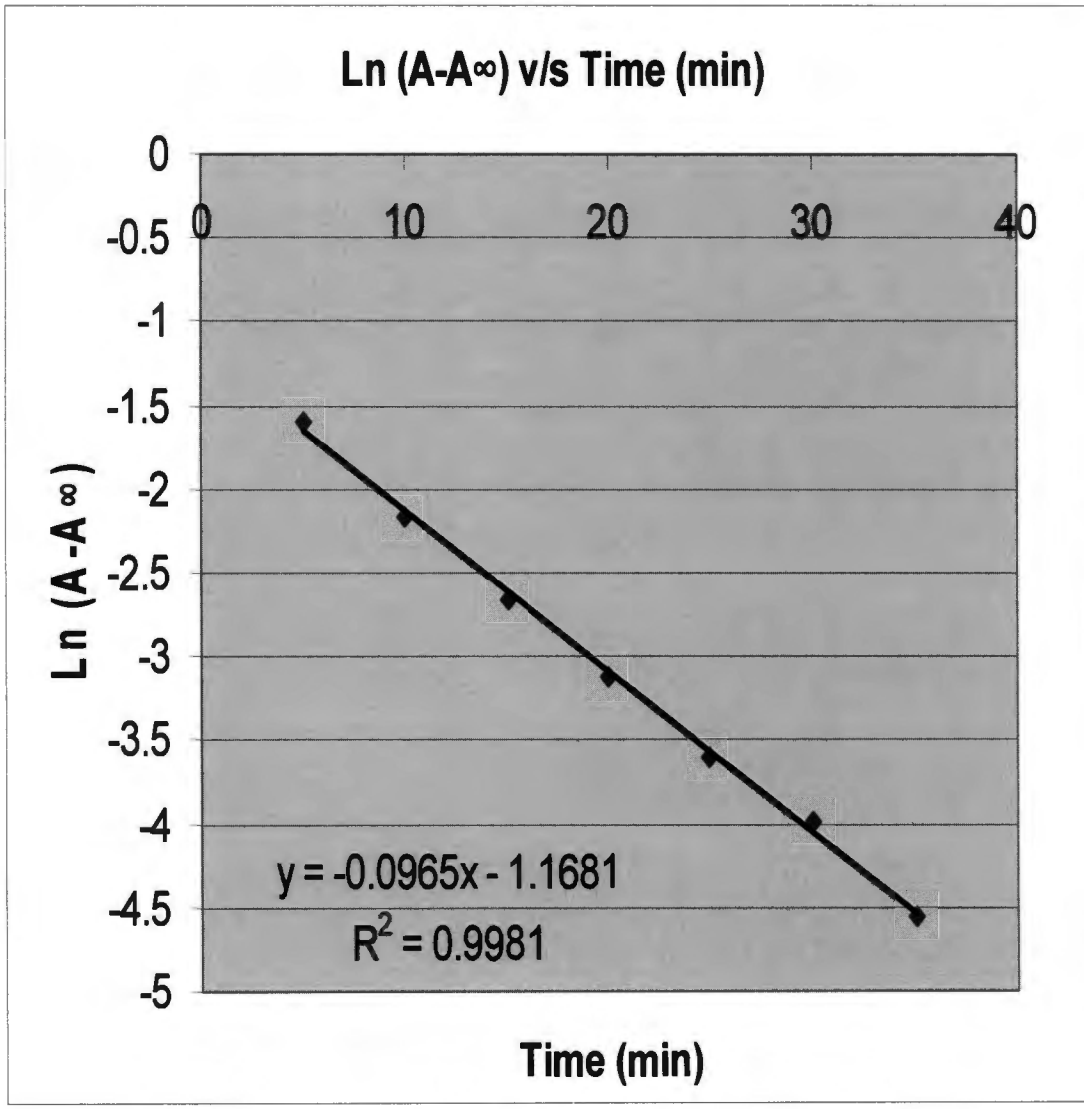

Figure 4.5.9 A plot for direct insertion of Cr(III) into mg(II)-pz at 20°C

Time (min)	4	8	12	16	20	24	28
Ln ($A-A_\infty$)	-1.8283	-2.7986	-3.5032	-4.1235	-4.7226	-5.3224	-5.9992

Table 4.5.10 Absorbance measurement for Cr(III) insertion into mg(II)-pz at 25°C

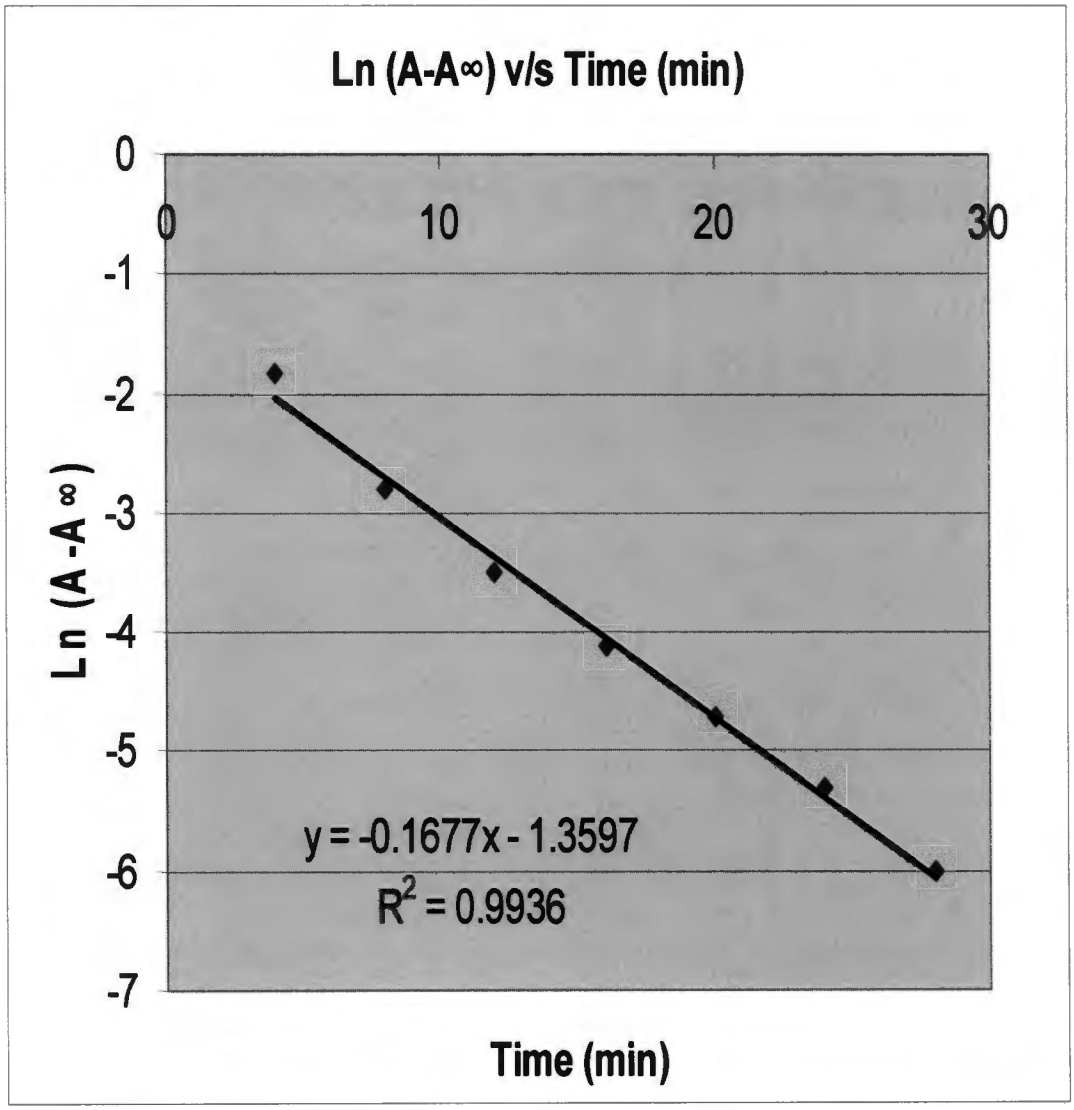

Figure 4.5.10 A plot for direct insertion of Cr(III) into mg(II)-pz at 25°C

Time (min)	3	6	9	12	15	18	21
Ln ($A-A_\infty$)	-1.5962	-2.0994	-2.6641	-3.1917	-3.8397	-4.7261	-5.4512

Table 4.5.11 Absorbance measurement for direct insertion of Cr(III) into mg(II)pz at 30°C

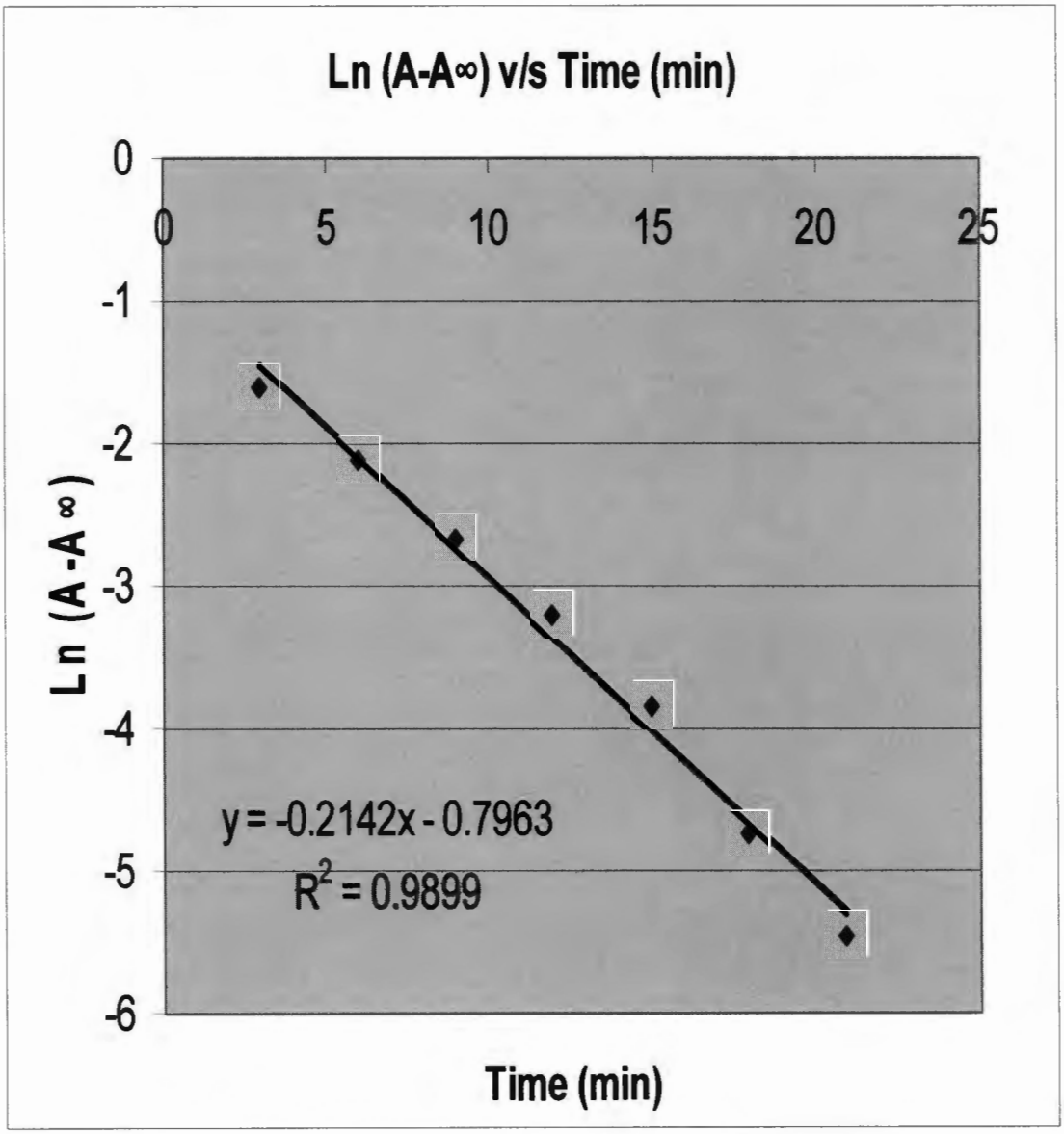

Figure 4.5.11 A plot of direct insertion of Cr(III) into mg(II)-pz at 30°C

Time (min)	2	4	6	8	10	12	14
Ln ($A-A_\infty$)	-1.4987	-2.1426	-2.6311	-3.4204	-4.1065	-4.662	-4.9923

Table 4.5.12 Absorbance measurement for Cr(III) insertion into mg(II)-pz at 35°C

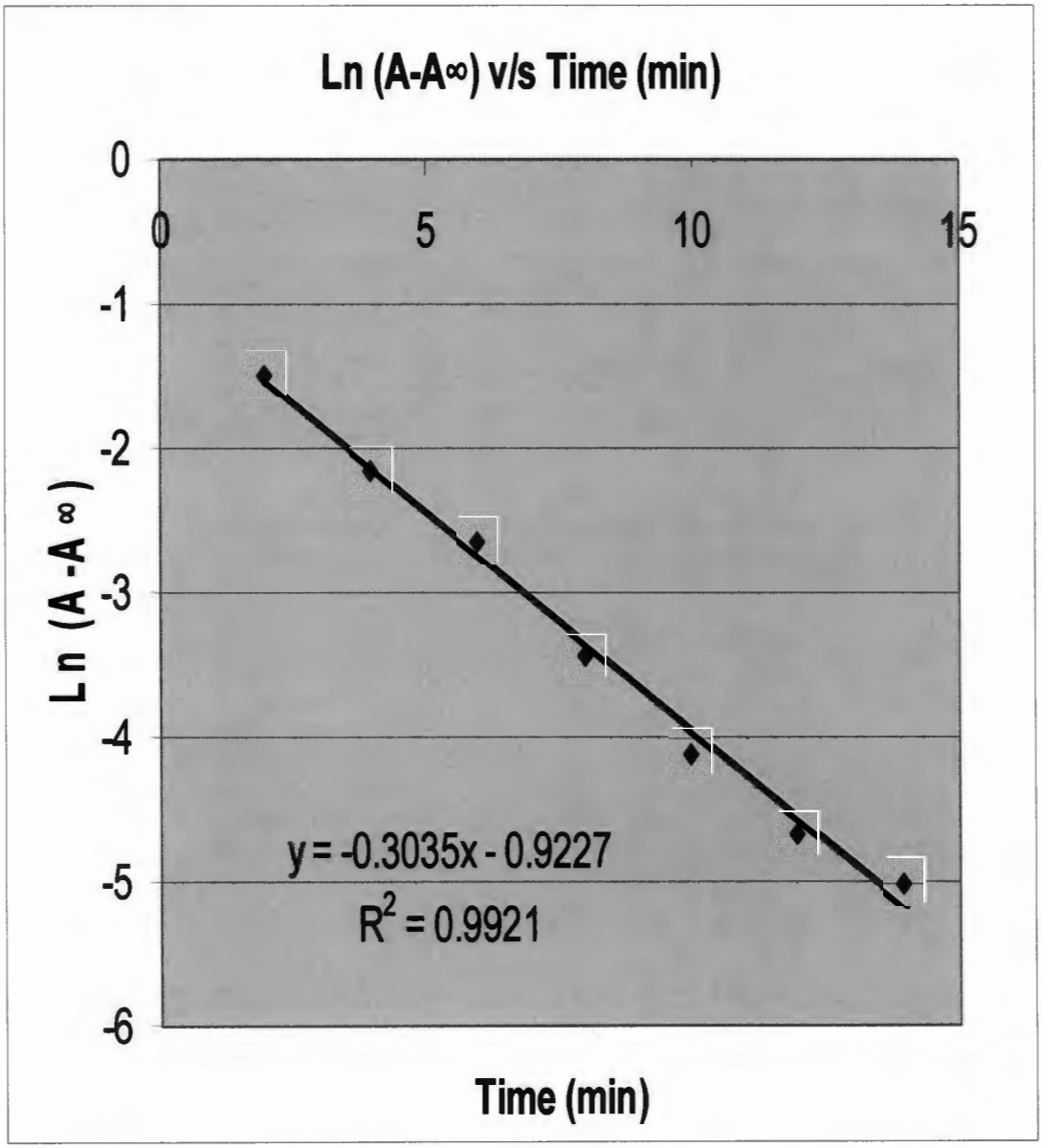

Figure 4.5.12 A plot for direct insertion of Cr(III) into mg(II)-pz at 35°C

4.5.3 Tables and plots of absorbance versus time for insertion of Cr(III) ion into 2,3,9,10,16,17,23,24octa-substituted phthlocyanine

Time (min)	5	10	15	20	25	30	35
Ln ($A-A_\infty$)	-1.4714	-1.6328	-1.9014	-2.0896	-2.1998	-2.5144	-2.7723

Table 4.5.13 Absorbance measurements for Cr(III) insertion into octa-phthalo at 15°C

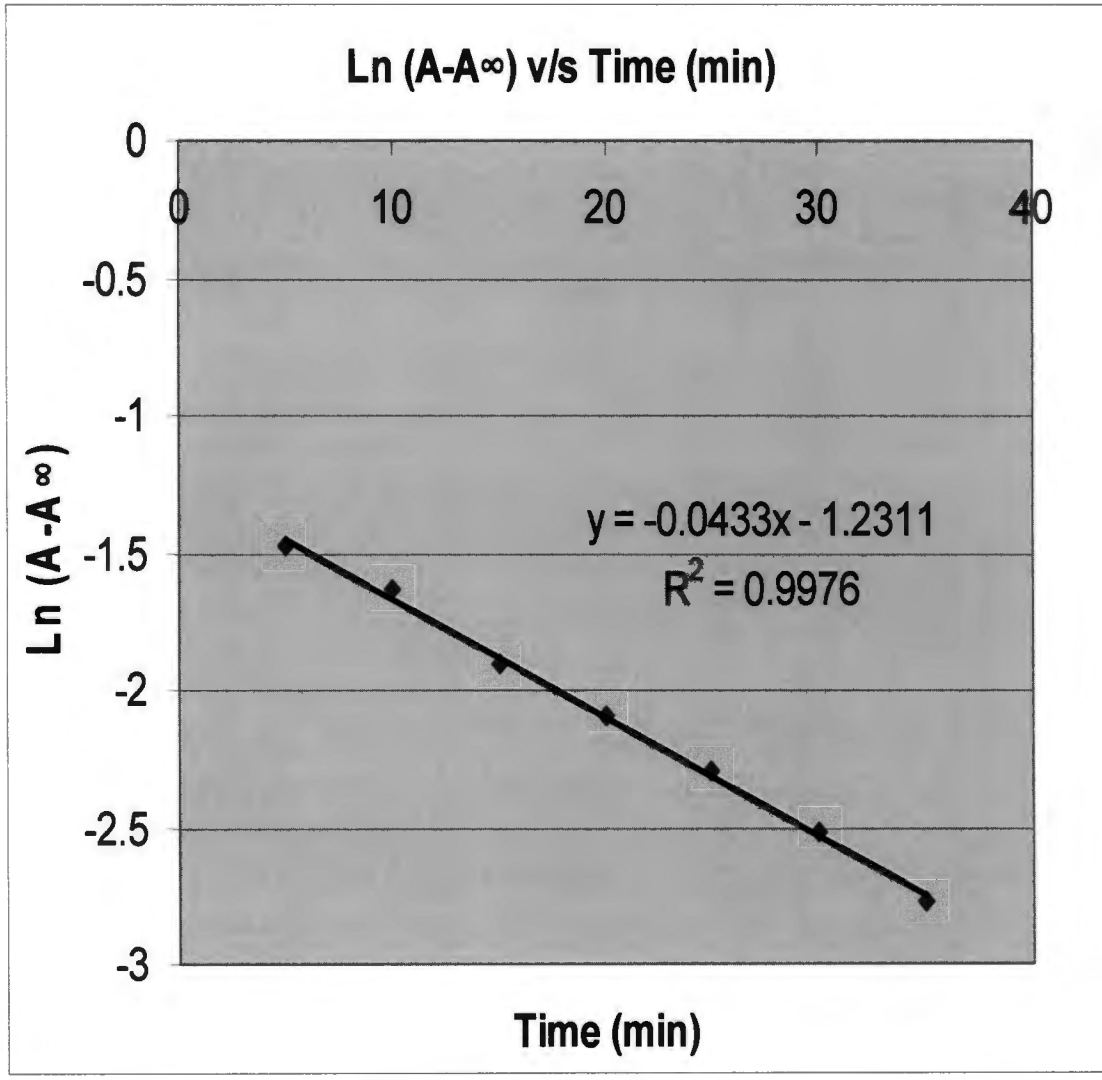

Figure 4.5.13 A plot for Cr(III) insertion into octa-phthalo at 15°C

Time (min)	5	10	15	20	25	30	35
Ln ($A-A_\infty$)	-1.3678	-1.5972	-1.9456	-2.276	-2.5783	-2.9121	-3.2113

Table 4.5.14 Absorbance measurements for Cr(III) insertion into octa-phthalo at 17°C

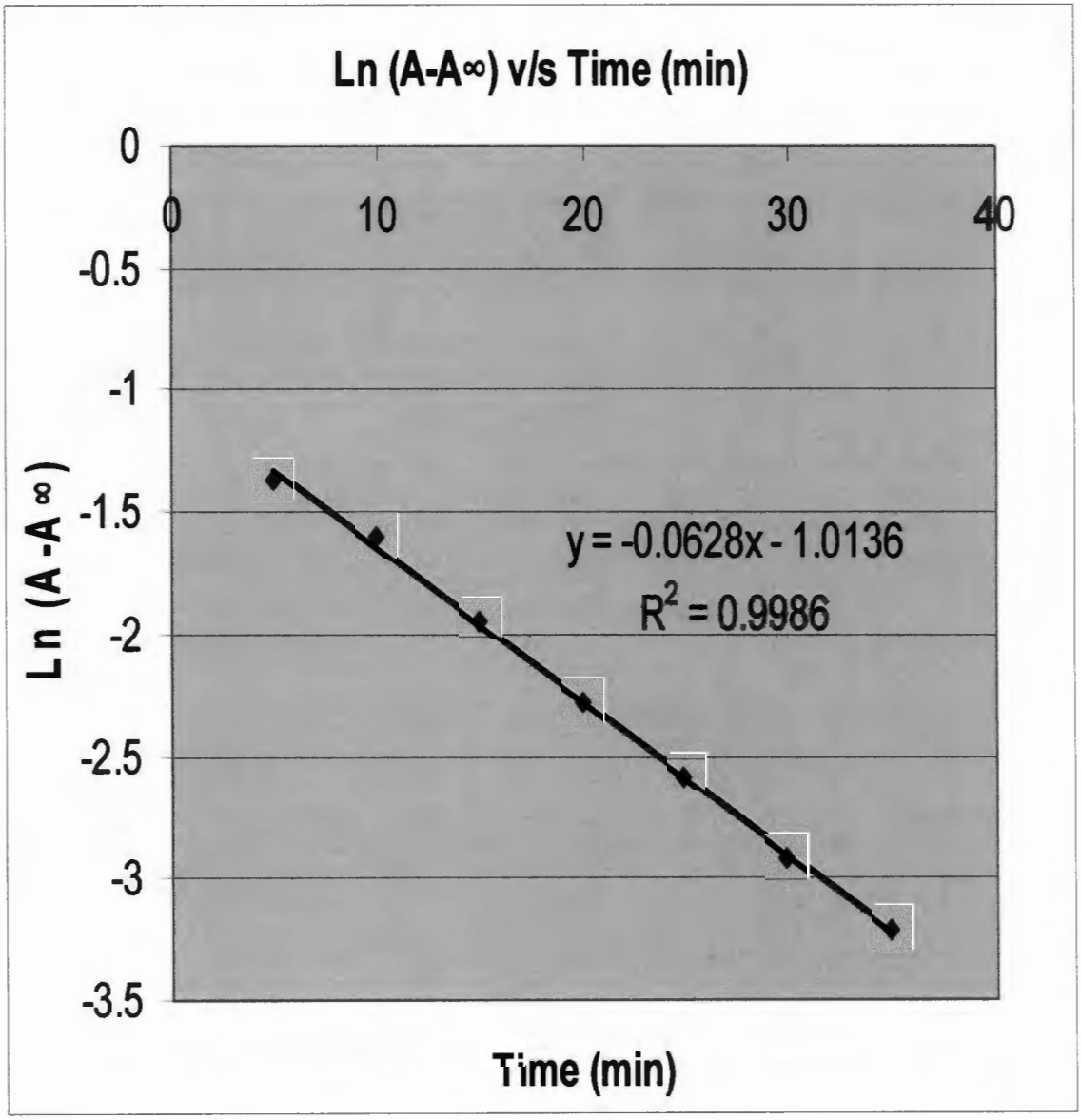

Figure 4.5.14 A plot for Cr(III) insertion into octa-phthalo at 17°C

Time (min)	5	10	15	20	25	30	35
Ln ($A-A_\infty$)	-0.955	-1.2997	-1.6766	-2.0875	-2.4521	-2.7798	-3.1121

Table 4.5.15 Absorbance measurements for Cr(III) insertion into octa-phthalo at 20°C

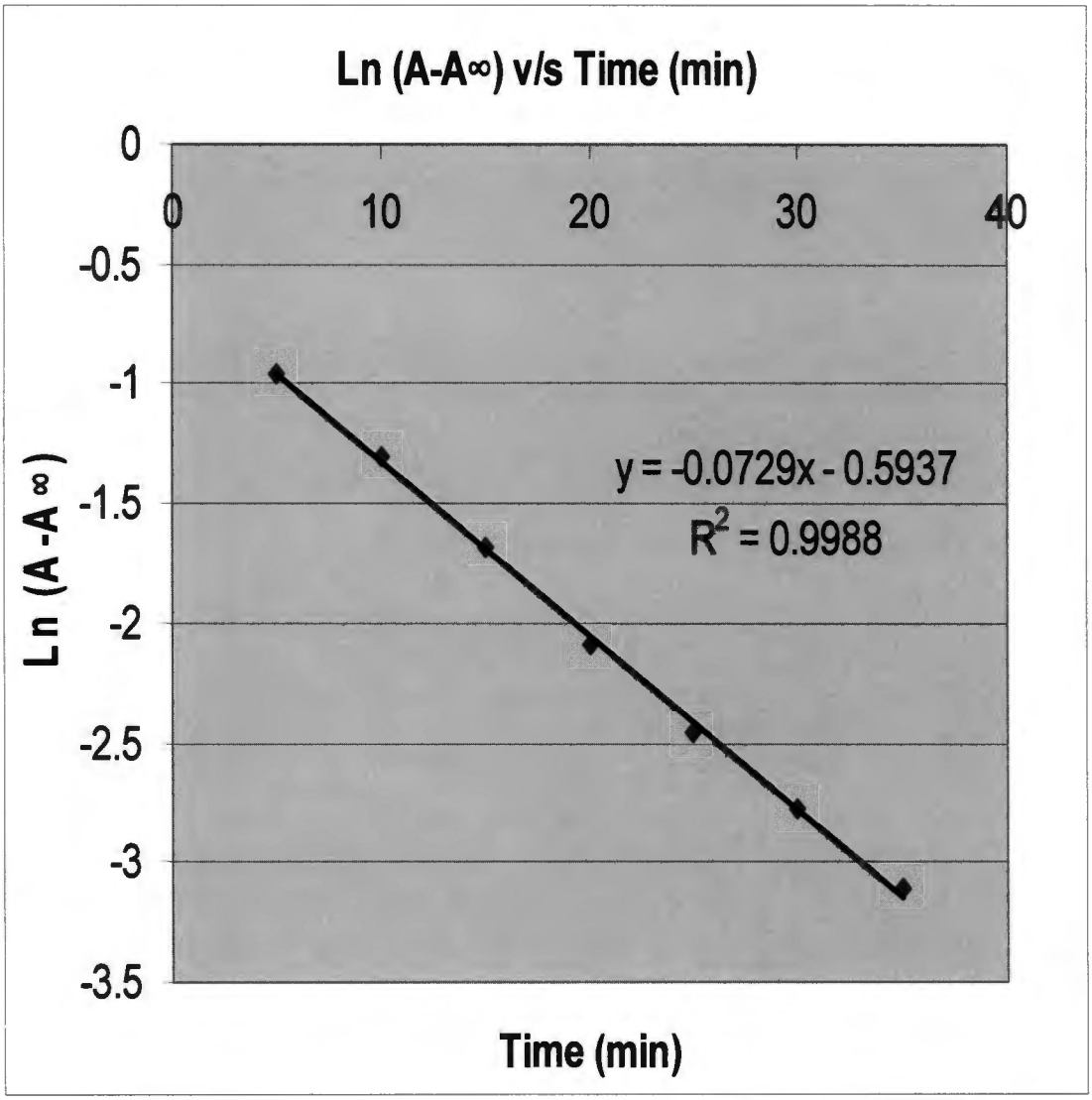

Figure 4.5.15 A plot for Cr(III) insertion into octa-phthalo at 20°C

Time (min)	5	10	15	20	25	30	35
Ln ($A-A_\infty$)	-1.7126	-2.0691	-2.6283	-3.0583	-3.4621	-3.8825	-4.2144

Figure 4.5.16 Absorbance measurements for Cr(III) insertion into octa-phthalo at 25°C

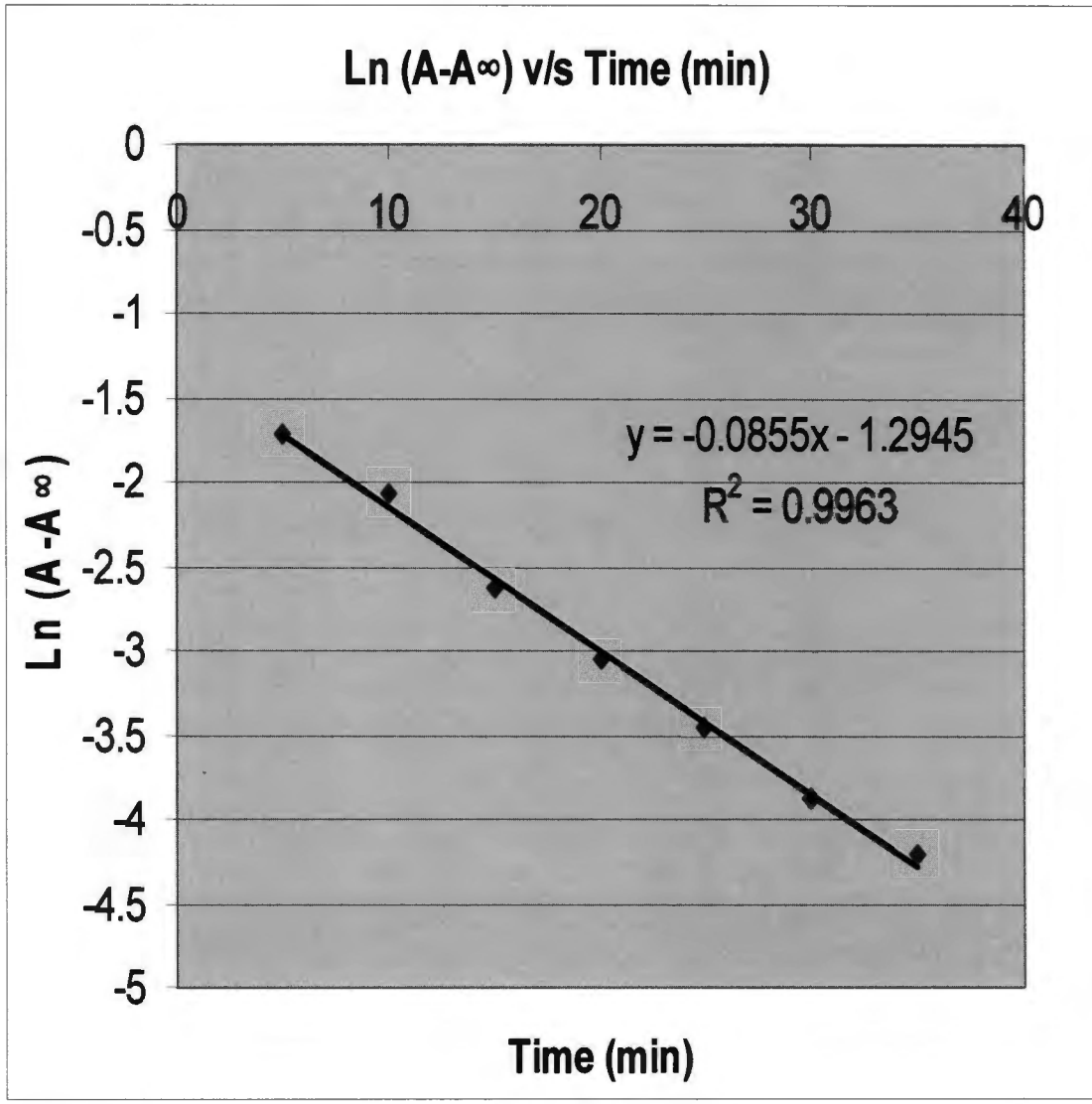

Figure 4.5.16 A plot for Cr(III) insertion into octa-phthalo at 25°C

Time (min)	5	10	15	20	25	30	35
Ln ($A-A_\infty$)	-1.045	-1.5114	-2.0867	-2.6736	-3.0552	-3.4458	-3.9468

Table 4.5.17 Absorbance measurements for Cr(III) insertion into octa-phthalo at 30°C

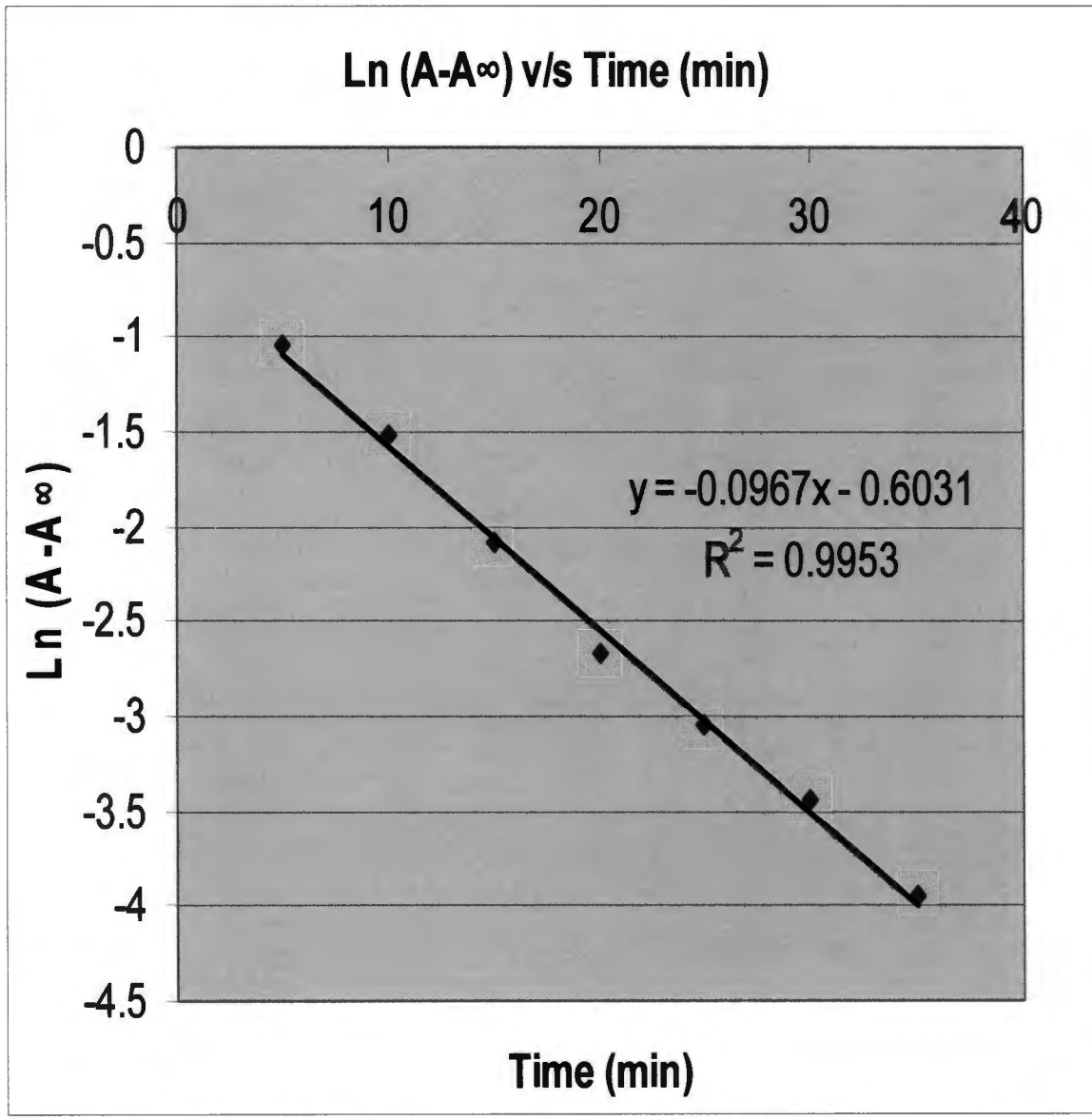

Figure 4.5.17 A plot for Cr(III) insertion into octa-phthalo at 30°C

Time (min)	5	10	15	20	25	30	35
Ln ($A-A_\infty$)	-1.2056	-1.6059	-2.0699	-2.6023	-3.2675	-3.7725	-4.1998

Table 4.5.18 Absorbance measurements for Cr(III) insertion into octa-phthalo at 35°C

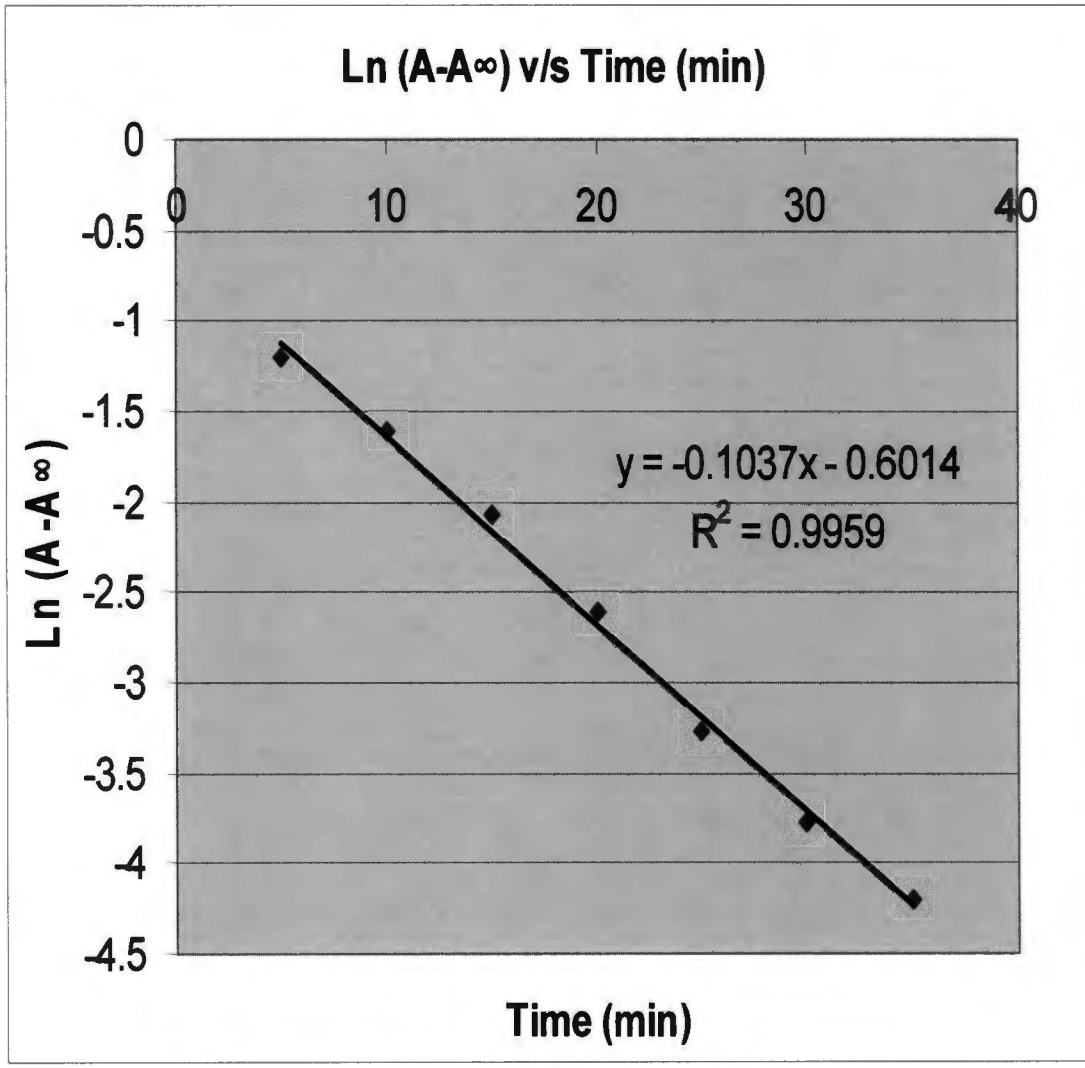

Figure 4.5.18 A plot for Cr(III) insertion into octa-phthalo at 35°C

4.5.4 Tables and plots of absorbance versus time for the reduction of octakis(propyl)porphyrazinechromium(III) complex with octakis(propyl)porphyrazinecobalt(II) complex

Time (min)	5	10	15	20	25	30	35	40
Ln ($A-A_\infty$)	-6.1658	-6.2146	-6.3199	-6.5023	-6.6454	-6.9078	-7.2644	-7.824

Table 4.5.19 Absorbance measurements for reduction at 15°C

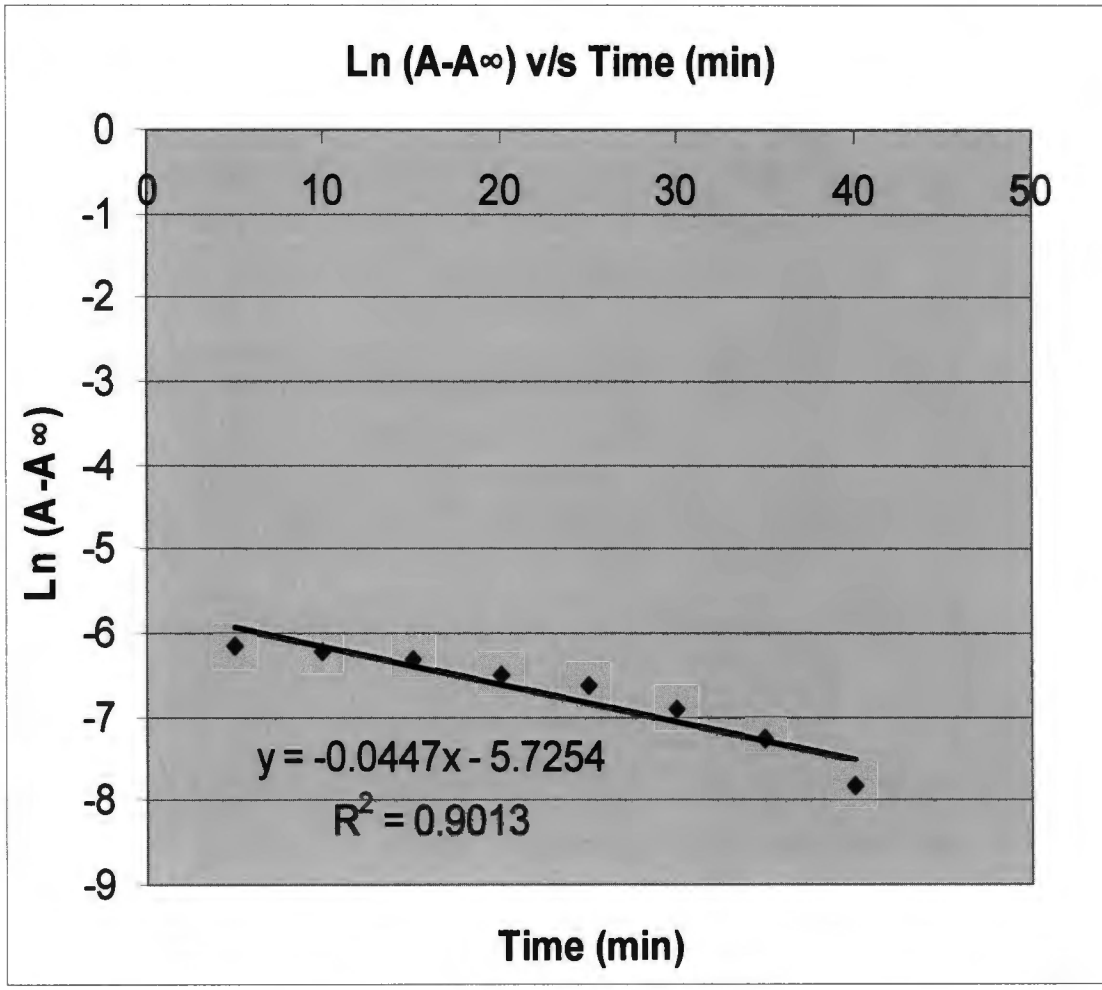

Figure 4.5.19 A plot for reduction at 15°C

Time (min)	5	10	15	20	25	30	35	40
Ln ($A-A_\infty$)	-5.6268	-5.7446	-5.9522	-6.1658	-6.3771	-6.5713	-6.9078	-7.4186

Table 4.5.20 Absorbance measurements for reduction at 17°C

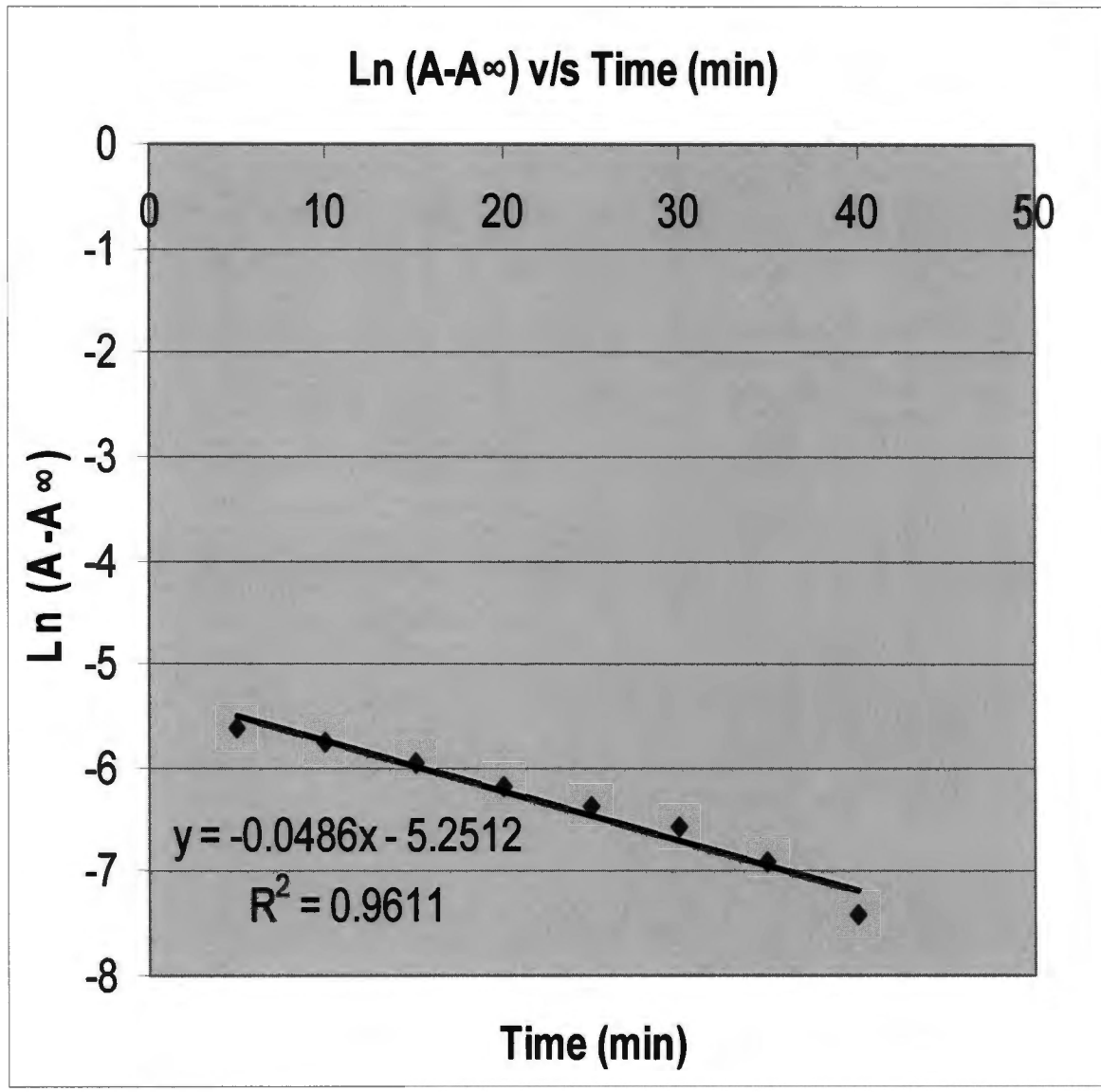

Figure 4.5.20 A plot for reduction at 17°C

Time (min)	5	10	15	20	25	30	35
Ln ($A-A_\infty$)	-5.203	-5.3602	-5.5994	-5.843	-6.1193	-6.4378	-6.8124

Table 4.5.21 Absorbance measurement for reduction at 20°C

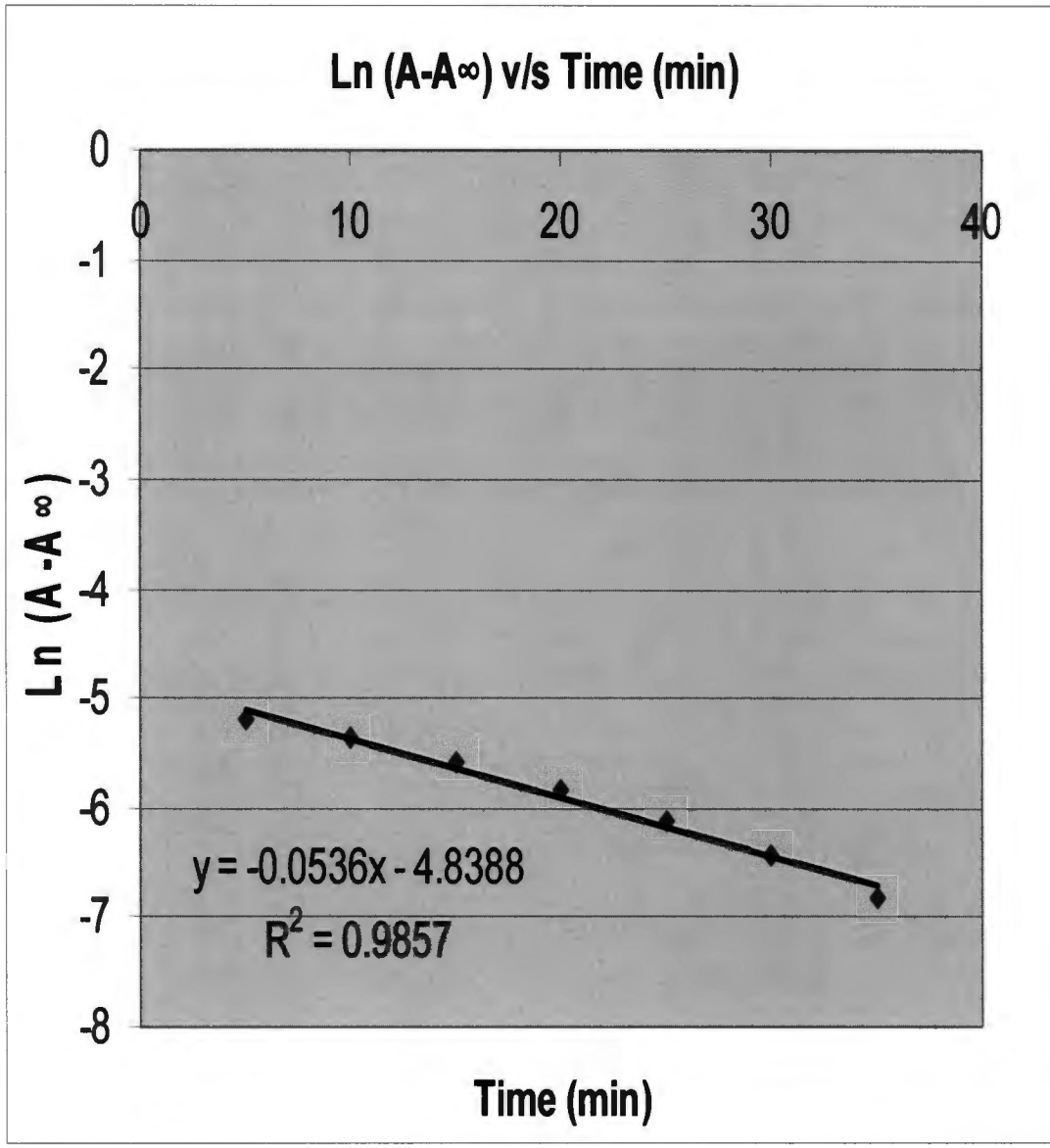

Figure 4.5.21 A plot for reduction at 20°C

Time (min)	5	10	15	20	25	30	35	40
Ln ($A-A_\infty$)	-5.384	-5.743	-5.9145	-6.2658	-6.7023	-6.9924	-7.4186	-7.8117

Table 4.5.22 Absorbance measurements for reduction at 25°C

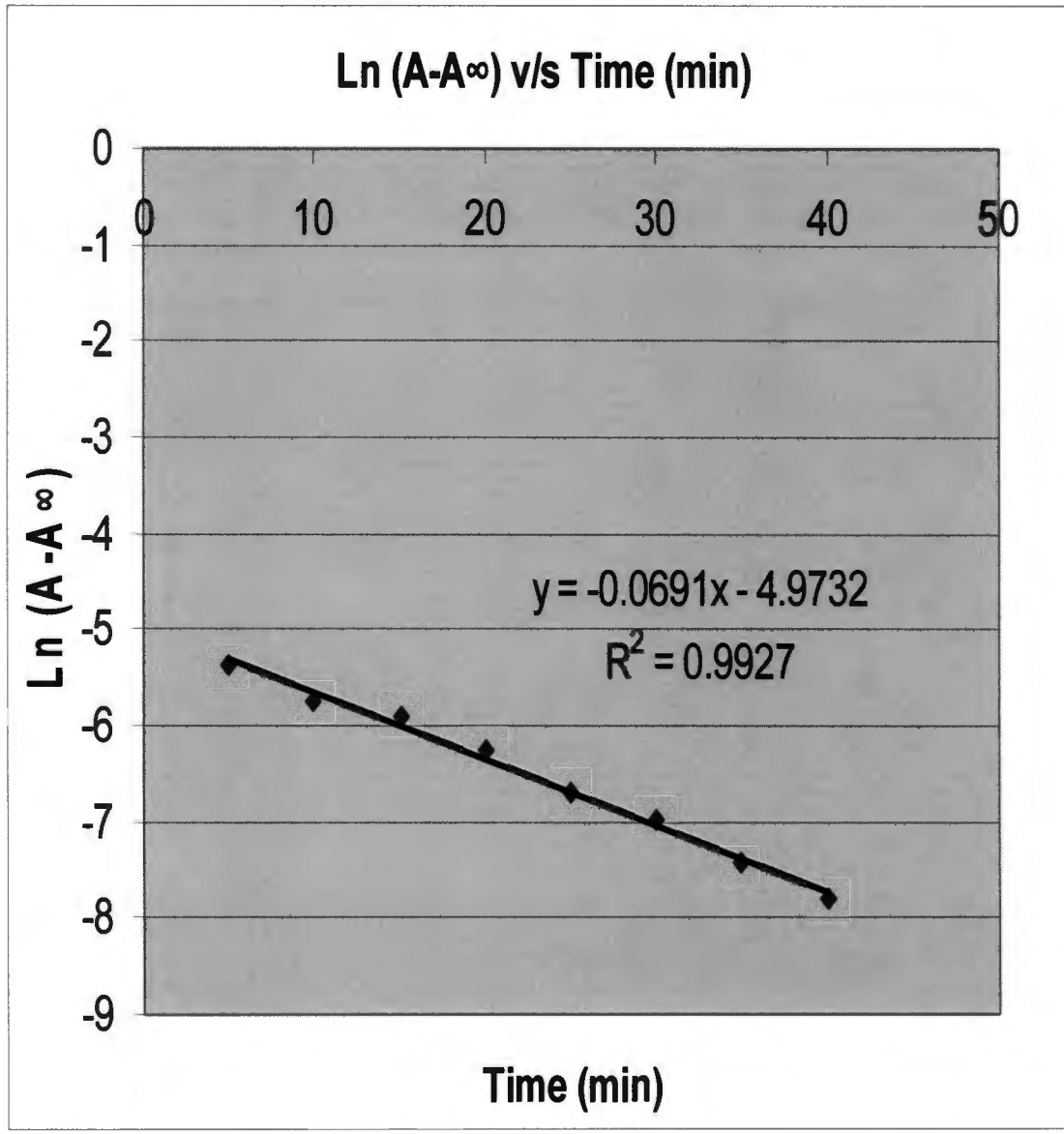

Figure 4.5.22 A plot for reduction at 25°C

Time (min)	5	10	15	20	25	30	35	40
Ln ($A-A_\infty$)	-5.9522	-6.4813	-6.8078	-7.1309	-7.5466	-7.9002	-8.4172	-8.8703

Table 4.5.23 Absorbance measurements for reduction at 30°C

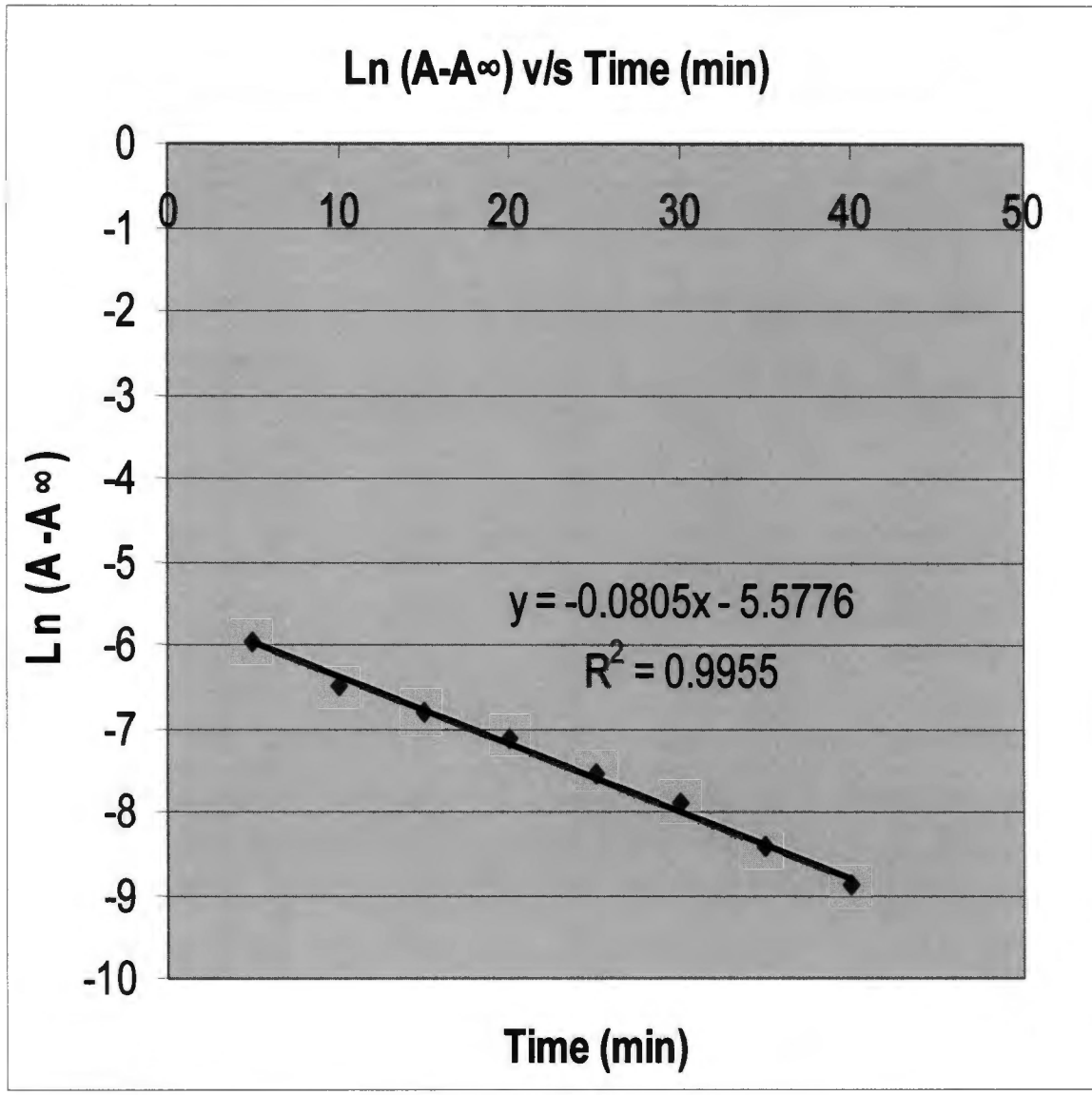

Figure 4.5.23 A plot for reduction at 30°C

Time (min)	5	10	15	20	25	30	35
Ln ($A-A_\infty$)	-3.4119	-4.2223	-4.7735	-5.5915	-6.2771	-6.9078	-7.6009

Table 4.5.24 Absorbance measurement for reduction at 35°C

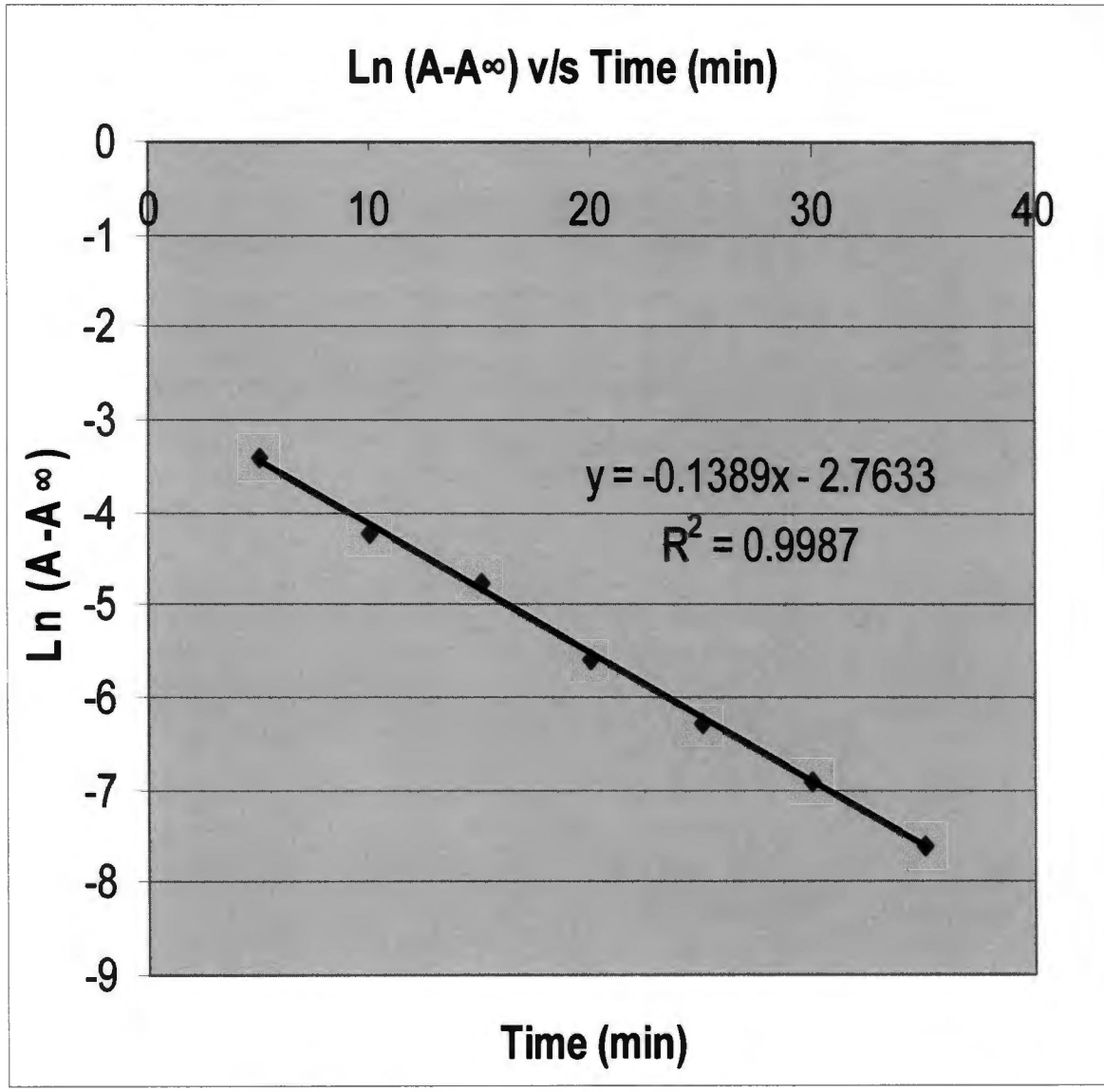

Figure 4.5.24 A plot for reduction at 35°C

4.6 CALCULATION OF THE ACTIVATION ENERGY USING ARRHENIUS EQUATION, $k = A\ e^{-E/RT}$

The individual rates constants for each reaction are summarized in Tables 4.6.1 to 4.6.4 while the plots of ln k versus 1/T for each reaction are shown on Figures 4.6.1 to 4.6.4, which were used to determine the activation energy.

4.6.1 Insertion of Cr(III) into the octakis(propyl)porphyrazine ligand

1/ T (K^{-1})	k (min^{-1})	Ln k
0.00347	0.0655	-2.7257
0.00345	0.0776	-2.5562
0.00341	0.0963	-2.3403
0.00336	0.1732	-1.7533
0.0033	0.2165	-1.5302
0.00325	0.3033	-1.1930

Table 4.6.1 ln k v/s 1/T for Cr(III) insertion into the octakis(propyl) porphyrazine ligand

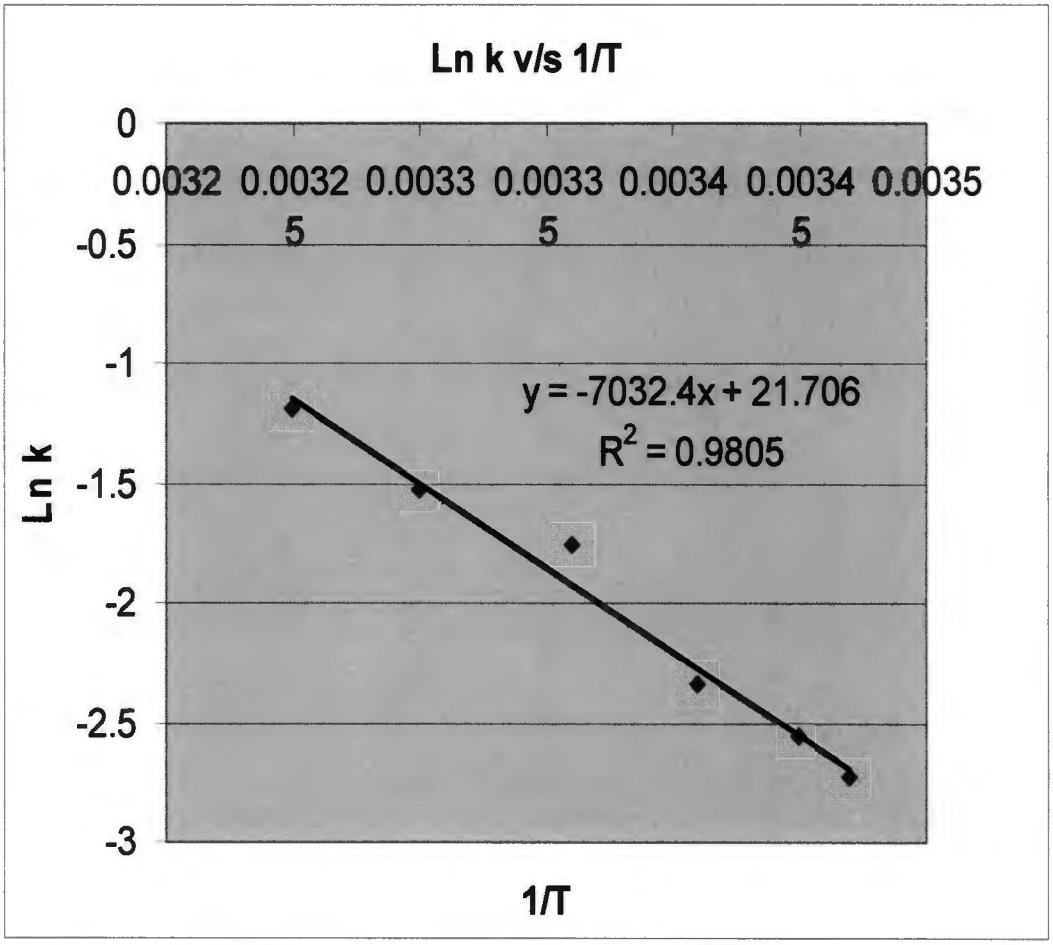

Figure 4.6.1 A plot of ln k v/s 1/T for Cr(III) insertion into the freebase

4.6.1.1 Activation energy of Cr(III) insertion into octakis(propyl) porphyrazine ligand

From the graph above, the slope E/R = 7032.4 K.

$\therefore E = 7032.4\ K \times 8.314\ J\ mol^{-1}\ K^{-1}$

$\therefore E = 58467.37\ J\ mol^{-1}$

$\therefore E = 58.47\ kJ\ mol^{-1}$

4.6.2 Direct insertion of Cr(III) into octakis(propyl)porphyrazine magnesium(II) complex

1/ T (K^{-1})	0.00347	0.00345	0.00341	0.00336	0.0033	0.00325
k (min^{-1})	0.0649	0.0768	0.0965	0.1677	0.2142	0.3035
Ln k	-2.7349	-2.5666	-2.3382	-1.7856	-1.5408	-1.1924

Table 4.6.2 ln k v/s 1/T for Cr(III) insertion into the mg(II)-pz complex

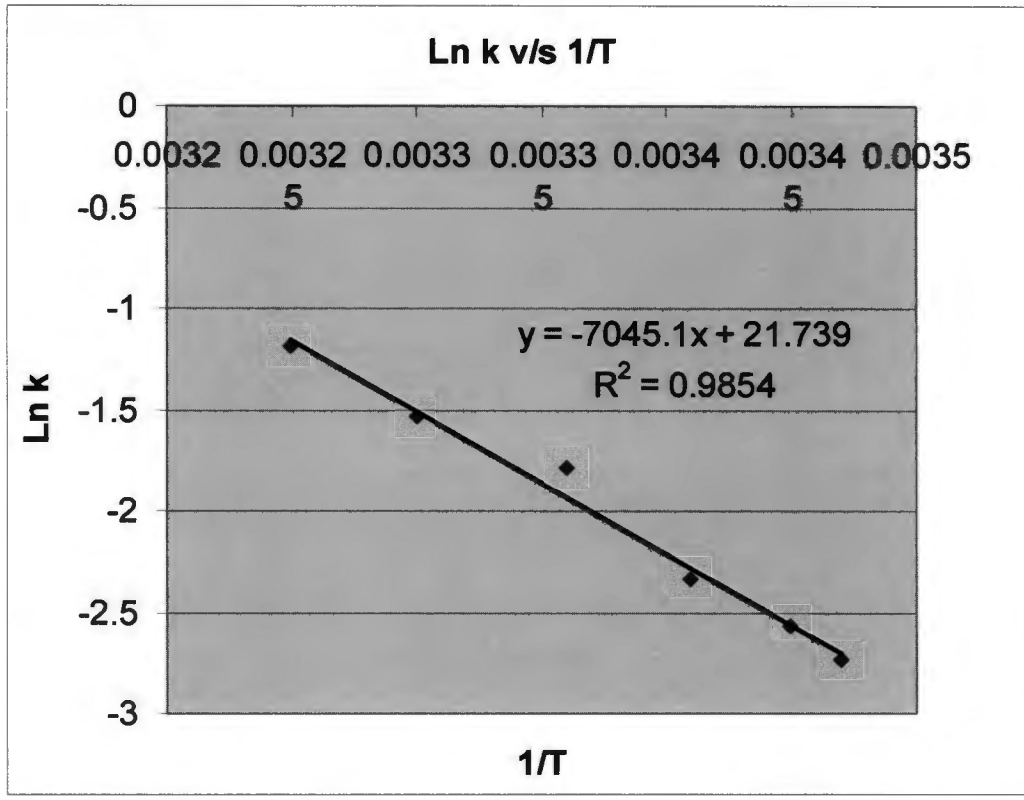

Figure 4.6.2 A plot of ln k v/s 1/T for the Cr(III) insertion into mg(II)-pz complex

4.6.2.1 Activation energy of Cr(III) insertion into mg(II)-pz complex

From the graph above, the slope E/R = 7045.1 K

$\therefore E = 7045.1\ K \times 8.314\ J\ mol^{-1}\ K^{-1}$

$\therefore E = 58572.96 J\ mol^{-1}$

$\therefore E = 58.57\ kJ\ mol^{-1}$

4.6.3 Insertion of Cr(III) into 2,3,9,10,16,17,23,24octa-substituted phthalocyanine

1/ T (K^{-1})	0.00347	0.00345	0.00341	0.00336	0.0033	0.00325
k (min^{-1})	0.0433	0.0628	0.0729	0.0855	0.0967	0.1037
Ln k	-3.1396	-2.7678	-2.6187	-2.4592	-2.3361	-2.2663

Table 4.6.3 ln k v/s 1/T for Cr(III) insertion into 2,3,9,10,16,17,23,24octa-substituted phthalocyanine

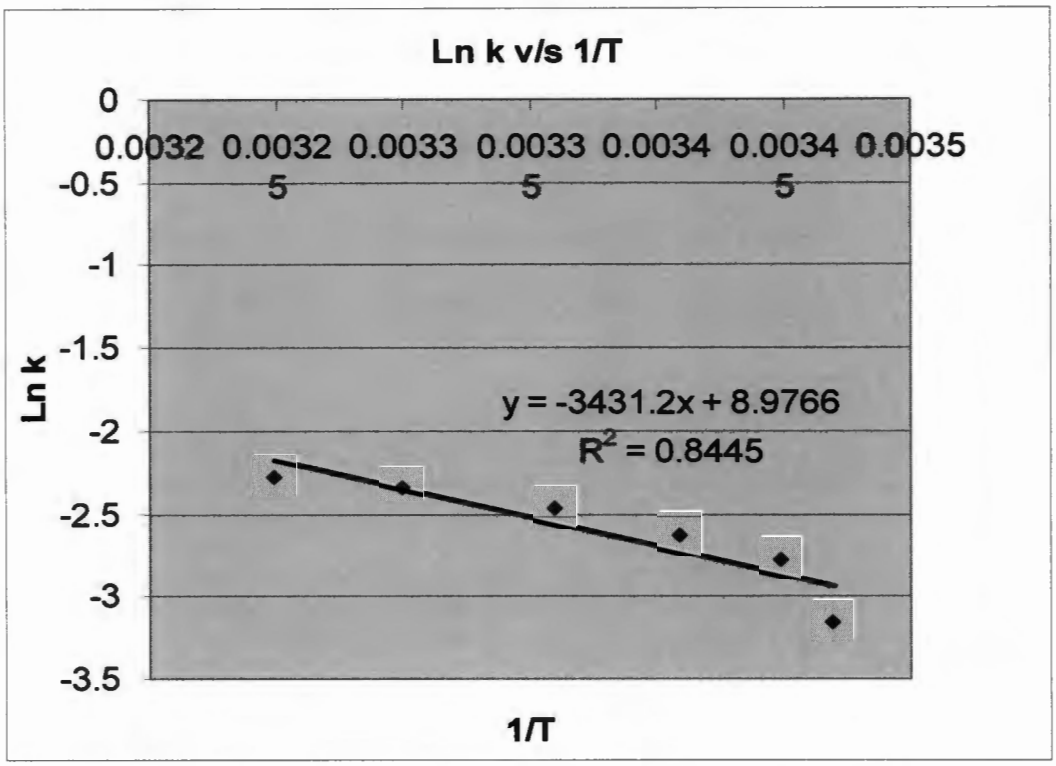

Figure 4.6.3 Plot of ln k v/s 1/T for insertion of Cr(III) ion into 2,3,9,10,16,17,23,24octa-substituted phthalocyanine

4.6.3.1 Activation energy of Cr(III) insertion into 2,3,9,10,16,17,23,24octa-substituted phthalocyanine

From the graph above, the slope E/R = 3431.2 K

$\therefore E = 3431.2\ K \times 8.314\ J\ mol^{-1}\ K^{-1}$

$\therefore E = 28526.99\ J\ mol^{-1}$

$\therefore E = 28.53\ kJ\ mol^{-1}$

4.6.4 Reduction of octakis(propyl)porphyrazinechromium(III) complex with octakis(propyl)porphyrazinecobalt(II) complex

1/ T (K^{-1})	0.00347	0.00345	0.00341	0.00336	0.0033	0.00325
k (min^{-1})	0.0447	0.0486	0.0536	0.0691	0.0805	0.1389
Ln k	-3.1078	-3.0241	-2.9262	-2.6722	-2.5195	-1.9740

Table 4.6.4 ln k v/s 1/T for Cr(III) reduction by Co(II)

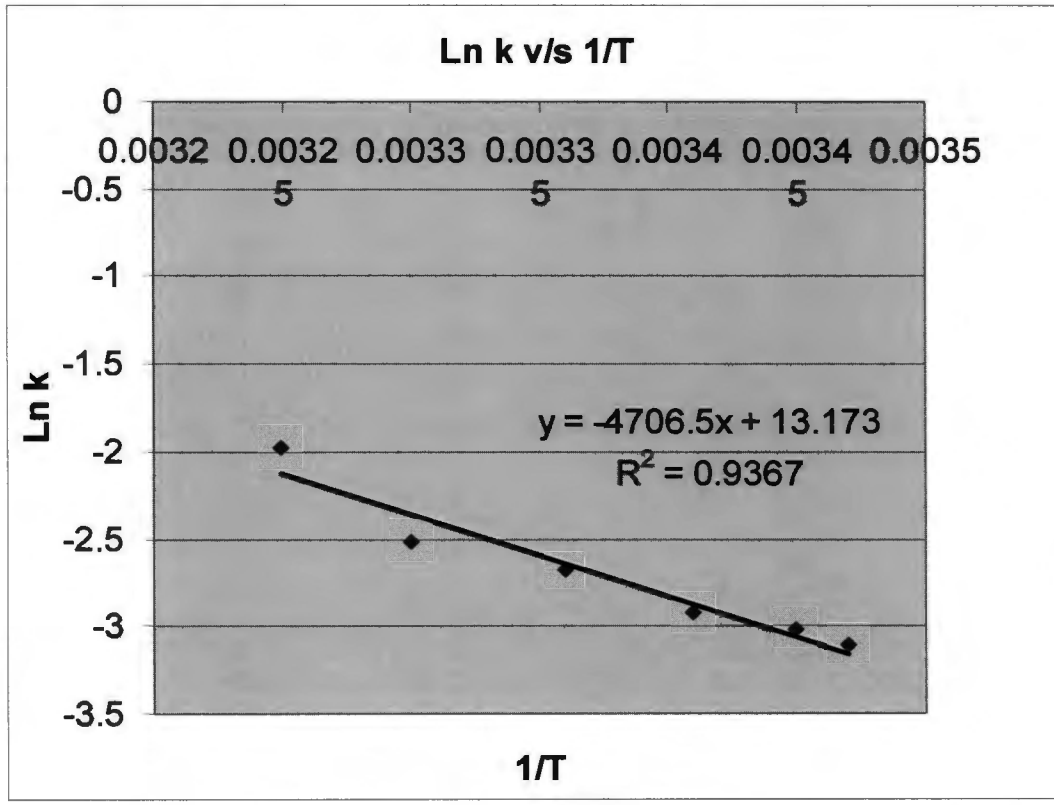

Figure 4.6.4 A plot of ln k v/s 1/T for reduction of octakis(propyl)porphyrazinechromium(III) complex with octakis(propyl)porphyrazinecobalt(II) complex

4.6.3.1 Activation energy for reduction

From the graph above, the slope E/R= 4706.5 K

$$\therefore E = 4706.5\ K \times 8.314\ J\ mol^{-1}\ K^{-1}$$

$$\therefore E = 39129.84\ J\ mol^{-1}$$

$$\therefore E = 39.13\ kJ\ mol^{-1}$$

CHAPTER 5

DISCUSSION

5.1 Preparation of the compounds

5.1.1 Octakis(propyl)porphyrazinemagnesium(II) complex

The octakis(propyl)porphyrazinemagnesium(II) complex was successfully synthesized from maleonitriles via the Linstead's template cyclization. The treatment of internal alkyne with one equivalent of bromine, in the presence of bromide ion, produced a *trans*-dibromoalkene. These vinylic dibromides were converted to fumaronitriles. The fumaronitriles were photoisomerised, using a mercury lamp, to the maleonitriles. After 30 hours the reaction reached photostationary state and was stopped. The mixture contains both the *cis*- and *trans*-isomers. Fractional distillation under high vacuum was used to separate these isomers. Even though the *trans*-isomer was isolated first at about 40°C, the desired *cis*-isomer was isolated with a low yield of 22 g. However with column chromatography the yield was improved.

It was observed that the yield of the octakis(propyl)porphyrazine magnesium(II) complex was higher when the maleonitrile was used as the starting material as opposed to the fumaronitrile. This was expected since in order to cyclizise, the two nitrile groups are supposed to be *cis*- to each

other. The magnesium(II)porphyrazine was fairly soluble in chloroform and dichloromethane respectively, and was separated from other additional porphyrazines formed during the reaction by column chromatography.

5.1.2 2,3,9,10,16,17,23,24octa-substituted phthalocyanine

The synthesis of the 2,3,9,10,16,17,23,24octa-substituted phthalocyanine was done when a solution of 4-nitrophthalonitrile was reacted with phenol, in the presence of tetrahydrofuran, at lower temperatures to form the 1,2-diisocyano-4-phenoxybenzene. 1,2-diisocyano-4-phenoxybenzene was further reacted with 1,8 diazabicyclo[5.4.0]-undec-7-ene, in the presence of methanol to give the 2,3,9,10,16,17,23,24octa-substituted phthalocyanine. Soxhlet extraction with methanol and acetone gave a green precipitate, which was dried at 60°C and purified by flash chromatography. (Yield = 0.294 g, 98%)

5.2 Demetallation of magnesium(II)porphyrazine

The demetallation of magnesium(II)porphyrazine was achieved by the reaction of magnesium(II) porphyrazine complex with trifluoro acetic acid, forming the freebase ligand. Rotary evaporation gave the ligand as a dark blue solid. This ligand was fairly soluble in dichloromethane and

chloroform. Both the ultraviolet-visible spectrum and infrared confirmed the removal of magnesium(II) from the macrocyclic ligand.

5.3 Characterisation of Compounds

5.3.1 ^{1}H and ^{13}C NMR spectra

The ^{1}H and ^{13}C NMR spectra of the molecules are described below as these indicate the positions and different shifts for each molecule in a compound. The ^{1}H NMR of 4,5-dibromo-4E-octene indicates a triplet that appears in the upfield position at 0.922 ppm, a quartet at 1.64 ppm and a triplet at 2.546 ppm in the downfield position. The triplet at the upfield position is for the aliphatic protons while the triplet in the downfield position is for the allylic protons. The ^{13}C spectra indicate alkyl carbon shifts in the upfield (δ 13.09, 21.24, and 35.67) position and carbon atoms with the double bonds at downfield (δ 115.35 and 129.10) position.

The ^{1}H NMR spectra of fumaronitrile indicate a triplet at the upfield at 0.89 ppm, a quartet at 1.58 ppm and a triplet at 2.44 ppm at the downfield position. The ^{13}C spectra indicate the alkyl carbon atoms at the upfield (δ 12.59, 20.77, and 35.19) and the carbon double at downfield (δ 114.94 and 128.70). As compared to the 4,5-dibromo-4E-octene, in the fumaronitrile,

the proton and carbon shifts are moved to an upfield position, this might be caused by the change in the substituents within a molecule.

Similarly the ^{1}H and ^{13}C spectra of maleonitrile resemble those of the fumaronitrile, with a slight shift on the allylic protons to the downfield, while the alkyl carbon is moved to the upfield and the carbon with the double bond is moved to the downfield. The ^{1}H NMR confirms the existence of the propyl groups and a single alkene signal, in both the maleonitrile and fumaronitrile, which are fully in agreement with the structure.

The ^{1}H NMR for 1,2-diisocyano-4-phenoxybenzene indicates several broad bands at a region of ~7.05 to 7.53 ppm, which represent aromatic protons. The ^{13}C shifts for the C-CN appears in the upfield position at 71.02 ppm, while C=C signals appear at a downfield position at 117-135.50 ppm.

The ^{1}H NMR for the octa-substituted phthalocyanine indicates the chemical shift of the N-H at the upfield position around 1-2 ppm, while the aromatic protons where observed at 7-8 ppm. The ^{13}C NMR indicates the shift at 114-135 ppm which is for the C=C, and the shift at 153-162 which was due to the C-OR in the peripheral positions. ^{1}H NMR confirms the aromatic nature of

the molecule, as observed in the appearance of the N-H, and C=C signals. The NMR spectrum was in agreement with the structure.

5.3.2 Ultraviolet-visible spectrum of compounds

The ultraviolet-visible spectrum was used to confirm different electronic transitions within the compound. The ultraviolet-visible spectrum of octakis(propyl)porphyrazinemagnesium(II) complex showed the electronic transitions (λ_{max} nm, absorbance), a Soret peak at 345.9 nm (0.694 abs), a shoulder at 547.7 (0.1686 abs),a peak in the blue region at 599.5 nm (0.817 abs) and a Q band at 638.5 (0.168 abs).

The ultraviolet-visible spectrum of the demetallated octakis(propyl)porphyrazine ligand has shown the electronic transitions (λ_{max} nm, absorbance) at different transitions, a Soret peak at 340 nm (1.363 abs), 558.0 nm (0.783 abs), a peak at 626.1 nm (1.244 abs) and a shoulder at 598.0 nm (0.234 abs). These results are closely related to those mentioned in the literature[9] as shown in Table 5.1 whereby a Soret peak was centered at 340.0 nm, and the peak at 558 nm was due to the n-π^* transitions from the lone pair electrons from the external nitrogen atoms into a π^* ring orbital, and a blue shifted peak at 626 nm.

Literature (nm)	338	554	630
Observed (nm)	340	558	626

Table 5.1 Absorption peaks for the freebase

Comparing the results of the freebase and the magnesium(II) complex, the major changes were on the Q-bands, for the magnesium(II) complex there was only one Q band at 599.5 nm and for the freebase ligand, the Q bands were split into two Q_x and Q_y at λ_{max} at 558.0 nm and 626.1 nm respectively. The peaks were shifted to the blue region, this shift was caused by the change in symmetry of two compounds from the D_{4h} to a D_{2h} symmetry.

The Soret peak was red shifted by ~5 nm. The electronic transitions observed with octakis(propyl)porphyrazinemagnesium(II) complex and the freebase porphyrazine are explained by Gouterman's four orbital model for porphyrinic macrocycles. Since the octakis(propyl)porphyrazine magnesium(II) is a D_{4h} symmetric macrocycle, the LUMO is doubly degenerate (e_g), and the Q and B bands are due to transitions from the highest occupied MO's (a_{1u} and a_{2u}) into the LUMO.

The removal of the central magnesium metal from the ligand results into the formation of a freebase porphyrazine and change from D_{4h} to a D_{2h}

macrocycle. The reduction in symmetry of the macrocycle removes the degeneracy of the e_g orbital and therefore LUMO gives rise to split Q-bands, as shown in Figure 5.1

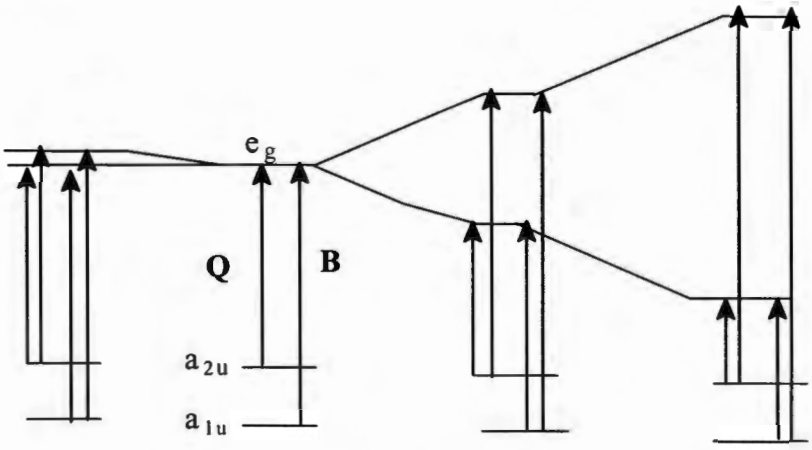

Figure 5.1 Orbital energy diagram showing electron transitions in porphyrazines

The ultraviolet-visible spectrum of the $Cr.Cl_3.6H_20$ ion in ethanol showed two broad peaks at 458.4 nm (2.6778 abs) and at 640.7 nm (1.9945 abs). These were the expected transitions of a d^3 ion, which were due to the following spin-allowed transitions $^4A_{2g} \rightarrow {}^4T_{2g}$ (F), $^4A_{2g} \rightarrow {}^4T_{1g}$ (F).

The ultraviolet-visible spectra of $Co(NO_3)_2.6H_20$ in ethanol showed one broad peak. This peak was due to the spin-allowed transition $^4T_{1g}$ (F) $\rightarrow {}^4T_{2g}$ (F) in a d^7 compound.

The electronic spectra of chromium(III) insertion into octakis(propyl)porphyrazine ligand showed a change at 462 nm, which confirms the insertion of chromium(III) ion into the freebase. The other peaks were blue shifted, a Soret peak at ~7.00 nm and the Q band at ~1.1 nm.

The electronic spectra of cobalt(II) insertion into octakis(propyl) porphyrazine ligand showed slight changes at a region around 500 nm-550 nm. The peak at a region at 550 nm confirms the insertion of the cobalt in the porphyrazine while the Soret peak is red shifted about 5.1 nm and a Q band is blue shifted about 1.8 nm.

The electronic spectra of chromium(III) insertion into the octakis(propyl)porphyrazinemagnesium(II) complex showed the changes at 470 nm, which confirms the insertion of chromium(III) ion in the complex. The other peaks were broad, a shoulder at 547 nm was red shifted about 10.1 nm while the Q band was blue shifted about 8.4 nm, and a Soret peak was not observed.

The electronic spectra of octa-substituted phthalocyanine showed a Soret band at 325.9 nm (1.8832 abs) which arises from the deeper π levels to the LUMO transition. Two split Q bands at 668 nm (1.048 abs) and at 704 nm

(1.124 abs) were observed. The transitions at the Q-band are also responsible for the green colour of the complex, and they are assigned to the π-π^* transitions, which are correlated with the $a_u \rightarrow b_{2g}$ and $a_u \rightarrow b_{3g}$ transitions.

The ultraviolet-visible spectrum confirms the reduction of chromium(III). The position of the signal of chromium(III) insertion into both the freebase and magnesium(II)porphyrazine was at 465 nm and 467 nm respectively, whereas the position during the reduction was shifted to 586 nm. This shift was caused by the conversion of chromium(III) to chromium(II) within the macrocylce.

5.3.3 The infrared spectrum

The frequencies of various groups are summarised in Tables 5.1 and 5.2 for the compounds. The most important absorption band for the octakis(propyl)porphyrazine ligand, which confirms the removal of the magnesium in the complex, is in a region of 3395.74 cm^{-1} which confirms the presence of NH groups, which is lacking in the magnesium(II) porphyrazine, as shown in Figure 5.2 and Figure 5.3.

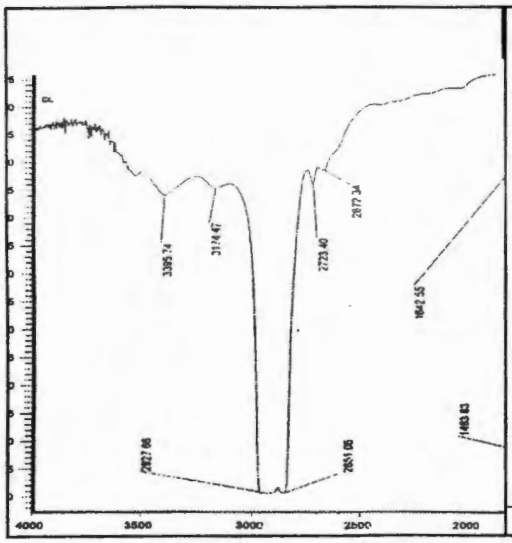

Figure 5.2 freebase

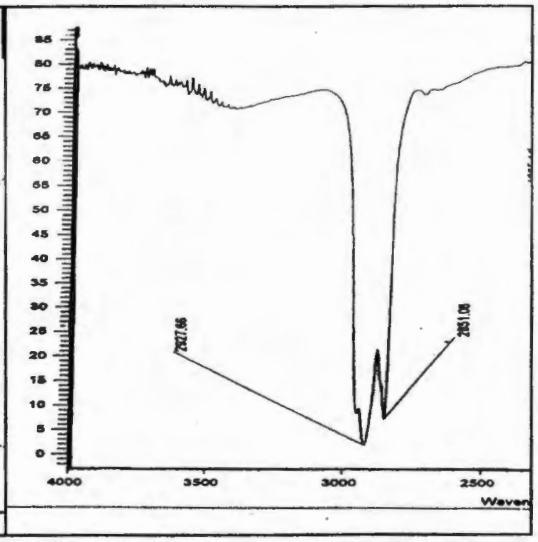

Figure5.3 magnesium(II)porphyrazine

Band	Signal strength	Assignment
2927.66	sh	~C-H stretch(aromatic)
2851.06	sh	C-H stretch (alkyl)
1665.11	m	C=C (stretch)
1463.83	sh	C=C (bending)
1378.72	sh	C-N
1208.51	w	C-N
842.55	w	C-H
723.40	m	C-H

Table 5.2 Absorption bands of the octakis(propyl)porphyrazine magnesium(II) complex and their assignments

There are comparable frequencies at particular regions for both the freebase and Mg(II)-pz, i.e. the C-H signals for propyl substituents at a region of 723.40 cm^{-1}, the C-N stetch within the macrocycle at a region of 1208.51

cm^{-1}, and other observed frequencies as indicated in Tables 5.2 and 5.3. These frequencies observed were in agreement with the formed macrocycle.

Band	Signal strength	Assignment
3395.74	vw	N-H stretch
3174.47	vw	C-H stretch
2927.66	w	C-H (stretch)
1463.83	sh	C=C bending
1378.72	sh	C-N stretch
1208.51	vw	C-N
723.40	m	C-H bending

Table 5.3 Absorption bands of the freebase and their assignments

5.4 Metallation of compounds

The individual reaction rate constants for the insertion of Cr(III) into the compounds are summarised in Table 5.4. Metallation of the freebase with chromium(III) chloride and cobalt(II) nitrate gave the chromium(III)porphyrazine and cobalt(II)porphyrazine, respectively. The two metal ions were both dissolved in ethanol, which was fairly miscible with dichloromethane in the freebase.

The rate constants for both the direct insertion and indirect insertion of Cr(III) into the freebase and mg(II)-pz respectively, are close, they only

differ by ~2-18. This difference might be caused by the slow fission of Mg(II)-pz, followed by the fast pick up of chromium(III) into the macrocycle. Hence the reaction for the direct insertion tends to be slower as compared to the insertion into the freebase.

Temperature	Cr(III) + freebase	Cr(III) + Mg-Pz	Cr(III) + Octa-phthalo
15°C	0.0655	0.0649	0.0433
17°C	0.0776	0.0768	0.0628
20°C	0.0963	0.0965	0.0729
25°C	0.1732	0.1677	0.0855
30°C	0.2165	0.2142	0.0967
35°C	0.3033	0.3035	0.1037

Table 5.4 Individual reaction rate constants for the insertion of Cr(III) into the compounds

The insertion of chromium(III) into 2,3,9,10,16,17,23,24octa-substituted phthalocyanine was occurring at a faster rate as compared to the insertion into Mg(II)-pz. This difference might be brought about by the difference in the nature of the two macrocyclic ligands. The 2,3,9,10,16,17,23,24octa-substituted phthalocyanine has benzene ring substituents, whereas the Mg(II)-pz has propyl substituents. These benzene rings donate more

electrons to the macrocycle core, thus it tends to attract the electropositive metal ions faster. Hence the rate of insertion in this macrocycle is faster as compared to that in the freebase and Mg(II)-pz.

5.4.1 Proposed mechanism for Cr(III) insertion

The insertion of Cr(III) into the octakis(propyl)porphyrazine ligand can occur according to either two mechanisms. The first mechanism would be a slow fission of the mg(II)-pz followed by a fast pick up of the Cr(III) by the resulting freebase. The second mechanism would be fast fission of the mg(II)-pz followed by a slow pick up of the Cr(III) by the freebase. Considering that the rate constants at 20°C for direct insertion and indirect insertion are closely similar as shown in Table 5.4, it is reasonable to assume that the second mechanism is taking place as shown in Equations 5.1 and 5.2.

$$Mg^{(II)}\text{-pz} \rightarrow Mg^{(II)} + Pz \quad \text{(fast)} \qquad 5.1$$

$$Pz + Cr^{(III)} \rightarrow Cr^{(III)}\text{-pz} \quad \text{(slow)} \qquad 5.2$$

5.5 Redox reaction

The rate constants for the reduction process are summarized in Table 5.5, showing it to be relatively slow compared to most redox reactions.

Temperature	15°C	17°C	20°C	25°C	30°C	35°C
Reduction of Cr(III)-pz by Co(II)-pz ($K. m^{-1}$)	0.0447	0.0486	0.0536	0.0691	0.0805	0.1389

Table 5.5 Individual reaction rates constants for the reduction reaction

Considering the absence of any potential bridging ligands in both coordination spheres, the mechanism is likely to be outer-sphere using an electron travelling procedure. Although outer-sphere redox processes are usually very fast, the slowness of this reaction can be attributed to the size of the macrocycle used. In this regard the electron transfer processes must satisfy the Frank-Condon restrictions which arise, in principle, from the fact that the act of electron transfer takes place within a time of $\sim 10^{-15}$ s, that is very much shorter than the time required for nuclei to change their positions in $> 10^{-13}$s.[46]

Therefore the oxidant and the reductant must reorganize themselves before the act of electron transfer, in a way that ensures that the energies of the oxidant and the reductant are identical in their transition states. This reorganization is likely to be slowed down considerably by the sizes of the macrocyclic ligands used in this work.

CHAPTER SIX

CONCLUSION

6.1 CONCLUSION

In conclusion, we were able to synthesise the octakis(propyl)porphyrazine magnesium(II) complex, and demetallate it under acid conditions to obtain octakis(propyl)porphyrazine ligand. Chromium(III) incorporation into the octakis(propyl)porphyrazine ligand, the octakis(propyl)porphyrazine magnesium(II) complex and into the 2,3,9,10,16,17,23,24octa-substituted phthalocyanine was achieved.

The reduction of the octakis (propyl)porphyrazinechromium(III) complex was achieved by using the octakis(propyl)porphyrazinecobalt(II) complex. These compounds have been fully characterised by spectrophotometric methods.

Kinetic studies for both metallation and reduction of the compounds have been followed, and thus a mechanism have been proposed for the complexation of chromium(III) in the octakis(propyl)porphyrazine magnesium(II) complex and octakis(propyl)porphyrazine ligand.

REFERENCES

1. Fitzgerald J , William T and Heather Owen. *J. Org.Chem.* 1991, 686

2. Fitzgerald J, Haggerty BS, Rheingold A N, May L. *Inorg. Chem.* 1992, 31, 2006

3. Ikeda Y, Konami H, Hotano M, Mochizuki K. *Chem. Lett.* 1992, 763

4. Tulinsky A, Ann N Y. *Acad.Sci.* 1973, 47, 206

5. Gouterman M. *J. Chem. Phys.* 1959, 30, 1139

6. Baerends E J, Ricciardi G, Rosa A, van Gisbergen. *Coord. Chem. Review.* 2002, 230, 5

7. Guo L, Ellis D E, Hoffman B, Ishikawa Y. *J. Inorg. Chem.* 1996, 35, 5304

8. Forsyth Timothy P, Montalban Anthony G, Barrett Anthony G M, and Brian Hoffmann. *J. Org. Chem.* 1998, 63, 331

9. Steven J Lange, Hanlin Nie, Charlotte L Stern, Anthony G M Barrett and Brian Hoffmann. *Inorg. Chem.* 1998, 37, 6435

10. Antonio Garrido Montalban, David J Williams, Anthony G M Barrett and Brian Hoffman. *J. Org. Chem.* 2000, 65, 2472

11. T F Baumann, M S Nassir, J W Sibert , A J P White. *J. Am. Chem. Soc.* 1996, 118, 10479

12. Sibert J W, Baumann T F, Olstead M M, Hope H, Barrett A G M and Hoffmann B M. *J. Am. Chem. Soc.* 1993, 115, 10487

13. Eichhorn D M, Williams D J, Barrett A G M, Hoffmann B. *J. Chem. Soc, Chem. Commun.* 1995, 1703

14. Mani N S, Beall L S, Miller T, Anderson O P, Hope H, Parkin S R, Williams D J, Barrett A G M and Hoffmann B M. *J. Chem. Soc. Chem. Commun.* 1998, 2095

15. Baumann T F, Sibert J W, Olmstead M M, Barrett A G M, Hoffman B M. *J. Am. Chem. Soc.* 1994, 116, 2639

16. Barett A G M, FRS-Research Paper, "Synthesis, Characterisation and Applications of Porphyrazines" www.ch.ic.ac.uk/barrett/porph.html. 09/07/2001.

17. Antonio Garrido Montalban, Anthony G M Barrett and Brian Hoffmann. *J. Org. Chem.* 1997, 62, 9284

18. A G Montalban, H G Meunier, R B Ostler and A G M Barrett. *J. Phys. Chem. A.* 1999, 103, 4352

19. Efstathia G Sakellariou, A G Montalban. *Journal of Photochemistry and Photobiology A. Chemistry.* 136, 2000, 185

20. Anderson K, Williams D J, Barrett A G M and Hoffman B M. *J. Heterolytic. Chem.* 1998, 35, 1013

21. Antonio G Montalban, Sven M Baum, Anthony Barrett and Brian Hoffmann. *Dalton Trans.* 2003, 2093

22. David P Goldberg, Anthonio Garrido Montalban, Andrew J P White, David J Williams, Anthony G M Barrett and Brian Hoffmann. *Inorg. Chem.* 1998, 37, 2873

23. Mani N, Barret A and Beall L S. *J. Chem. Soc. Chem. Commun.* 1994, 1943

24. Kobashayi N, Ashida T, Komani H. *Inorg. Chem.* 1994, 33, 1735

25. Montalban A G, Michel S L J, Baum S M, Benjamin J Vasper, Andrew J P White, David J Williams, Anthony G M Barrett and Brian Hoffman. *J. Chem. Soc. Dalton Trans.* 2001, 3269

26. Kormoh M K, Yormah T B R and Fode D V A. *AJST, Vol.3, No.1*: June 2002

27. Casula M, Illuminati G, Ortaggi G. *ibib.* 1972, 11, 444

28. Kormoh M L. *Afr. J. Sc and Tech (AJST)*. 1995, B7(2), 74

29. Cunningham G.E, Burley R.W and Friend M.T. *Nature (London)*. 1952, 169, 1103

30. Velazquez C S, Fox G A, Broderick W E, Anderson O P, Barrett A G M and Hoffmann B M. *J. Am. Chem. Soc.* 1992, 114, 7416

31. O'Shea D F, Miller M A, Matsueda H, Lindsey J S. *Inorg. Chem.* 1996, 35, 7325

32. Stuzhin P A, Khelevina O G. *Coord. Chem. Rev.* 1996, 147, 41

33. Shamim A, Hambright P. *Inorg. Chem.* 1990, 19, 564

34. Lahiri G K, Summers J S, Stolzenberg A M. *Inorg. Chem.* 1991, 30, 5049

35. Hanlin Nie, Anthony G M Barrett and Brian M Hoffman. *J. Org. Chem,* 1999, 64, 6791

36. Kobayashi N, Togashi N, Osa T, Ishii K, Yamauchi S and Hino H. *J. Am. Chem. Soc.* 1996, 118, 1073

37. Cook A S, Williams D B G and White A P. *Angew. Chem. Int. Ed. Eng.* 1997, 36, 760

38. Trabanco A A, Montalban A G, Rumbles G, Barrett A G, Hoffman B. *Synlett*. 2000, 5, 7

39. Nathalie Bellec, Anthonio Garrido Montalban, D Bradely Williams, Andrew S Cook, Mairin E Anderson, Xidon feng, Anthony G M Barrett and Brian M Hoffmann. *J. Org. Chem*. 2000, 65, 1774

40. Phthalocyanine-Wikipedia-Free-encyclopedia. http://en.wikipedia.org/wiki

41. Michael J Cook, Research Focus, "Synthesis and Evaluation of Novel Pthalocyanines Derivatives" p1-8. www.uea.ac.uk/cap/wmcc/mjc.html. 18/11/2002

42. Oleg A Golubchikov and Tatjana A Ageeva. *Molecules*. 2000, 5, 1461

43. Dennis P Piet, David Danovich, Han Zuilhof and Ernst J R Sudhölter. *J. Chem. Soc. Perkin, 2*. 1999, 1653

44. B G Coxand and H Schineider. *Pure and Appl Chem*. Vol 62, No.12, 1990, 2259

45. Antonio G Montalban, Joachim H G Steinke, M E Anderson, A G M Barrett and B Hoffman. *Tetrahedron Letters 40*, 1999, 8151

46. M L Tobe; "Inorganic Reaction Mechanisms" *The Camelot Press Ltd*, London, 1972